

RÉPUBLIQUE ALGÉRIENNE DÉMOCRATIQUE ET POPULAIRE
MINISTRE DE L'ENSEIGNEMENT SUPÉRIEUR ET DE LA RECHERCHE
SCIENTIFIQUE
UNIVERSITÉ FERHAT ABBAS DE SÉTIF
FACULTÉ DES SCIENCES ET SCIENCES DE L'INGENIEUR
THESE DE DOCTORAT ES SCIENCE
Département d'Optique et de Mécanique de Précision

Par

Ihaddadène Nabila

THEME

**Contribution à l'étude de la fissuration par fatigue des
ciments osseux ” Biomatériaux appliqués aux prothèses de
hanche”**

**Contribution to the study of fatigue cracked surfaces of
bone cements ”Biomaterial used in hip prosthesis”**

Membres du jury:

Président:	Prof. Zegadi Rabah	Université de Sétif
Rapporteur :	Prof. Bouzid Said	Université de Sétif
Examineur :	Dr. Mazouz Hamoudi	Université de Batna
Examineur :	Dr. Marouche Abdallah	Université de M'sila
Examineur :	Dr. Smata Lakhdar	Université de Sétif
Membres invités :	Dr. Bouzid Abderazek	Université de BBA

Année Universitaire 2008-2009

Acknowledgements

First of all (On Sky scale), Thanks be to God for my life. You have made my life more bountiful. May your name be exalted, honored, and glorified.

On Earth scale, this research work would not have been possible without the help of many people who I would like to thank lots.

I especially want to thank my advisor, Prof. Said Bouzid, for his entire confidence made in me. I was delighted to interact with Prof. Luca Cristofolini by attending Rizzoli Orthopaedic Institutes and having him as my co-advisor. He was abundantly helpful and offered invaluable assistance, support and guidance. Thanks Prof. Luca for all.

I can't forget Paolo Erani who was always accessible in Rizzoli Laboratory and willing to help me with my research. Thanks Paolo.

Prof. Rabah Zegadi, Prof. Abdellah Marouche, Dr. Lakhdar Smata, Dr. Hamoudi Mazouz and Dr. Abderazek Bouzid deserve special thanks as my thesis committee members.

I would like to convey thanks to Prof. Slimane Barhoumi (Rector of f M'sila's University) as my research was supported in part by the University of M'Sila.

Furthermore, Dr Rachid Ahmed Ouamer has always been a constant source of encouragement during my doctoral study. He offers advice and suggestions whenever I need them. Thanks Dr Rachid.

My deepest gratitude goes to my family for their unflagging love, and support throughout my life; this work is simply impossible without them. I cannot ask for more from my sister, Razika, as she is simply perfect. I have no suitable word that can fully describe what she does for me. I remember her constant support when I encountered difficulties and I remember, most of all, her delicious dishes. Special thanks to my aunt Mrs Nouara Zaamoum.

I would also like to thank Prof. L'H. Yahia who opened my mind to work on hip replacements.

For all people who I haven't cited and helped and inspired me during my doctoral study thanks a lot.

Nabila
Tanmirt inwen terni

Contents

INTRODUCTION

I Physico-Chemical properties of PMMA bone cement

I.1 History of acrylic bone cements	1
I.2 Chemico-physical properties of acrylic bone cements	2
I.2.1 Chemistry of the acrylic cement	2
I.2.1.1 Acrylic bone cement components	2
I.2.1.2 Polymerization process	4
I.2.1.2.1 Polymerization reaction	6
I.2.2 Polymerization heat	6
I.2.2.1 Effect of PMMA bead size	8
I.2.2.2 Effect of initiator to activator ratio	8
I.2.2.3 Effect of radiopacifiers	9
I.2.2.4 Effect of liquid to powder ratio	9
I.2.3 Residual monomer	9
I.2.4 Volumetric Shrinkage	10
I.2.5 Viscosity	10
I.2.6 Porosity	12
I.2.6.1 Cement mixing methods	13
I.2.7 Molecular weight	15
I.2.8 Glass transition temperature	16
Summary	18

II Mechanical properties of bone cements

II.1 Introduction	20
II.2 Quasi-static proprieties	21
II.2.1 Tensile properties	21
II.2.2 Compressive properties	22
II.2.3 Flexural properties	23
II.2.2.4 Shear properties	25
II.3 Dynamic proprieties	27
II.3.1 Fracture Toughness	27
II.3.2 Fatigue properties	33
II.3.2.1 Fatigue resistance	33
II.3.2.3 Fatigue Crack Growth (FCP)	38
II.3.3 Creep	40
Summary	43

III Materials and methods

III.1 Experimental Groups	44
III.2 Preparation of the cement specimens	46
III.3 Fatigue crack propagation tests	46
III.4 Roughness measurement	48
III.4.1 Roughness parameters	50
III.4.1.1 Ra Roughness	50
III.4.1.2 Rt Roughness	50
III.4.1.3 Rsm Roughness	50
III.5 Treatment of fractured surfaces	51

III.6 Count of cleaved pre-cured beads	52
III.6 Scanning Electron Microscopy	53
III.7 Statistical analysis	54
Summary	55
IV Results and discussion	
IV.1 Crack growth rate	56
IV.2 Roughness measurement	57
IV.3 Count of cleaved pre-cured beads	66
IV.4 Fractography	72
IV.5 Limitations	78
CONCLUSION	
Annex 1 Medical definitions	
Annex 2 Engineer definitions	
Annex 3 Results”Statistical analysis”	
References	

INTRODUCTION

Acrylic bone cements have been widely used in total hip replacements since 1960s as a fixation agent between the implant and the host bone. Hip Arthroplasty, is the definitive, surgical treatment for the severe pain and loss of function caused by hip arthritis. In this surgical procedure, the damaged arthritic cartilage and bone in hip joint are surgically removed and replaced by components of metal and plastic that provide bearing surfaces for the new artificial hip joint.

PMMA bone cement is prepared in the operating room at the time of surgery mixing the two components; polymethylmethacrylate (PMMA) powder and methyl methacrylate (MMA) liquid monomer at an approximate ratio of two to three parts powder to one part monomer, according to the manufacturer instructions. Typically, the powder component consists of PMMA (and or copolymers), radiopacifier such as Barium sulphate (BaSO_4) or Zirconium dioxide (ZrO_2) and di-benzoyl peroxide (BPO) as an initiator. The liquid component contains the monomer MMA, dimethyl-p-toluidine (DMPT) as an accelerator and the inhibitor (Hydroquinone). The mixed cement is initially a viscous fluid that can be poured into bone cavity prepared to receive a prosthetic device. After curing, PMMA must assure a rigid fixation of the prosthetic components. Curing process is the result of the polymerisation of methyl methacrylate (MMA) monomer, in the presence of pre-polymerised PMMA, initiated by benzoyl peroxide (BPO) and activated at room temperature by the presence of a tertiary amine the most classical being N,N dimethyl-p-toluidine (DMPT).

A number of new formulations of acrylic bone cements have been developed with components that differ slightly or markedly from those in the current generation of commercial formulations. Thus alternative monomers, polymers, inhibitors, accelerators and radiopacifiers have been proposed in order to reduce toxicity and improve handling and mechanical properties. The incorporation of antibiotics in polymethylmethacrylate (PMMA) bone cements for the treatment and prevention of infection in orthopaedics has become clinical practice during the last two decades.

The average person takes about 1000000 steps in one year and thus, in hip joint, about 10^6 fatigue cycles (repeated loads) per year are applied to the bone cement. After long term use, it does fail under cyclic loading. Fatigue bone cement is a critical failure mechanism leading to revision surgery. This mechanism includes crack initiation and subsequent crack propagation under cyclic loading. However the exact mechanism of cement failure is not well defined. Acrylic cements used in total hip replacement contain small pockets of trapped air or monomer and exhibit regions of incomplete mixing between polymerized methyl-methacrylate (MMA) monomer and the PMMA powder, in addition to voids created by radiopacifier particles (such as BaSO_4). These porous regions can become highly stressed due to the stress concentrating effects of the voids and may act as sites for the initiation of small cracks. The formation of these microcracks may take place during the cure of the acrylic

cement (by thermal stressing and residual stressing due to the shrinkage of the cement) or when the prosthesis becomes loaded in uses. These flaws (micro-voids or small cracks), under in vivo loading first extend slowly by coalescence of voids and microcrack propagation (stable crack) and then later there is fast (unstable) growth culminating in the fracture of the cement layer. Pore size and pore size distribution were found to affect the crack initiation and fatigue resistance. Porosity can be affected by the mixing method. PMMA bone cements have been traditionally mixed by hand in the operating theatre. Improved mixing techniques have been developed but they have not yielded consistently superior cements.

Although the fatigue crack propagation has been widely studied in the past to assess the effect of the environment and the effect of different additives (antibiotics, radiopacifiers, reinforcing agents, etc.) added to the basic formulation, crack surfaces remain qualitatively inspected. It has been reported previously, that the fractured surface appearance showed two different morphologies in relation to the crack propagation rate; rough fatigue surface and smooth catastrophic fracture. In the present study, untitled:

Contribution to the study of fatigue cracked surfaces of bone cements "Biomaterial used in hip prosthesis"

Two quantitative inspections of the fractured surfaces were elaborated based on roughness measurement and amount of cleaved pre cured beads. In this investigation three different morphologies were observed in the fractured surfaces; slow fatigue propagation which is relatively smooth, rough fast cyclic propagation and smooth sudden fracture.

This study focuses on four chapters. Two chapters are discussed in the theoretical part; two others in the experimental section. The first one deals with the physico-chemical properties of PMMA bone cement, followed by mechanical properties of acrylic cements in Chapter Two. Chapter three describes the material and methods used in the experiments, the last one reports the results found and discusses them. My thesis begins with an introduction and ends with a conclusion.

Finally, I have added some medical and chemical definitions in the two first annexes for engineers and non engineers' users respectively, to facilitate the comprehension of the terms that appear confused. The terms written in bold are explained in the two annexes.

PHYSICO-CHEMICAL PROPERTIES OF PMMA BONE CEMENT

Chapter

I

*This Chapter gives answers to the following questions:
What is PMMA bone cement?
Why we use it? (Domains of concern)
How it can be obtained?
What are PMMA's negative effects?
What are PMMA's physical properties?*

I.1 History of acrylic bone cements

Acrylic bone cements are the most frequently used materials for the fixation of a total joint prosthesis,^(1,2,3,4,5) although other means of prosthetic component fixation are preferred in certain cases such as bony in-growth or press fit. These polymeric materials composed principally of poly methyl methacrylate (PMMA) have been widely known since 1930.

Originally, PMMA better known as Plexiglas or Perspex, was utilized above all for producing safety glass, but in the thirties, both an English company called ICI⁽¹⁾ and a German researcher, Otto Röhm, proposed the use of PMMA in dentures (dental prostheses),^(2,6) their product, however, had technical difficulties (vacuum preparation and a high **polymerization** temperature, above 100°C).

The date of 1940 marked the beginning of the modern era of PMMA with the discovery of its cold **polymerization** (which occurs at room temperature) by Schnebel⁽⁶⁾(1940) and the two German companies Degussa and Kulzer⁽²⁾(1943). This process, using tertiary aromatic amines DMPT as a co-initiator is still valid to this day. During the forties, PMMA was used for implantation in the human body⁽⁶⁾ (reconstruction of the skull 1941, filling the defects of the skeleton 1943, **hip** implant 1949.....). Since the end of the World War II, PMMA bone cements were developed independently in several countries.⁽²⁾

After understanding the potential of PMMA, Kiaer (1951), Haboush (1953) and Wiltse (1957) proposed it as 'cement' in **hip** prosthesis surgery.^(2,6) This marked the fifties; Indeed, Sir John Charnley gave rise to the modern history of bone cement by using it for the first time in 1958^(2,7) to fix cephalic prosthesis on the **femur**. He called the material used 'bone cement on acrylic basis'.

The positive results regarding the **biocompatibility** of PMMA implants at an early date (Henrichsen et al.1953; Wiltse et al.1957; Lehmann and Jenny 1961; Hullinger 1962)⁽²⁾ led to clinical interest in this material. Rather, since its availability was guaranteed, acrylic bone cements were used in various medical fields such as dentistry, cranioplasties, plastic surgery, orthopedic surgery, etc.

In 1969, professor Buchholz made a first tentative to add some antibiotics to the cement, to decrease the incidence of infection, this date marks the beginning of the cements with antibiotics.⁽⁷⁾ Thus, the first antibiotic-loaded bone cement marketed was Refobacin-Palacos R (addition of Gentamicyn sulfate in Palacos R) by Merck and Kulzer.^(2,7)

A uniform and reproducible testing basis for acrylic bone cements was developed, first, in the US (ASTM F451) in 1978. A short time later, based on the American standards, the protocol ISO 5833/1 (1979) was developed.⁽²⁾ Today, all bone cements must fulfill the requirements of either ISO 5833/2 (1992) or ASTM F451 standards.^(2,3)

Acrylic bone cement, so-called two-component systems is commonly prepared by mixing a solid part made of a pre-polymerized poly methyl methacrylate (PMMA), benzoyl peroxide (BPO) as an initiator, and radio-pacifiers, with a liquid part containing methyl methacrylate (MMA), N, N-dimethyl-p-toluidine as an accelerator and inhibitor. Each cement manufacturer recommends a specific **monomer** to **polymer** ratio, expressed as grams per milliliter.⁽⁸⁾ Methods of cement mixing that are extrinsic factors may affect the properties of the final product.

Since PMMA bone cement's conception, efforts at improving its properties have been made by changing either the solid or the liquid part (incorporation of various ceramics into the powder such as hydroxyapatite, calcium phosphates and bioglass. Co-**monomers**, cross-linking agents, and new activators have been added to the liquid **monomer**).^(3,8) Currently, many types of cement are available on the market for orthopedic interventions, with a wide variety of physical, chemical and mechanical properties.

In orthopedic surgery, PMMA based cement is routinely used to fill cavities in bone, reinforce weakened bone and act as a fixation agent for surgically implanted joint replacement prosthesis (our domain of interest). In 2000's, about one million implants are fixed with bone cement world wide.⁽⁹⁾

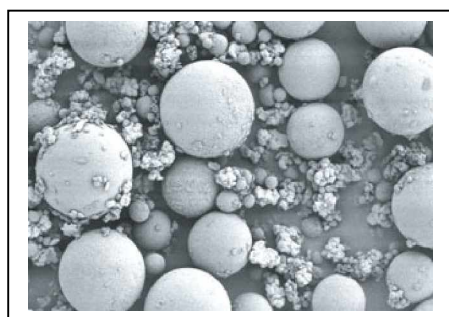
I.2 Chemico-physical properties of acrylic bone cements

I.2.1 Chemistry of the acrylic cement

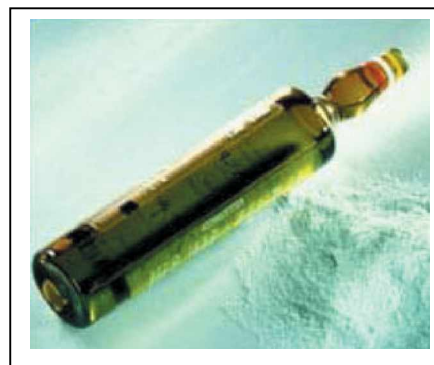
I.2.1.1 Acrylic bone cement components

Most commercially available cements consist of two separate components (Figure I.1): a powder containing spherical pearls of pre-polymerized PMMA (and or **copolymers**), with an average diameter of some tens of microns (μm)^(2,4) and a liquid made principally of monomer methyl methacrylate MMA. The di-benzoyl peroxide (BPO) initiator is incorporated into the powder and the chemical activator, mostly N, N-dimethyl-p-toluidine (DMPT) is added to the liquid in order to encourage the **polymer** and **monomer** to polymerize at room temperature (cold curing cement). The BPO can be either contained in the **polymer** balls or added to the **polymer** as a powder.⁽²⁾ To prevent spontaneous **polymerization** of the liquid during storage, a small quantity of retardant hydroquinone (HQ) is added as a stabilizer or an inhibitor. In the commercial bone cements, radiopacity is accomplished by the addition of an inorganic compound, like barium sulphate (BaSO_4) or zirconium dioxide (ZrO_2) to the powder, in a proportion ranging between 8% to 13% for the barium sulphate and 9-15% for the zirconium dioxide. The ZrO_2 particles are larger than those of BaSO_4 with a medium size of around $10\mu\text{m}$, as shown in Figure I.2. Bone cements with zirconium dioxide have a higher opacity than those containing barium sulphate. Colorant (chlorophyll or methylene blue) is added to both the liquid and the powder, to make the cement more easily visible in the operating room especially during revision procedures. The powder component in antibiotic loaded bone cement, additionally, contains an antibiotic (such as gentamicyn) or a combination of antibiotics (such as gentamicyn and clindamycin).

The actual production of the cement dough is performed by nurses in the operating room at the time of surgery, mixing the two components of the commercial package conveniently pre-dosed by the manufacturer at an approximate ratio of two to three parts powder to one part **monomer**.⁽²⁾

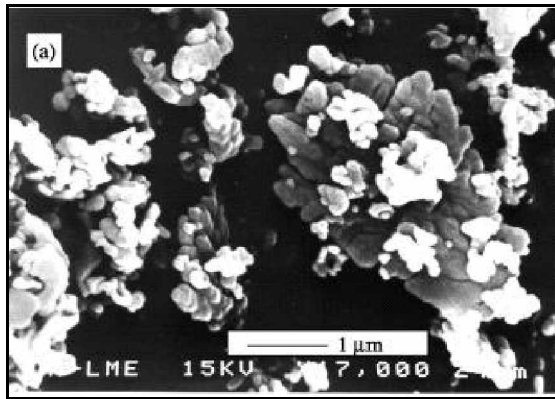
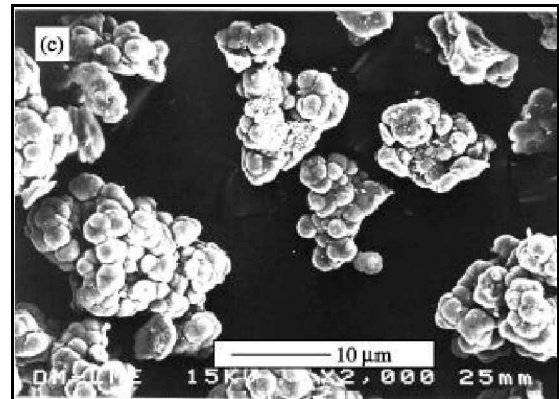


(a) Powder



(b) Liquid

Figure I.1 Powder and liquid components of PMMA bone cements.⁽⁷⁾

Barium sulfate(BaSO_4)Zirconium dioxide (ZrO_2)*Figure I.2* SEM of inorganic fillers.⁽¹⁰⁾

In Table I-1, are listed the most commercial acrylic bone cement formulations, in popular use.

Table I-1 Name and main composition of most widespread PMMA based bone cements.⁽⁴⁾

Name	Source	Powder Composition	Liquid Composition
Simplex P	Howmedica, Inc. (Rutherford, NJ, USA). Shannon Industrial Estate Co.(Clare, Ireland).	Copolymer (PMMA/Styrene) 75%	MMA 97.4%
		PMMA 15% BPO n.a BaSO ₄ 10%	DMPT 2.6% Hydroquinone 75ppm
Zimmer Regular ⁽⁵⁾	Zimmer, Inc. (Warsaw, IN, USA).	PMMA 89.25% BPO 1.19% BaSO ₄ 10.00%	MMA 97.27% DMPT 2.73% Hydroquinone 75ppm
Zimmer LVC (Low viscosity)	Zimmer, Inc. (Warsaw, IN, USA).	Copolymer (PMMA/Styrene) 89.25% BPO 0.75% BaSO ₄ 10%	MMA 97.27% DMPT 2.73% Hydroquinone 75ppm
Zimmer Osteobond	Zimmer, Inc. (Warsaw, IN, USA).	Copolymer (PMMA/Styrene) 87.5% BPO 1.2-2.5% BaSO ₄ 10%	MMA 99.25% NNDT 0.75% Hydroquinone 75ppm
Palacos R	Manufacturer: Haereus, Kulzer Gmbh, Germany. Distributed by: -Smith & Nephew Orthopedics, Inc (Memphis, TN, USA) -Schering-Plough (Welwyn, UK). -Merck (Darmstad, Germany).	Copolymer (PMMA/PMA) 84% BPO - ZrO ₂ 15% Chloropyll 200ppm	MMA 98% DMPT 0.02% Chloropyll 267ppm
CMW-1	Wright Medical Technology (Arlington, TN, USA).	PMMA 88.85% BPO 2.05% BaSO ₄ 9.10%	MMA 98.2% DMPT 0.82% Hydroquinone 20ppm Ethanol 0.945% Ascorbic acid 0.02%
CMW-3	Johnson and Johnson/ Depuy	PMMA 88.00%	MMA 96.54%

	(Warsaw, IN, USA).	BPO	2.00%	DMPT	2.49%
		BaSO ₄	10%	Hydroquinone	20ppm
				Ethanol	0.945%
				Ascorbic acid	0.02%
Cemex RX	Tecres SpA (Sommacampagna, VR, Italy).	PMMA	88.27%	MMA	99.1%
		BPO	2.73%	NNDT	0.9%
		BaSO ₄	9%	Hydroquinone	75ppm
Cemex Extra Low viscosity	Tecres SpA (Sommacampagna, VR, Italy).	PMMA	85.00%	MMA	98.20%
		BPO	3.00%	DMPT	1.80%
		BaSO ₄	12.00%	Hydroquinone	75ppm
Cemex Isoplastic	Tecres SpA (Sommacampagna, VR, Italy).	PMMA	84.3%	MMA	9.1%
		BPO	2.7%	NNDT	0.9%
		BaSO ₄	13%	Hydroquinone	75ppm
Cemex System	Tecres SpA (Sommacampagna, VR, Italy).	PMMA	85.00%	MMA	98.20%
		BPO	3.00%	NNDT	1.80%
		BaSO ₄	12.00%	Hydroquinone	75ppm
Cemex Fluoride LV	Tecres SpA (Sommacampagna, VR, Italy).	PMMA	85.00%	MMA	98.20%
		BPO	3.00%	DMPT	1.80%
		BaSO ₄	6.00%	Hydroquinone	75ppm
		NaF	6.00%		

The main differences between these twelve formulations are in their molecular weights and the relative amounts of **homopolymer** and **copolymer**, with other differences being in the quantity of other components (Radiopacifying agents, Chlorophyll...). Altering the concentrations of the individual reagents affects setting time, **polymerization** temperature and the material properties of the solidified product.

According to Lewis,⁽⁵⁾ the most widespread acrylic cements used in the United States are: Simplex P (Howmedica, Inc; Rutherford, NJ USA), Zimmer Regular and Zimmer low viscosity cement (LVC, Zimmer, Inc; Warsaw, IN), Palacos R (Smith & Nephew Orthopedics, Memphis, TN) and CMW-1 and CMW-3 (Wright Medical Technology, Arlington, TN). In the Norwegian Arthroplasty Register,⁽¹¹⁾ Palacos w/gentamicyn is the most used cement (66%) in both primary and revision **Total Hip Arthroplasty (THA)**. Currently, in Emilia Romagna (Italy) there are four commercial formulations in popular use for THA: Surgical Simplex P, Cemex, Amplicem3 and Palacos R.⁽¹²⁾ In Algeria I haven't unfortunately, succeed to gather any information.

All Cemex cements deviate most distinctly from the original 2:1 ratio.⁽²⁾

I.2.1.2 Polymerization process

At the moment of mixing, the solid particles of **polymer** are swollen by **monomer** and, due to the effect of the system (Activator/ Initiator), **polymerization** starts inside and around the swollen particles, transforming the MMA multi-molecular liquid system into a solid PMMA macro-molecular one in a very aggressive exothermic reaction.

The **polymerization** process of acrylic bone cements can be divided into four basic steps⁽²⁾ as shown in Figure I.3: the mixing phase, the waiting phase, the working phase, and the hardening phase.

I. Mixing phase

During the mixing phase, the liquid is added to the powder or inversely, forming a homogenous mass after thorough mixing. Some cements can be easily mixed, others can be

homogenized only with great difficulty. The cement should be mixed homogeneously in order to minimize the number of pores (see Sect. I.2.6). Moreover, the more powerfully and longer the dough is mixed, the more porous it will be.⁽²⁾

II. Waiting phase

During this period, the cements accomplish a suitable viscosity for delivery of bone cement. It remains sticky dough.

III. Working phase

The working phase is the time during which the cement can be manipulated with ease. Rather, the surgeon can easily apply cement to the **femur**, during this time period. The dough must not be sticky, and its viscosity should be suitable for application (see Sect. I.2.5).

IV. Hardening phase

The hardening phase indicates the moment at which the cement is completely hardened. Hardening is influenced by the cement temperature, the operating room temperature as well as the body temperature.

The surgical preparation of PMMA bone cement can be divided into three time periods: mixing time (includes mixing and waiting phases), working time and hardening time. These time periods which present the handling properties of the material, depend strongly up on the environmental temperature^(2,4,7) as well as on the mixing system.^(2,13) According to ISO 5833 standard, the manufacturer is obliged to present the handling properties of his material in form of a graph⁽²⁾ as outlined in Figure I.4 for Palacos high viscosity cement.

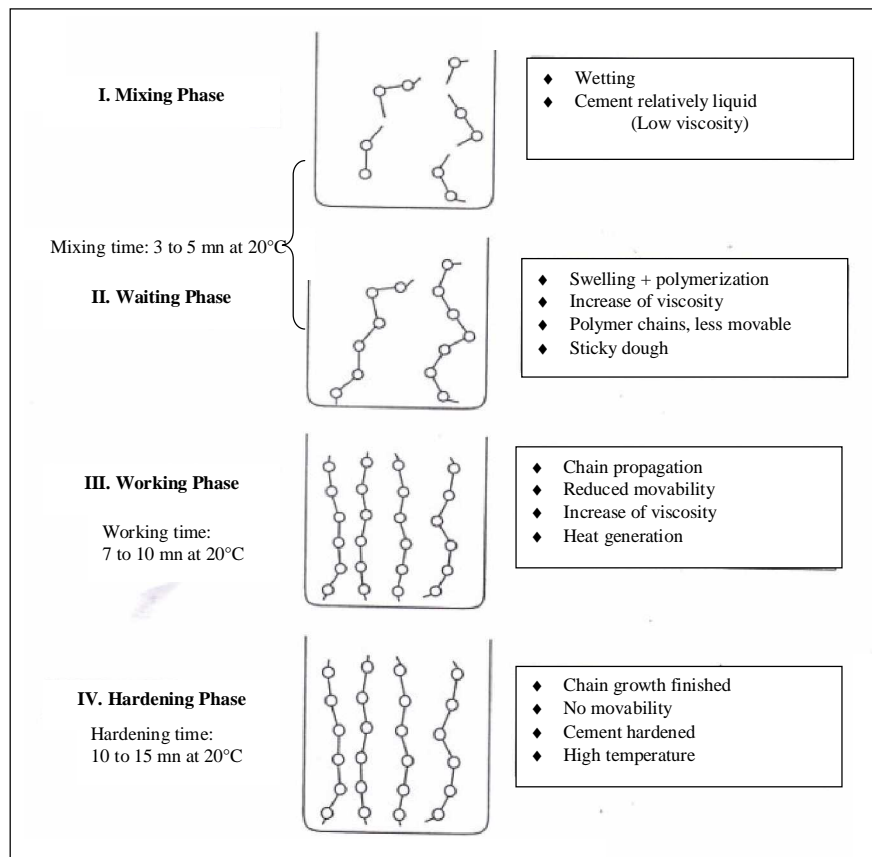


Figure I.3 Schematic graph of the **polymerization** process of PMMA-based bone cements.⁽²⁾

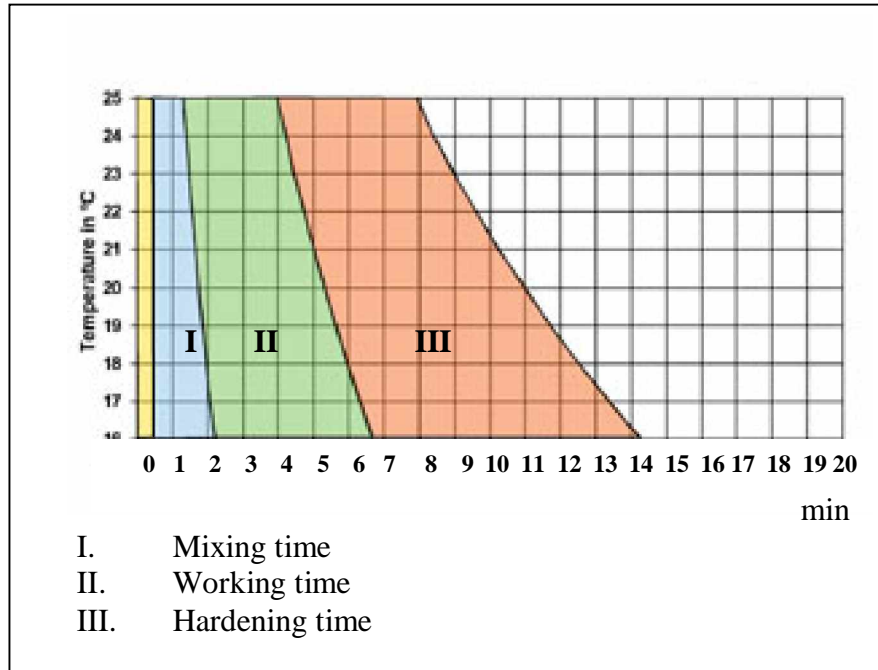


Figure I.4 Handling properties of Palacos HV cement.⁽⁷⁾

Breush et al. 1999⁽²⁾ reported that the mixing time of bone cement is standardized in only two thirds of all cases, whereas, the working time is standardized in approximately 88% of all cases. The hardening phase of the cement under operating conditions can significantly differ from the statements in the manufacturer's instructions conducted in laboratory under defined conditions of temperature, humidity, etc.⁽²⁾

I.2.1.2.1 Polymerization reaction

Polymerization begins by the addition mechanism in which DMPT cleaves BPO initiator at room temperature, forming a phenyl radical as shown in Figure I.5.

The activated initiator attacks the double bond of the MMA **monomer** forming a **monomer** radical that can attack the double bond of the next **monomer** by the adding mechanism shown in Figure I.6, propagating, thus, the **polymer** chain. The growing **polymer** chains encapsulate the PMMA beads within a solid matrix. It is assumed that the smallest beads of the PMMA phase (<20µm) undergo complete dissolution in the presence of MMA **monomer** increasing the viscosity of the curing mass. In contrast, the surface of the bigger particles are partially dissolved and incorporated in the cured bone cement maintaining the spherical shape. When two reactive radical chain ends meet, they react to form non-reactive completed **polymer** chains, within 10-15 min after the start of mixing at 20°C.

Negative effects of PMMA bone cement have been attributed to its high temperature reached during polymerization,^(2,4,5,7,13) **monomer** release to the surrounding tissues,^(2,4,5,7,13) and volumetric shrinkage.^(2,4,5,7)

I.2.2 Polymerization heat

The conversion of MMA to PMMA is an exothermic reaction, releasing an energy of 52 kJ per mole of MMA.^(2,4,7,13,14) This important energy that gives rise to the increase of the local temperature (peak temperature) is caused only by the **monomer** MMA.

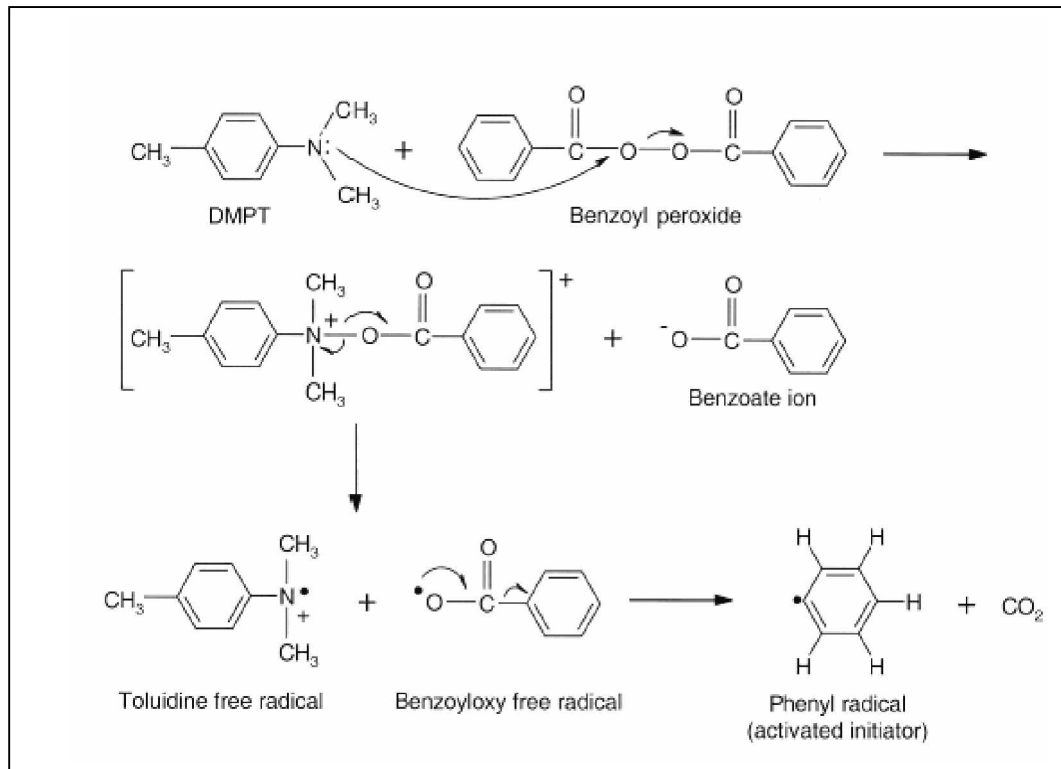


Figure I.5 Formation of phenyl radical by reaction of DMPT with the BPO initiator.⁽¹⁴⁾

The temperature peak depends on the MMA-PMMA ratio,⁽¹⁵⁾ the composition of the liquid and solid components,⁽¹⁶⁾ the concentration of BPO and DMPT, the average size of the PMMA,^(4,14,17,18) etc.

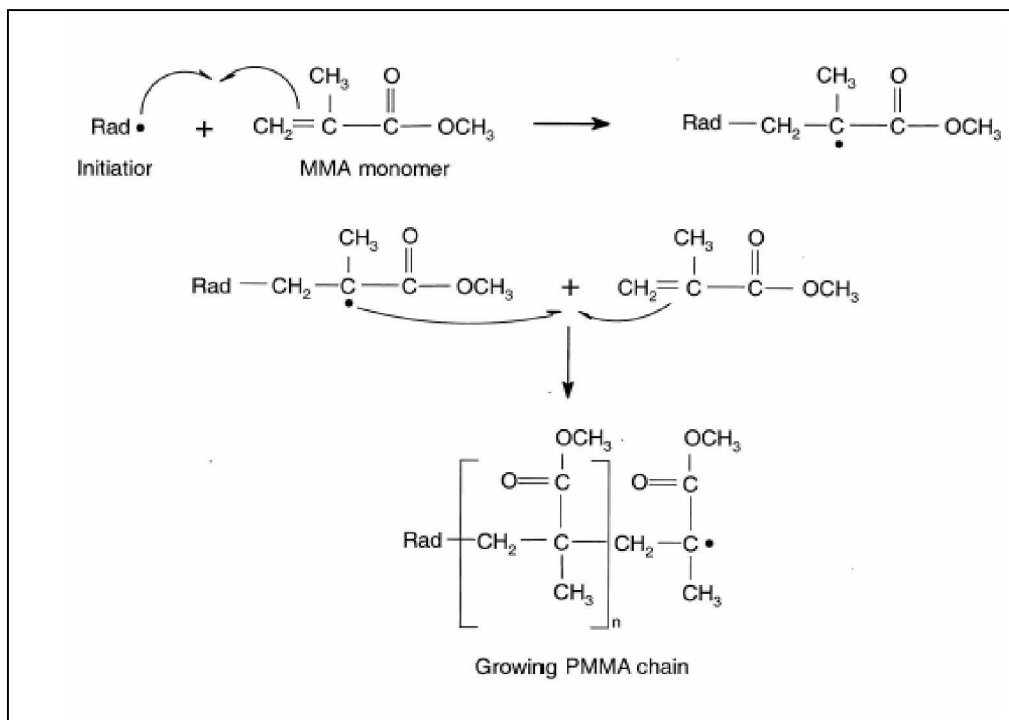


Figure I.6 Polymerization of PMMA by an addition reaction.⁽¹⁴⁾

For a long time, the maximum temperature reached during the hardening phase of PMMA cements was known to cause tissue necrosis (50-60°C) and hinder the efficacy of joint prostheses.^(2,4,7,14,19) In real conditions (in vivo), there are several factors that contribute to dissipate the heat produced, including the thin layer of cement (3-5 mm), the blood circulation, heat dissipation in the vital tissue connected with the cement, and heat dissipation of the system attained via the prosthesis.^(4,20,21)

A temperature/time diagram (Figure I.7) shows best the progress of the **polymerization** temperature

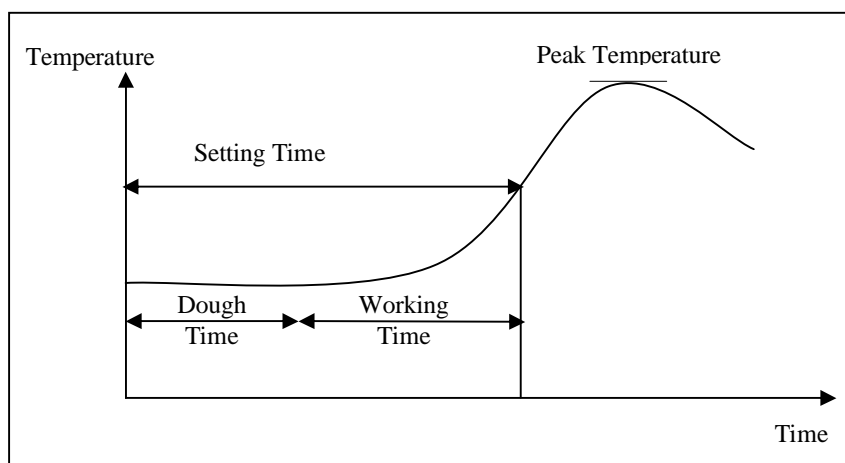


Figure I.7 Diagram temperature/time of bone cement.⁽⁴⁾

The temperature increases only slowly during the mixing phase. It starts to rise rather quickly with increasing viscosity of the cement dough. During the hardening phase, the temperature rises explosively and soon reaches its maximum (gel effect). After this, a speedy decrease in temperature is registered due to the polymerization behavior.

The effect of each component on the kinetic control of the **polymerization** process of bone cement is detailed as follows:

I.2.2.1 Effect of PMMA bead size

Park and Lakes⁽²²⁾ considered that the properties of bone cement could be affected by the powder size, shape and distribution. Indeed, the characteristics of the curing process of acrylic cements, the peak temperature and setting time are better when using PMMA particles of relatively large diameter and wide size distribution, lower peak **polymerization** temperature and longer setting time.^(17,18)

It has been found that there is a linear relationship between the average size of PMMA beads and the peak temperature for acrylic systems, prepared in the same experimental conditions.^(4,17)

I.2.2.2 Effect of initiator to activator ratio

Classical kinetic parameters were strongly related to BPO and DMPT concentrations. Moreover, the rate of radical formation is dependent on the concentrations of the activator and initiator. Pascual et al.⁽¹⁷⁾ reported with use of the more conventional liquid/powder cement mixture that, the peak temperature increases by increasing the concentration of both components. Inversely, this impact is unclear when using two liquid solutions.⁽²³⁾ Increasing

the concentration of both BPO and DMPT will speed up the overall **polymerization** process, decreasing setting time.^(17,23)

I.2.2.3 Effect of radiopacifiers

In the cured cement, radiopaque particles are found in the interbead matrix filling the spaces between the relatively large pre-polymerized beads. A number of studies^(17,24,25) reported that radiopacifiers such as BaSO₄ or ZrO₂ had no noticeable influence on the curing properties of bone cement.

I.2.2.4 Effect of liquid to powder ratio

At high L/P ratios, an abundance of **monomers** react exothermically, increasing the peak **polymerization** temperature. Moreover, the relative concentration of initiator (a component of powder) is decreased, so the **monomers** are activated slowly, increasing setting time.^(26,27)

I.2.3 Residual monomer

Generally, **polymerization** of MMA is never completed since the mobility of the **monomer** is greatly decreased (increase of viscosity) at high conversion rates, thus residual **monomer** remains in the final product. The proportion of non converted residual **monomer** remaining in the hardened cement is in the range of 2-6%^(2,7)(Figure I.8). Within 2 to 3 weeks, this rate falls to 0.5 %⁽²⁸⁾, due to a slowly progressing, continuous **polymerization**. The main part of the eluted **monomer** quickly passes into blood stream and disappears just as quickly. A more reduced share of the residual **monomer** is either speedily exhaled or metabolized⁽²⁹⁾ in the Krebs's cycle (Figure I.9).

Investigations of Schlag et al.1976 show that MMA cannot be the cause of loosening or respiration and circulation reactions.⁽²⁾

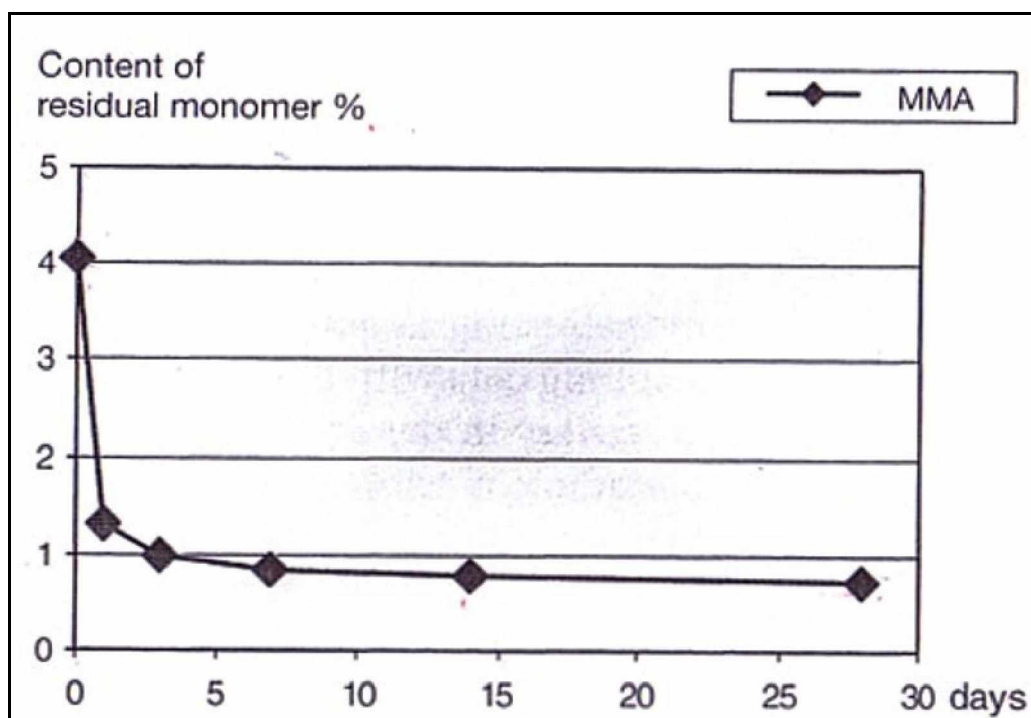


Figure I.8 Diagram Residual monomer.⁽²⁾

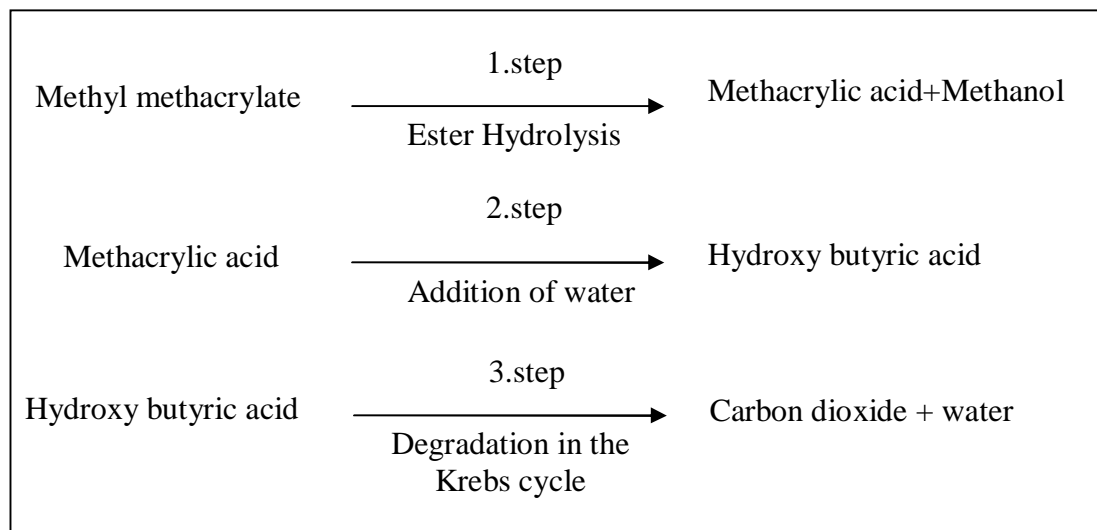


Figure I.9 Metabolization of MMA.⁽⁷⁾

I.2.4 Volumetric Shrinkage

During the **polymerization** process, only a few large **polymer** molecules develop from the multitude of **monomer** ones, this determines a volumetric shrinkage (Material contract). Indeed, the **monomer** molecules are separated by an intermolecular distance of 4 \AA , whereas after the reaction, due to the formation of covalent bonds, they will be separated by atomic bond distances of 1.9 \AA .⁽⁴⁾

Pure MMA shows a shrinkage of approximately 21-22% as shown in Figure I.10 during **polymerization**,^(2,7) which is intolerable for an application as cement for joint prosthesis fixing. However, mixing **monomer** and pre-polymerized **polymer** particles reduces considerably the volumetric shrinkage, theoretical contract, in this case varies from 6-7%.⁽⁷⁾ Besides, the presence of porosity (air bubbles) reduces furtherly the amount of volumetric shrinkage making it as much as 2-4% of the initial volume (Figure I.10). Vacuum mixing (to avoid pores) leads to a slightly higher shrinkage (Davies et al.1990).⁽²⁾

Volumetric shrinkage of the cement is not disadvantageous since, its contraction at the cement bone interface will favor the building of new bone. Moreover, the shrinkage of the material will be compensated, *in vivo*, by its dilatation due to a slightly absorbent characteristic.

I.2.5 Viscosity

Viscosity is a physical parameter, which characterizes a material's resistance to flow. Materials with a high viscosity do not flow readily; materials with a low viscosity are more fluid.

The viscosity of the acrylic bone cement used in THA is an important material property for determination of the proper handling characteristics. In the operating theater, the cement viscosity must be low enough (not too low) to make it very easy to force the dough through the delivery system (syringe) and cause it to flow and penetrate into the interstices of the spongy bone, under any given pressure, in a very short time.^(2,4,5,7)

However, cement with too low viscosity cannot withstand the bleeding pressure in the **femur**.^(2,7) Blood is included in the cement, resulting in gaps and laminate formation.^(2,4,7) These inclusions with a high fracture risk affect the mechanical stability of the implant.⁽³⁰⁾

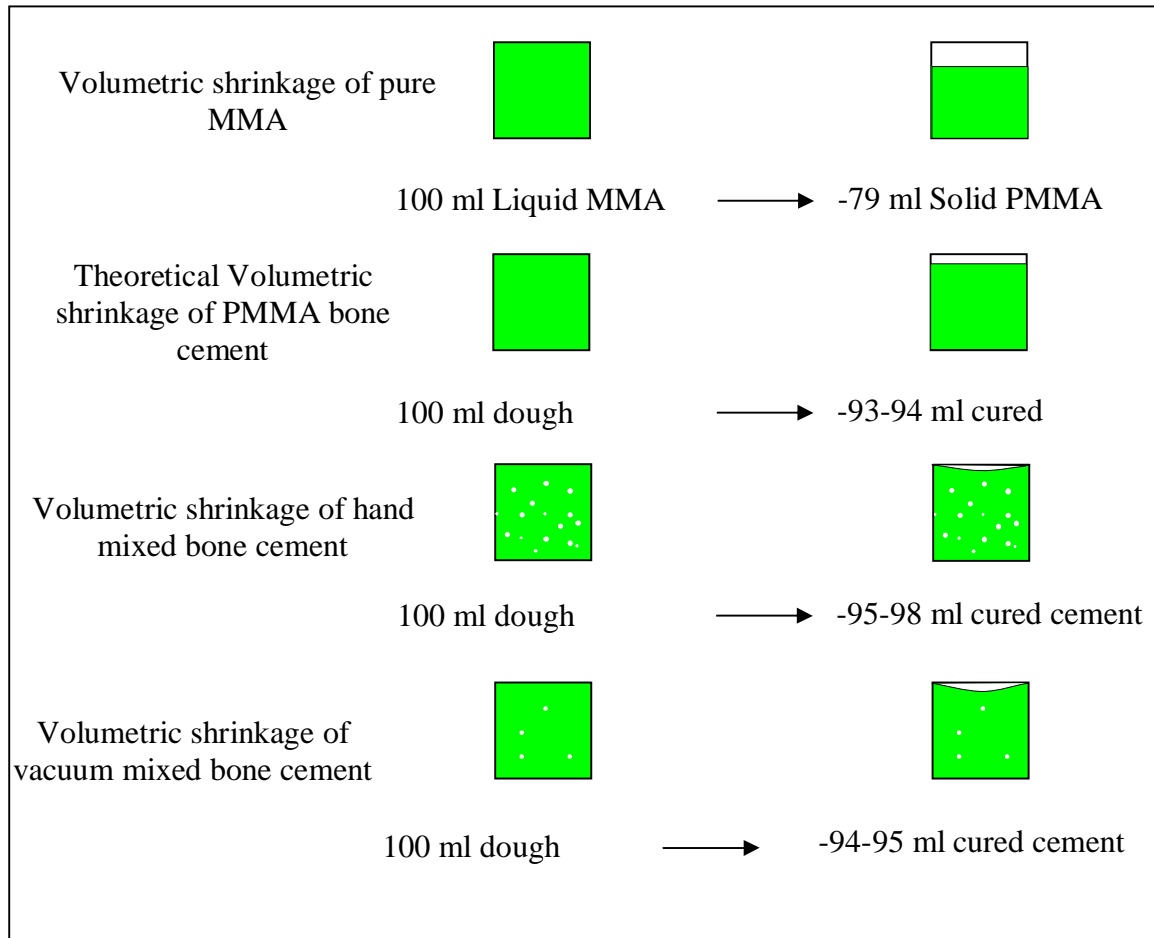


Figure I.10 Volumetric shrinkage of PMMA based cement.⁽⁷⁾

High viscosity cement may introduce cement interface (cement-bone and cement-implant) gaps. This phenomenon due to a poor cement penetration into the bone tissue and/or poor cement flow properties.⁽⁴⁾

Dynamic viscosity, η , of bone cement decreases with an increase in shear rate, and increases with an increase in time as the **polymerization** reaction proceeds^(4,5) (pseudo plastic behavior of bone cement).

The ideal cement would display a low and practical unchanged viscosity with time during the working period, followed by a very short time to full **polymerization**⁽³¹⁾ (increase of viscosity).

Cement viscosity is increased by the addition of fibers, greater molecular weight of the **polymer**, solubility of the **polymer** in the **monomer**, variation in the powder composition or bead size distribution, and the temperature of the cement components.⁽⁴⁾ Pre-chilling the cement components reduces the viscosity of some cement formulations.^(4,7)

Acrylic cements on the market are divided according to their viscosity into low, medium, and high viscosity cements. In Table I-2 are summarized the handling characteristics of these three cement categories.

In vitro determination of viscosity is usually accomplished with the use of a capillary extrusion or rotational (plate and cone) rheometer.⁽⁵⁾

Table I-2 Handling characteristics of low, medium and, high viscosity cements.

Cement Type Handling properties	Low viscosity(LV)	Medium viscosity (MV)	High viscosity(HV)
Mixing phase	-Long lasting liquid phase. -Low viscosity wetting phase. -The dough Remains sticky for 3 mn.	-Low viscosity wetting phase. -The dough is no longer sticky after 3 mn at the latest.	-Short wetting phase. -Quickly lose of their stickiness.
Working phase	-Quickly increase of viscosity. The dough becomes warm fast. Short working phase 1-2 min	-Slow and continuous invariance increase of viscosity	-Unchanged viscosity -Slow increase toward the end of this phase. -Long working phase.
Hardening phase	Time period 1-2 mn	Time period 1.5-2.5 mn	Time period 1.5-2 mn

I.2.6 Porosity

The structure of bone cement is porous on both the macroscopic and microscopic scales (see Figure I.11). Thus, there are two types of pores in fully polymerized cement: macropores (pore diameter >1mm) and micro pores (pore diameter \approx 0.1-1mm).⁽³²⁾

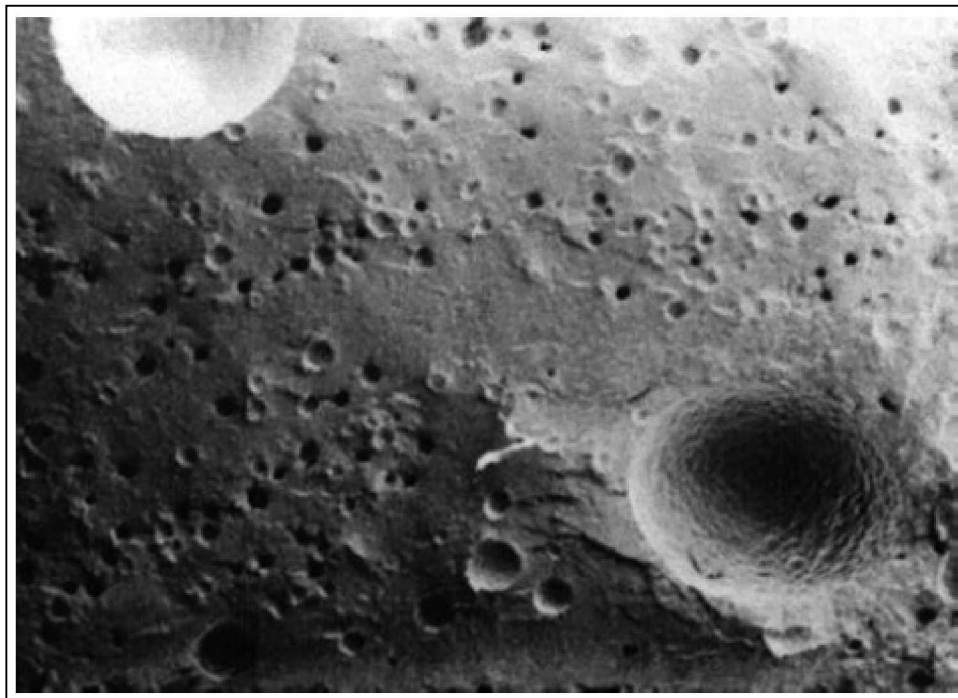


Figure I.11 Porosity of bone cement.⁽³³⁾

Porosity in the cement occurs due to air initially present in the liquid **monomer** and

powder **polymer** constituents,^(2,4,34,35,36) incorporation of air during wetting and mixing of the components,^(1,2,4,17,34,35,36) entrapment of residual **monomer** during **polymerization**^(2,4,17,34,35,36) (evaporation of the volatile **monomer**), entrapment of air during the dough transfer,^(4,34,35,36) and introduction of blood or tissue into the cement during implantation.^(1,2)

Porosity of the cement can be influenced by the mixing method (see Sect. I.2.6.1). Relative to hand mixing, centrifugation or vacuum mixing are methods of pore reduction. The pre-cooling of the **monomer**, **polymer** and mixing vessels lead to a significant reduction of the number and the volume of pores.⁽²⁾ Another source of micro-porosity in PMMA bone cement is the inclusion of radiopacifiers,⁽³⁷⁾ BaSO₄ or ZrO₂. These particles do not adhere to newly polymerized PMMA matrix, but they are contained in small cavities that behaves as small pores (0.1-30µm), occupying up to about 6% of the cement volume.⁽³⁸⁾ Pressurization of the implanted doughy cement (delivery system) has also been proposed as means to reduce porosity.^(4,5)

The presence of pores in the fully polymerized material may have a detrimental and a beneficial effect on the stability of the implant, and hence, on the artificial joint life. Pores would act as stress risers and crack nucleation sites for micro cracks, leading to early cement failure. However they may also act as crack decelerators.^(39,40) Thereby, prolonging the life of the implant. The current consensus is that every effort should be made to substantially reduce the number and size of both macro and micro-pores in order to improve the mechanical properties of the acrylic cements.

Apparent density measurements,⁽³⁵⁾ use of a high powered optical or metallurgical microscope with incident light,⁽⁴¹⁾ comparison of radiographs of the specimen with that of a standard metal plate containing holes of 1 to 10 mm in diameter, and use of a computerized image analysis system^(42,43) are the usual methods for the in vitro determination of porosity.

I.2.6.1 Cement mixing methods

Mixing method has an important role in determining the mechanical properties of acrylic cements. There are four (4) cement-mixing methods: manual or hand mixing, centrifugation, vacuum mixing and, combined mechanical mixing.

In manual mixing, the powder component is added to the liquid in a polymeric bowl (see Figure below) and manually stirred with a polypropylene spatula at 1 Hz or 2 Hz (not grater than 2 Hz in order not to beat air into the mixture)^(2,44) for a period of time between 45 and 120 s.



Figure I.12 Bowl and spatula for hand mixing.⁽⁴⁵⁾

In *centrifugation mixing*, the hand mixed mass is immediately poured into a syringe that is then promptly placed in a centrifuge at 2300-4000 rpm for a period of time between 30 and 180 s.⁽⁴²⁾ Centrifugation is a method of pore reduction compared to hand mixing. The extent of such reduction depends on the storage temperature of the liquid **monomer** prior to mixing.⁽⁵⁾

For *vacuum mixing*, a number of proprietary (Simplex Enhancement Mixer, Stryker High Vacuum System, MITAB, Optivac, Stryker MixevacII, Sterivac, Mitvac, Cemvac Merck, Bonelock and Cemex Systems) and experimental chambers^(35,36) have been used. Each chamber or proprietary has its own steps to follow. Depending on the chamber (or proprietary) used, vacuum is applied and the cement components are mixed at reduced pressure to obtain the dough. Compared to hand mixing, considerable reduction in porosity (micro-porosity) was observed for vacuum mixing.

A number of combined mixing devices have been used: hand mixing in stainless bowl on vibrating plate (50 vibrations/s)⁽⁴⁶⁾, a motor coupled to eccentric unit that creates the action of vibration (motion in two directions), in which a cement holder is fixed, the motor is typically run at 500 rpm for 120 s during the mixing of the constituents,⁽⁴⁷⁾ and a proprietary machine called the Universal Mixing Machine that simultaneously mixes and centrifuges the cement constituents for typically 12 s.⁽⁴⁸⁾

Other emergent techniques for mixing exist also, based on a combination between ultrasonic cleaner and vibration after hand mixing,⁽⁴⁹⁾ pressurization under vacuum mixing.⁽⁵⁰⁾

One new combined mixing method proposed by Lewis consists of the application of a passive vacuum to the cement constituents followed by their simultaneous mechanical mixing and centrifugation. This technique leads to cement with excellent physical and mechanical properties.

The usual procedure after mixing is to inject immediately the cement dough into a cartridge or tube. The dough is usually pressurized with a cement gun into the bone cavity.^(4,5)

Cemex System is instead the unique device being a mixing and delivering system at a time: powder and liquid are pre-dosed and contained in a syringe like container⁽⁴⁾ (see Figure below).



Figure I.13 Cemex system: a mixing and delivering system at a time.⁽⁴⁵⁾

I.2.7 Molecular weight

When powder **polymer** and liquid **monomer** are mixed, macromolecules that have a variable number of linked **monomers** will be created. Therefore, different molecular weights co exist in the solidified product.^(2,51) It is assumed that **monomer** dissolves the smaller particles of the powder (<20µm) forming thus, the interbead matrix and partially dissolves the surface of the bigger particles (pre-polymerized beads) which are thus completely incorporated in the cured cement.⁽⁵²⁾

Gel permeation chromatography (GPC) is used to determine the molecular weight (Mw) of the two **polymer** phases (**polymer** powder and cured cement).^(26,33,52)

The typical distribution of the molecular weights of the various macromolecules that form a polymeric product is similar to the shape of a ball, whose width is tied to the distribution of the molecular weight (see Figure I.14)

The values of the average molecular weights can be defined as follows:

1-The average numerical molecular weight (Mn), expresses the average according to the number of the macromolecules present. This parameter is of a highly interest in the study of reaction mechanisms.

$$\overline{M}_n = \frac{\sum N_i M_i}{\sum N_i} \quad (\text{I-1})$$

Where,

M_i is the mass of the nth macromolecule present and N_i is the nth macromolecule present.

2-The average ponderal molecular weight (Mw) expresses the average according to the mass of the macromolecules present, which is connected to the mechanical characteristics and processability of the material.

$$\overline{M}_w = \frac{\sum N_i M_i^2}{\sum N_i M_i} \quad (\text{I-2})$$

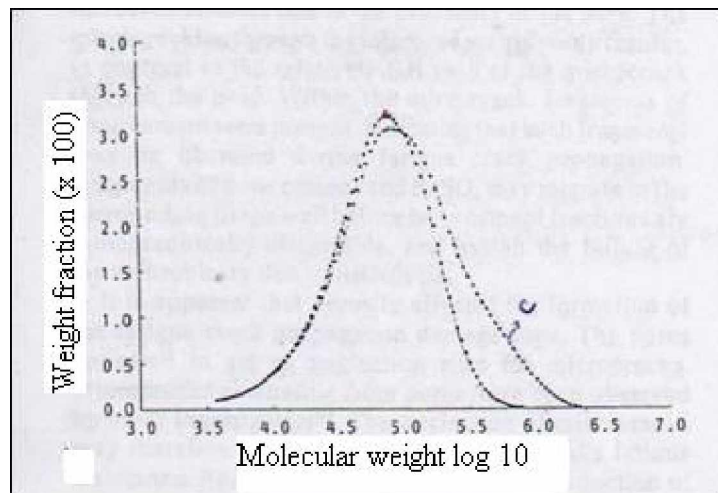


Figure I.14 The typical distribution of the molecular weights of bone cements.⁽³⁹⁾

Bone cement like any implantable biomaterial must be sterilized before its introduction into the body. It's well known that ethylene oxide gas (EtO) or gamma irradiation is used to

sterilize the powder constituents, whereas the liquid **monomer** typically is sterilized by membrane filtration.⁽³³⁾

The structure of **polymers** seems to be affected by sterilization techniques.⁽⁵³⁾ When irradiated, PMMA undergoes chain scission leading to a reduction in its molecular weight.^(33,53,54,55) Large decreases in molecular weight of the PMMA powder were observed with increasing gamma irradiation dose.⁽³³⁾ However, fumigation with ethylene oxide has no influence on the molecular weight of the cement.^(33,54,56) Additionally, the molecular weight of the PMMA can further decrease over time during in vivo use.⁽⁵⁷⁾

The molecular weight influences the swelling properties, the mechanical properties and the working phases of the different cements.

I.2.8 Glass transition temperature

On heating, PMMA bone cements change their state from glass-like and brittle to elastic at glass transition temperature (T_g), the material starts to soften and the Brownian motions cease.⁽²⁾ These micro-movements influence the thermal expansion coefficient, the bending modulus and mechanical and electric absorption of the material (Material's parameters).⁽²⁾

Recently, T_g is used as characteristic of bone cements (Thanner et al 1995).⁽²⁾ Several methods can be used to determine the glass transition temperature: torsional fatigue testing, shear modulus determination and the dilatometric method DSC (see Figure I.15)

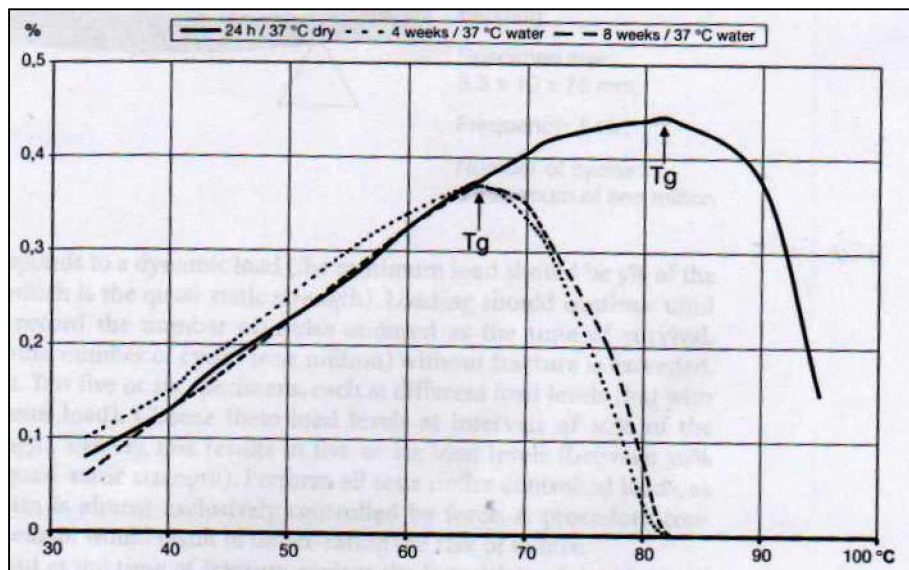


Figure I.15 Determination of the glass transition temperature using the dilatometric method.⁽²⁾

Glass transition temperature depends on the molecular weight, water content and the molecular structure of the monomer used (hydrophilic/hydrophobic behaviour).

Experiments reveal⁽²⁾ that there is no change in temperature when bone cements (samples) are stored in dry environment, a continuous decrease in temperature can be registered when stored in water at 37°C. However, there are no further changes, when the samples are water-saturated.

Bone cements are always in a humid environment at 37°C after implantation and become saturated with water after only a few weeks, thus, cements with T_g 's of 40-50°C (dry specimens) could lead to disastrous clinical results.⁽²⁾

According to Kühn,⁽²⁾ Cemex cement and simples P present a relatively high Tgs in dry environment and remain above body temperature (~70°C) after 8 weeks of storage in water at 37°C.

Another transition temperature reported by various authors is beta β transition. This last is related to the rotation of the bonds in the cement molecule.^(58,59)

Summary

This chapter allows us to retain the following points:

- Polymethylmethacrylate (PMMA) widely known since 1930 was used for the first time, in 1958 as a fixation agent of a femoral implant, by Sir John Charnley, who named it bone cement on acrylic basis.
- In reality, acrylic bone cements were used in various medical fields such as dentistry, cranioplasties, plastic surgery, orthopaedic surgery, etc.
- Acrylic bone cement, so-called two-components system is commonly prepared by mixing a solid part made of a pre-polymerized poly methyl methacrylate (PMMA), benzoyl peroxide (BPO) as an initiator, and radio-pacifiers, with a liquid part containing methyl methacrylate (MMA), N, N-dimethyl-p-toluidine as an accelerator and inhibitor. Each cement manufacturer recommends a specific **monomer** to **polymer** ratio, expressed as grams per milliliter.
- Bone cement is formed from an exothermic reaction of benzoyl peroxide initiator present in Polymethylmethacrylate (PMMA) powder and N,N-dimethyl-p-toluidine in methylmethacrylate **monomer** liquid transforming after few minutes (10 to 15 mn), the MMA multi-molecular liquid system into a solid PMMA macro-molecular one.
- Negative effects of PMMA bone cement have been attributed to its high temperature reached during **polymerization**, **monomer** release to the surrounding tissues, and volumetric shrinkage.
- For a long time, the maximum temperature reached during the hardening phase of PMMA cements was known to cause tissue necrosis and hinder the efficacy of joint prostheses. In real conditions (In vivo), there are several factors that contribute to dissipate the heat produced, including the thin layer of cement (3-5 mm), the blood circulation, heat dissipation in the vital tissue connected with the cement, and heat dissipation of the system attained via the prosthesis.
- The proportion of non converted residual **monomer** remaining in the hardened cement is in the range of 2-6%. Within 2 to 3 weeks, this rate falls to 0.5 %, due to a slowly progressing, continuous **polymerization**. The main part of the eluted **monomer** quickly passes into blood stream and disappears just as quickly.
- Volumetric shrinkage (Material contract of approximately 2-4 %) of the cement is not disadvantageous since, its contraction at the cement bone interface will favor the building of new bone. Moreover, the shrinkage of the material will be compensated, in vivo, by its dilatation due to a slightly absorbent characteristic.
- Viscosity is a physical parameter, which characterizes a material's resistance to flow. Acrylic cements on the market are divided according to their viscosity into low, medium, and high viscosity cements. In the operating theater, the cement viscosity must be low enough (not too low) to make it very easy to force the dough through the delivery system (syringe) and cause it to flow and penetrate into the interstices of the spongy bone, under any given pressure, in a very short time. Therefore, cement viscosity is an important material property in determining the proper handling characteristics.
- The structure of bone cement is porous on both the macroscopic and microscopic scales. In general, pores are referred to as micropores or as macropores, depending on whether their maximum dimension is smaller or larger than 1 mm. Pores in the cement arise from different causes. These include the evaporation of the liquid **monomer** during curing, entrapment of air during mixing and mixture application, inclusion of radiopacifiers, interoperative bleeding, bone preparation, and cement implantation technique. There are four

(4) cement-mixing methods: manual or hand mixing, centrifugation, vacuum mixing and, combined mechanical mixing. Relative to hand mixing, centrifugation, or vacuum are methods of pore reduction.

- As with any implantable biomaterial, acrylic cement must be sterilized before its introduction into the body. Sterilization methods have been shown to affect molecular weight. Large decreases in molecular weight of the PMMA powder were observed with increasing gamma irradiation dose. However, fumigation with ethylene oxide has no influence on the molecular weight of the cement. Additionally, the molecular weight of the PMMA can further decrease over time during in vivo use.

- On heating, PMMA bone cements change their state from glass-like and brittle to elastic at glass transition temperature (T_g). Glass transition temperature depends on the molecular weight, water content and the molecular structure of the **monomer** used (hydrophilic/hydrophobic behaviour).

MECHANICAL PROPERTIES OF ACRYLIC BONE CEMENTS

Chapter

II

It is believed that mechanical failure of the bone cement layer is the cause of aseptic loosening. For this reason it is necessary to know the mechanical properties of bone cements.

II.1 Introduction

Bone cements, as aforementioned by many authors, are used for the fixation of artificial joints. When used in **total hip Arthroplasty**, PMMA fill the free space between the metallic component and the predetermined bone site. This technique allows a stable fixation of the prosthesis to the bone.^(2,60,61) The interaction between the cement and the adjacent bone tissue and between the cement and the prosthesis is only mechanical.^(2,62,63) The main task of PMMA is to transfer complex, varying physiological loads from the prosthesis to the bone.^(1,2,5,33,64)

The in vivo integrity and performance of bone cement are necessary for longevity of the prosthetic system.^(2,60) Indeed, if the external **stress** factors are superior to the ability of the cement to transfer the force, a break will result. PMMA fragments thus formed could trigger phenomena of peri-prosthetic osteolysis and lead to the mobilisation and even failure of the prosthesis.^(60,65) However, the state of **stress** in the cement mantle is influenced by many factors, tied on the thickness of the cement layer, structure of the cement (distribution and dimension of the pores),⁽¹⁾ the shape of the metallic implant and materials that constitute it, and the bond conditions of the prosthesis.

It is believed that mechanical failure of the bone cement layer at any or all of the weak link zones (the implant-cement interface, the cement mantle, and the cement-bone interface) is the cause of aseptic loosening.^(66,67) For this reason it is necessary to test the mechanical properties of bone cements under standard conditions. Numerous studies have focused on improving the static and dynamic properties of bone cement in order to maximise its resistance to applied **stress**.

The American Society for Testing and Materials (ASTM-F451) and the International Standards Organization (ISO 5833) have fixed minimum values for the critical properties (Table II-1), these standards are limited as they cover some mechanical properties in compression and bending.^(2,3)

Table II-1 ISO Critical values for mechanical properties of bone cements.^(2,65)

Compression strength (MPa)	Bending strength (MPa)	Elastic or Bending modulus (MPa)
>70	>50	>1800

Compressive strength was the first mechanical criterion implemented by American society for testing and Materials standards (ASTM) in the USA in 1978.⁽²⁾ All surgical grades PMMA must fulfil these minimum requirements.

Several data on the mechanical properties of bone cements can be found in literature. However, there is no consensus on any unique value for any of the mechanical properties due to the different kind of cements and many trial techniques and conditions that have been used.⁽¹⁾

Mechanical property determinations can be performed at different times after polymerization, or specimens can be stored for various time periods (some as long as two years)⁽¹⁾ in air, de-ionized water, distilled water or physiological solutions (Isotonic saline, or serum) at room temperature or at elevated physiological body temperature.^(2,5) However, complex storage conditions and long storage times are prohibitive for most studies.⁽¹⁾ ASTM and ISO standards recommend storage in air or distilled water at 37°C for periods of 1 to 7 days for most mechanical property testing of Acrylic bone cement.⁽²⁾

The manner in which the cement is prepared, handled and chemically composed affects its

mechanical properties.^(1,59) Temperature and loading rate at the time of testing, also affect the measured mechanical properties.⁽¹⁾

PMMA bone cement fails during in vivo use at **stress** levels far below the critical values seen in their static tests (Table II-1). In reality, the cement mantle is subjected to cyclical loads (repeated loads) and the fatigue phenomena appear to be the cause of mechanical failure of the PMMA mantle.^(1,5,60,62,68,69) Failure of the cement most commonly occurs by the growth of fatigue cracks until a critical size when unstable propagation of the crack occurs and cement fractures.

Mechanical fatigue testing can be conducted as **tensile**, **compressive** or bending tests.⁽²⁾ Unfortunately, mechanical fatigue testing on bone cement is not currently regulated by any international standard.⁽⁶⁵⁾

II.2 Quasi-static properties

II.2.1 Tensile properties

In clinical service the **hip implant** is subjected to static or quasi-static **tensile** forces during daily activities.^(5,65) In vitro determination of the quasi-static **tensile** properties involves the use of a dog-bone specimen, as exhibited in Figure II.1, at a cross-head displacement speed ranging from 5-30.5 mm/min.^(49,70) The same experiments were also carried out with a cross head speed of 1 mm/min according to ISO 527 standard.⁽¹⁰⁾

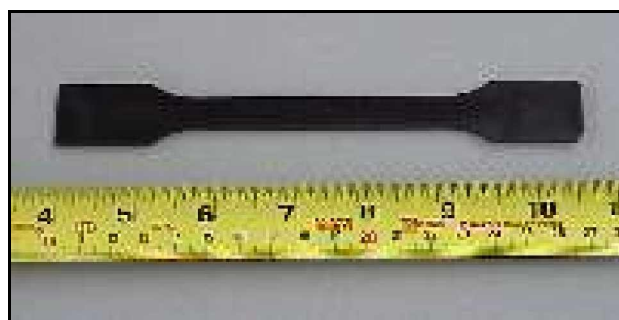


Figure II.1 A dog bone specimen used in tensile tests.

The values of the ultimate **tensile** (UTS), **tensile modulus of elasticity** (E_t) and **tensile strain** at the fracture point (ϵ_{\max}) are determined from the applied load versus elongation curve that is fully linear, since cement is brittle or quasi-brittle material.⁽⁵⁾ Davis et al.⁽⁷²⁾ in their study, found no significant difference in **tensile** strengths of three types of bone cements; Simplex P, LVC and Zimmer Regular bone cement.

A number of studies^(10,14,15,44,71) have shown that the addition of Barium Sulphate (BaSO_4) decreases significantly **tensile** strength, which, however, is not observed when Zirconium dioxide (ZrO_2) is added. These inorganic fillers interrupt the polymerizing matrix and produce pores that act as fracture initiation sites, in the case of BaSO_4 , diminishing cement **tensile** strength. The cauliflower like morphology of ZrO_2 particles allowed for mechanical anchorage, which could avoid the decrease in the **tensile** strength.⁽¹⁰⁾ Pascual et al.⁽²⁷⁾ considered that the quasi-static **tensile** properties couldn't be affected by the powder size distribution, however, the **tensile** strength and the **tensile strain** of the test specimens were higher for formulations with lower DMPT content.

All commercially available cement requires mixing powder and liquid. The mixing methods have a large impact on the **tensile** properties, in fact, vacuum or centrifugation

mixing lead to a mean of 44% increase in UTS relative to hand mixing. Typical values of maximum **tensile stress** are between 24 MPa and 49 MPa.⁽⁵⁾

II.2.2 Compressive properties

The **hip implant** is subjected to static or quasi-static direct **compressive** forces, during certain daily activities, for example, in the one legged stance.^(5,73) Additionally, in **hip Arthroplasties**, the cement mantle may act as a **compressive** wedge between the femoral stem and the bone tube.^(74,75) Therefore, compression tests should be justified. In vitro determination of **compressive** properties has been carried out according to the ASTM-F451 or ISO 5833 standards for acrylic bone cements.^(2,5,10,65,71) Compression trials, are performed on cylindrical samples of 6 mm in diameter and 12 mm in height (see Figure below) at a cross-head speed of 20^(2,5,10,65) or 25.4^(5,73) mm/min.

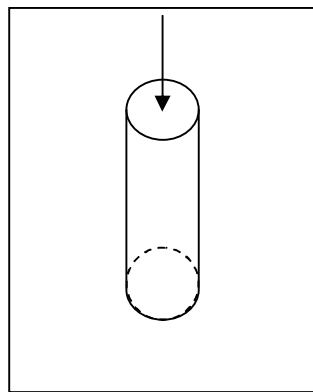


Figure II.2 Compressive test specimen.

The ultimate **compressive** strength (UCS) and **compressive** modulus (E_c) should be estimated from the **stress-deformation** curve shown in Figure II.3. The slope of the first part of the curve characterises the stiffness of the material (E-modulus) and the maximum of the curve (**yield point**) defines the stress and **strain** beyond which the material will deform plastically. The ultimate **compressive strain** (e_{maxc}) is obtained as the **strain** at the UCS point. The “2% offset” method is used to obtain the ultimate **compressive** strength and the ultimate **compressive strain** (e_{maxc}).

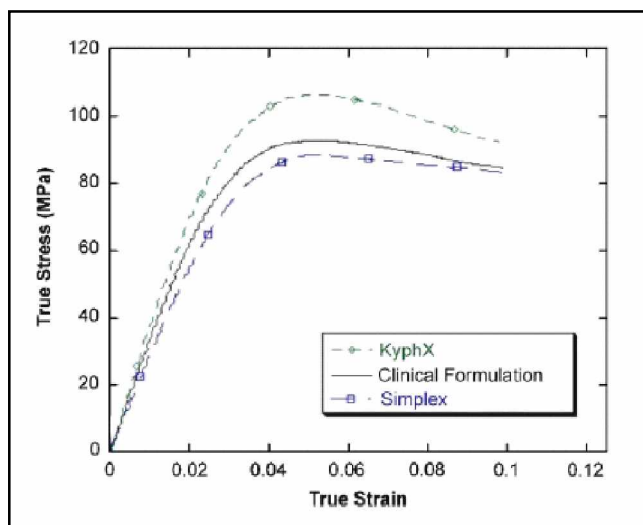


Figure II.3 Compressive strain curve.⁽⁷⁶⁾

For a given mixing method, the formulation exerts a profound effect on the quasi-static **compressive** properties (see Figure II.4).

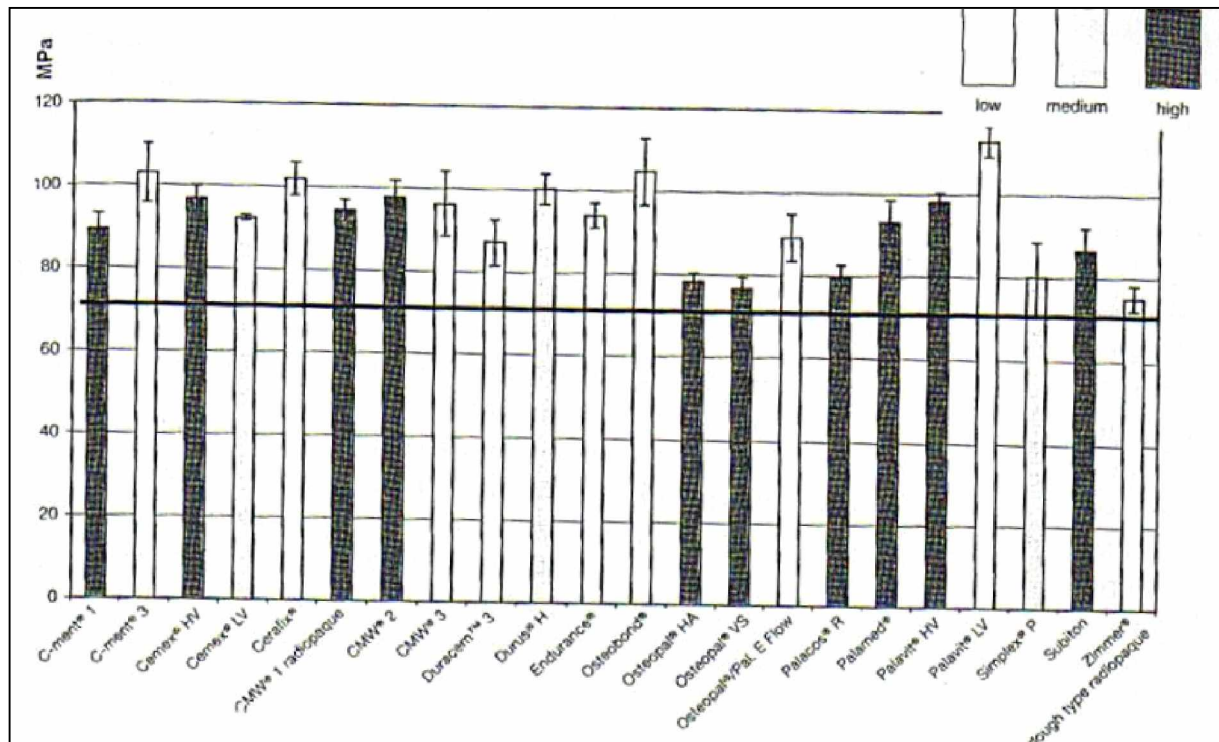


Figure II.4 Compressive strength of plain bone cements, according to ISO 5833 standards.⁽²⁾

The addition of inorganic fillers to PMMA bone cement has been shown to reduce quasi-static **compressive** strength,^(15,77) because they could act as flaw sources.⁽⁴⁴⁾ **Compressive** strength and elastic moduli seem to be poorly affected by the size of PMMA particles.⁽¹⁷⁾ Lautenschlager et al.⁽⁷⁸⁾ showed that Simplex P loaded with Gentamicyn led the **compressive** strength to drop below 70 MPa. The same result was observed for Simplex P loaded with a mixture of Meropenem and Vancomycin.⁽⁶⁵⁾ Some authors^(65,79,80) reported that **compressive** strength of PMMA bone cements decreased with increasing dosages of antibiotic.

The **compressive** strength of PMMA bone cement has shown a slight increase in the first three months after mixing and fairly constant values after that.^(44,81) The test parameters are of decisive importance, in fact, increases in **strain** rates result in quasi-static property increases⁽⁵⁹⁾ (**modulus of elasticity** and **ultimate strength**) due to the viscoelastic nature of PMMA.

Concerning mixing methods, Trieu et al.⁽⁴⁸⁾ reported that for Simplex P, there was no statistically significant difference between (UCS) and (E_c) of hand mixing (HM) and simultaneous mechanical mixing and centrifugation (MEC) specimens. These findings are in contrast, with the results obtained by Lewis⁽⁷³⁾ for CMW-3 Cement. In addition, Trieu et al.⁽⁴⁸⁾ found in their study that (UCS) and (E_c) were significantly lower for (MEC) specimens when compared to vacuum mixing, however, these differences were not significant in Lewis' investigation.⁽⁷³⁾

II.2.3 Flexural properties

Flexural properties are related to the life of the arthroplasty because during in vivo loading

of the artificial joint, a combination of **shear**, tension and compression **stresses** are found and therefore the study of bending tests are justified.⁽⁵⁾

In vitro determination of flexural properties of bone cements (flexural strength and modulus) has been performed in accordance with the ASTM-790⁽⁸²⁾ or ISO 5833 standards. The flat samples used in the ISO bending strength tests (see Figure below) have to be immersed for 50 ± 2 h in water or Ringer solution at $37 \pm 1^\circ\text{C}$ ^(2,65) to simulate physiological conditions. According to ISO 5833, bending trials are performed at a cross head speed of 5 mm/min.

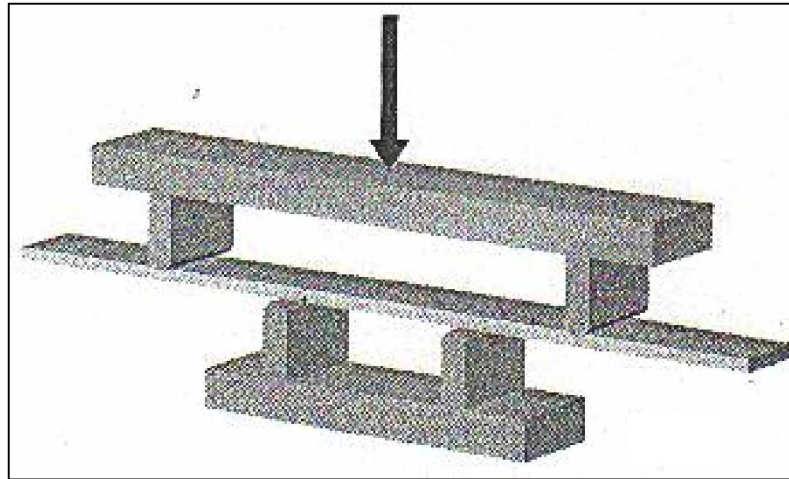


Figure II.5 Bending trials on a flat sample using a four-point test bench.⁽⁶⁵⁾

The flexural strength value is obtained from the follow relation:

$$F_s [MPa] = \frac{3Fa}{bh^2} \quad (\text{II-1})$$

Where

F [N] is the applied force;

b [mm] is the average width measured for the sample;

h [mm] is the average thickness measured for the sample;

a [mm] is the distance between the two force application points on the sample on the testing device.

The **modulus of elasticity** known as the flexural modulus (E_b) is a measure of the stiffness of a material. The higher the modulus, the less the material is deformed.⁽²⁾ The bending elastic modulus is also calculated, using the follow formulation:

$$E_b [MPa] = \frac{\Delta F \cdot a}{4fbh^3} \quad (\text{II-2})$$

Where

f is the difference between the arrow values corresponding to the loads 15 N and 50 N;

$\Delta F = 35\text{N}$ is the interval of variation of the load applied between the two points of evaluation of the arrow f .

The values of flexural strength (F_s) and flexural modulus (E_b) are influenced by the usual

variables: cement formulation, mixing method, and curing and aging conditions.^(1,2,5) The values of bending strength and elastic modulus of the most common commercial bone cements (according to ISO standards) are given in Table II-2.

Table II-2 ISO test values of flexural properties of the most commercial bone cements.⁽⁶⁵⁾

Cement Types	Bending Strength (MPa)	Elastic Modulus(MPa)
Palacos R	66±2	2912±315
CMW-3	59±4	2698±239
Cemex System	58±4	3223±360
Cemex Rx	61±4	2956±196
Cemex Isoplastic	59±9	3029±179
Simplex P	77±3	2679±39

It has been shown^(15,83) that the addition of BaSO₄ to PMMA bone cement causes a reduction in its flexural strength. Numerous studies on the effect of adding antibiotics to bone cements assert that loaded cements show a reduction in their flexural properties.^(65,78,84,85) Askew et al.⁽⁸⁵⁾ demonstrated in their investigation that mixing the cement under vacuum up to 700 mmHg increased the flexural properties of the cement by reducing its porosity. However, these properties show a positive but a weak **strain** rate dependency.⁽⁸⁶⁾

Short Storage times, less than 60 days, in water in the same manner, probably do not affect the mechanical properties of acrylic bone cement since the absorption of water by PMMA cement is very slow as it is hydrophobic.^(2,87) According to Kühn,⁽²⁾ the bending strength was found to be not affected by the environment storage (dry for 16h or wet for 50h), whereas, the flexural modulus depend on.

Finally, various studies in literature,⁽⁵⁾ have been performed on the flexural properties of acrylic cement using different specimen sizes ranging from 5×6×50 mm to 10×10×110 mm, support spans (25.4 or 50.0 mm), loading rates ranging from 0.033 to 7.6 mm/s, and loading types (3-point or 4-point).

II.2.2.4 Shear properties

During certain normal daily activities, the three weak link zones are subjected to **shear** forces.^(5,88,89,90) Thus **shear** properties of the cement are relevant to the life of the implant. Lewis in his art review⁽⁵⁾ cited only two reports^(47,91) of the in vitro determination of the ultimate **shear** strength (USS) of bone cements, while, numerous papers of **shear** properties of bone cement interface and cement stem interface exist in literature.^(88,89,90,92) In one study⁽⁹¹⁾ the acrylic specimens were rectangular in cross section, measuring 55×51×6,5 mm; in the other study⁽⁴⁷⁾ they were circular measuring 9 mm in diameter and 24 mm in length. Two different loading rates were used in these studies^(47,91) 1.3 and 0.18 mm/min.

The load versus displacement response for the bone cement experienced a linear response followed by yielding and an exponential type decay to complete failure.

The values of USS are affected by cement formulation, mixing method, and curing and aging conditions as shown in table II-3. The addition of BaSO₄ to PMMA bone cement has been shown to reduce its quasi static **shear** strength.^(83,93) This latter was found to decrease in loaded bone cements.⁽⁷⁸⁾

Shear strength of PMMA bone cement shows a positive but weak strain rate dependency.⁽⁸⁶⁾

Table II-3 USS data for most commercial bone cements cited by Lewis.⁽⁵⁾

Formulation	Mixing Details	Curing, Aging, And Test Environment Conditions	Shear Strength (Mpa) From		Reference
			Double Shear Test	D732	
Simplex P	Manual; per manufacturer's instructions	Cure time of 24-48h	42.7	-	Linden
	Mechanical mixer(vibration/shaker);500 rpm for 120s	Cure time of 24-48h	48.4		Linden
	Manual; 1 storke/s	Aged in 37°C water for at least 24h; Tested in37°C water	-	37.0	Kindt-Larsen et al.
	CC stored at 5°C prior to vacuum mixing; 20 kPa(absolute)	Aged in 37°C water for at least 24h; Tested in37°C water	-	69.0	Kindt-Larsen et al.
Zimmer LVC	Manual; per manufacturer's instructions	Cure time of 24-48h	48.7	-	Linden
	Mechanical mixer(vibration/shaker);500 rpm for 120s	Cure time of 24-48h	50.2	-	Linden
	CC stored at 5°C prior to manual mixing; 1storke/s	Aged in 37°C water for at least 24h; Tested in37°C water	-	33.0	Kindt-Larsen et al.
	CC stored at 5°C prior to vacuum mixing; 20 kPa(absolute)	Aged in 37°C water for at least 24h; Tested in37°C water	-	62.0	Kindt-Larsen et al.
Palacos R	CC stored at 5°C prior to manual mixing; 1storke/s	Aged in 37°C water for at least 24h; Tested in37°C water		33.0	Kindt-Larsen et al.
	CC stored at 5°C prior to vacuum mixing; 20 kPa(absolute)	Aged in 37°C water for at least 24h; Tested in37°C water	-	50.0	Kindt-Larsen et al.
CMW TM -1	CC stored at 5°C prior to manual mixing; 1storke/s	Aged in 37°C water for at least 24h; Tested in37°C water	-	32.0	Kindt-Larsen et al.
	CC stored at 5°C prior to vacuum mixing; 20 kPa(absolute)	Aged in 37°C water for at least 24h; Tested in37°C water	-	63.0	Kindt-Larsen et al.

CC: Cement components

II.3 Dynamic proprieties

II.3.1 Fracture Toughness

During normal daily activities, a cemented femoral implant is stressed cyclically by physiological loads of up to five times body weight.^(1,5,94,95) Additionally, bone cement used in **hip implants** contains discontinuities such as voids, flaws or other **stress** concentrations, resulting from porosity and irregular PMMA bone interface.^(37,96) This combination of features is well known to make the cement vulnerable to fracture, thus threatening the life of the prosthesis. Indeed, numerous studies have reported that failure of the femoral arthroplastic components is mediated by extensive fractures in the cement mantle.^(44,97,98) Initiation of such cracking is generally thought to begin with debonding of the bone cement from the metal prosthesis⁽⁶⁶⁾ and /or from voids associated with porosity either in the cement mantle⁽⁹⁹⁾ or at the biomaterial interfaces.⁽¹⁰⁰⁾ Under applied physiological loads, catastrophic failure of PMMA bone cement will inevitably result in failure of the entire cemented implant which is complicated by a complex biological response of the bone (PMMA debris realised from micro-cracking can trigger a localized immune response that leads to **bone resorption**⁽¹⁰¹⁾) leading to aseptic loosening.^(63,64,66,101,103)

Accordingly, the fracture property of the fully polymerized cement is very important. Fracture mechanics approach has been widely adopted as the appropriate way of characterizing mechanical behaviour of the cement mantle.⁽⁵⁹⁾ The fracture mechanics analysis⁽¹⁾ takes into consideration three variables, namely applied **stress**, flaw size and a material property related to the resistance of the material to the propagation of the flaw. There are two approaches to the identification of this material property: the energy approach and the **stress** intensity approach.

According to the energy approach, the crack extension occurs when the energy available for crack growth is adequate to overcome the resistance of the material to the creation of new surface. For an infinite plate (see Figure II.6) made of a linear elastic material with a through the thickness crack of length $2a$ and subjected to a **tensile stress** σ , the energy release rate, G , which is the rate of change of potential energy with increasing crack area is defined as follows:

$$G = \frac{\sigma^2 \times \pi \times a}{E} \quad (\text{II-3})$$

Where

σ is the applied **stress**;
 a is half the crack length;
 E is young's modulus.

As the applied **stress** or the crack length increase, G , increases, until it reaches a critical value, G_c , when unstable crack occurs.

The **stress** intensity approach is based on analysis of the **stress** concentration that occurs at the tip of a crack. The analysis depends on the mode of loading and the existence of plane **strain** conditions. For a linear elastic material presenting a sufficient thickness B for plane **strain** conditions, the **stress** concentration at the tip of the crack in Figure II.6 can be described by a Mode I (**tensile** load applied perpendicular to the plane of the crack and its direction of propagation), plane **strain**, **stress** intensity factor given by the follow formulation:

$$K_I = \sigma \sqrt{\pi \times a} \quad (\text{II-4})$$

Where:

σ is the applied **stress**;

a is half the crack length;

K_I is the Mode I **stress intensity factor**.

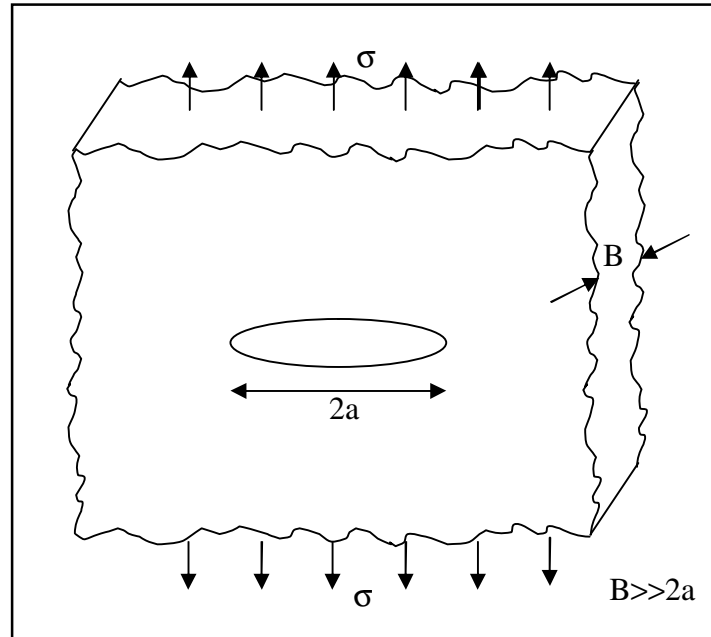


Figure II.6 Infinite plate with a through-the-thickness crack.⁽¹⁾

Similarly, as the applied **stress** or the crack length increase, K_I increases, and when it reaches a critical value, K_{IC} , unstable (catastrophic) crack propagation occurs. This critical value of the Mode I, plane **strain, stress intensity factor** is called the **fracture toughness**, a measure of material's ability to resist catastrophic crack propagation. The material's resistance to the combined effects of **stress** and flaws (known as fracture toughness) depends only on the geometry of the crack,^(1,63,95) not the geometry of the object hosting the crack.

The assumptions⁽¹⁾ in linear elastic fracture mechanics (LEFM) are that the material be linearly elastic and the material fractures in a brittle manner, that is, without plastic deformation prior to crack propagation. Really, real materials, such as PMMA bone cement, rarely behave in such a restricted manner. In order to resolve this problem certain criteria have been established to allow the description of the behaviour of real materials in terms of linear elastic fracture mechanics. The zone of plastic deformation at the crack tip (plastic zone, damage or craze zone) must be very small compared to the thickness and the crack length of the material structure. The applicability of linear elastic fracture mechanics (LEFM) to the study of crack propagation and fracture of PMMA bone cement has been clearly established.^(59,63,64,95,103)

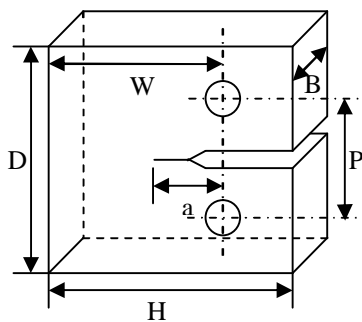
Under clinical conditions, the cement is loaded in Mode I^(5,96) and linear elastic conditions exist, so, the fracture toughness was obtained in vitro as the critical value of the Mode I **stress intensity factor** (K_{IC}) for various cements.

Despite the absence of a standard specific to acrylic resin, two procedures based on the recommendation of two American standards have been used to determine the K_{IC} value of bone cement.^(10,58,59,63,64,103,104,105) The two existent specifications are: the ASTM-E399-90

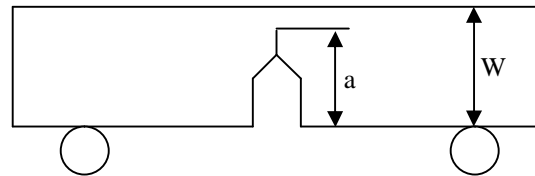
(reapproved in 1997) for metallic materials and the ASTM-D 5045-99 for plastic materials. Guandalini et al.⁽⁹⁵⁾ studied the equivalence of the two testing methods, they found no difference when the same pre-cracking technique was used. While E339 suggested precracking the specimens by applying a cyclic load, in the D5045 the precrack had to be created using a razor blade. The cyclic load precracking technique appeared to be more repeatable than that based on sawing the specimen using a razor blade. This latter must be accurately controlled to ensure any influence on the results. Guandalini et al.⁽⁹⁵⁾ assessed, also, that a sharp tip was at the basis of a correct calculation of the value of fracture toughness.⁽¹⁰⁶⁾ Cayard et al.⁽¹⁰⁷⁾ reported that the use of razor notching in plastics has been shown to yield crack tip radii and crack tip residual **stress** zones that are equivalent to those obtained by fatigue precracking. This result justifies the use of razor blade by many investigators when precracking the specimen according to the ASTM E-399 specification.^(10,33,59,63,64,103,108)

The general testing protocol involves a test specimen with a machined (for ASTM D5045) or fatigue grown crack (for ASTM E-399). The specimen is monotonically loaded in Mode I loading, and the load at the time of initiation of crack propagation is determined. This measured load and crack length known a priori or measured after fracture, are then used to determine the fracture toughness.

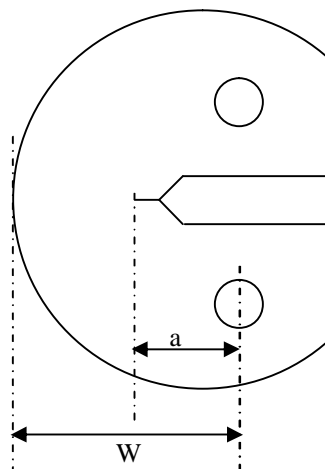
Various specimen configurations and sizes were used in determining the K_{IC} values. Figure II.7 shows the three plate type test specimens currently described in the ASTM E-399 for use in measurement of plane **strain** fracture toughness, K_{IC} .



Compact tension specimen (C(T))



Single Edge Notched bend specimen (SNEB)



Compact Disk Tension specimen CD(T)

Figure II.7 Plate-type specimen shapes used for K_{IC} measurement.

Fracture toughness of non homogenous material, like PMMA, is a function of both material and structure. Porosity seems to have a controversial effect on the fracture properties of bone cement.^(5,33,44,47,63,103,109) In fact, Topoleski and colleagues⁽³⁹⁾ hypothesized that internal pores may enhance the material's fracture toughness by blunting any cracks that propagate through them. Rinnac et al.⁽¹⁰⁹⁾ pointed out that existing cracks and surface imperfections counteract any beneficial stabilizing effects of pores since these existing flaws are substantially larger than the most internal pores in the material. Therefore, reducing the porosity should not have an effect on fracture toughness. Following the same idea, Vila et al.⁽¹⁰³⁾ suggested that the **stress** intensity of the crack tip predominates over the **stress** concentration from porosity. This fact would explain why fracture toughness seems not to be dependent on porosity. Pores have been identified as **stress** risers and crack initiating sites that reduce crack growth resistance.^(33,47,63,110) In fact, a statistically significant inverse relationship between porosity and fracture toughness was found by Ries and colleagues.⁽⁶³⁾ It is clear that internal porosity is reduced greatly by vacuum^(33,46,103,111) or centrifugation⁽¹¹²⁾ mixing techniques. Ries et al.⁽⁶³⁾'s finding agrees with the finding of others^(33,110) showing that vacuum mixing instead of hand mixing leads to improve fracture roughness of several brands of bone cement. Concerning the effect of macro-pores on the fracture toughness of bone cement, the collected data pointed out that pore dimension and location affect the final result.⁽⁹⁵⁾ Indeed, the crack initiates earlier in sharp notch specimens than in round notch specimens. Also, the pores located at 10 mm from the crack tip of the K_{IC} specimen have a negligible effect on the fracture toughness of the material.⁽¹¹³⁾ As a consequence, Guandalini et al.⁽⁹⁵⁾ recommended a K_{IC} specimen criterion rejection based on the presence of macropores on the fracture surface up to 10 mm away from the crack tip.

The effect of the inorganic radiopacifiers on the fracture toughness of the cement depends on their size and morphology. In fact, Genebra et al.⁽¹⁰⁾ reported that the addition of ZrO_2 had a beneficial effect on the fracture toughness due to the mechanical anchorage of the ZrO_2 particles in the polymeric matrix. The information concerning the influence of $BaSO_4$ on the fracture toughness of the cement is somewhat controversial. Whereas some authors report that the addition of $BaSO_4$ improves fracture toughness,^(1,59,114,115) by promoting interaction between the moving crack front and the matrix, "second phase dispersion" others, in contrast, claim that this parameter decreases with the addition of this Radiopacifying agent.⁽¹¹⁶⁾ An other trend, reports that the fracture toughness is not affected by the incorporation of $BaSO_4$.^(10,117)

The presence of non reacted monomer in the acrylic matrix which acts as a plasticizer leads to blunting the crack tip, thus, toughening the material.^(59,118)

Molecular weight, MW, of a polymer is known to directly affect its mechanical properties. Moreover, a decrease in molecular weight of PMMA bone cement can cause degradation in its mechanical properties.^(15,119,120) As aforesaid in sect I.2.7, sterilization methods and physiological aging have been shown to affect PMMA's molecular weight. Thus fracture toughness (a mechanical property) depends on sterilization method.^(33,121) However, Ries et al.⁽⁶³⁾ reported no relationship between fracture toughness and time in vivo of retrieved simplex bone cement. Kim et al.⁽⁵⁶⁾ pointed out that many mechanical properties, especially fracture toughness of PMMA, might be insensitive to MW values over 2×10^5 g/mol. Graham et al.⁽³³⁾ showed markedly reduced changes in fracture toughness of PMMA samples of MW over 1×10^5 g/mol. These findings were confirmed in Ries' paper⁽⁶⁵⁾ with MW tested ranging from 170 000 to 210 000 g/mol. Figure II.8 shows the variation in fracture toughness with molecular weight for different kinds of commercially available bone cement that are mixed under vacuum or centrifuged from Graham et al..⁽³³⁾ A reduction in MW can lead to diminished fracture toughness.

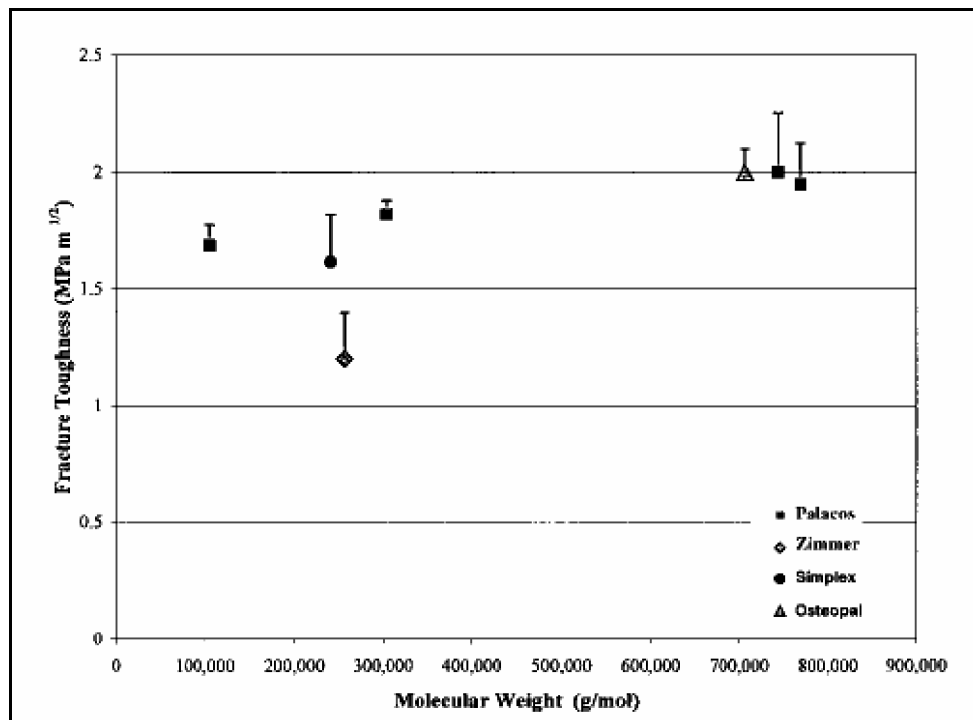


Figure II.8 Effect of molecular weight, MW, on fracture toughness of PMMA bone cement.⁽³³⁾

The effect of molecular weight on fracture toughness according to the theory of defect crazing is believed to involve the formation of defects known as crazes that precede the nucleation of macroscopic cracks in plastics.^(33,56) A decrease in molecular weight or a reduction in the length of the polymer chains limits the chains' ability to bridge the defect and prevent fracture. Once the polymer chain is long enough to bridge the craze, further increases in molecular weight provide little enhancement in fracture properties.^(33,122) This could explain the results obtained by Graham et al.,⁽³³⁾ Kim et al.⁽⁵⁶⁾ and Ries et al.⁽⁶³⁾

Physiological environment affects fracture toughness behaviour of PMMA bone cement.^(1,64,103) Specifically, the PMMA is more resistant to fracture in Ringer's solution (a simulated physiological environment) than in 45% relative air humidity. This increase was attributed to the plasticizing effect of the water intake in the cement.^(64,103,123)

While the ASTM-399 does not fix the cross head rate, the ASTM D-5045 fixes it to 10 mm/min. A variety of loading rates have been used in fracture toughness tests of PMMA bone cement ranging from 0.01 mm/min to 10 mm/min deformation rate. Lewis et al.⁽⁵⁸⁾ demonstrated in tests conducted in air at room temperature that fracture toughness of low and medium viscosity cement increased weakly (5-10%) with loading rate ranging from 0.1 mm/min to 10 mm/min. Whereas this increase was found to be important for high viscosity cement (33%). Another study performed by Vallo et al.⁽⁵⁹⁾ showed that K_{IC} increased with a cross head speed ranging from 0.5 mm/min to 10 mm/min. These effects were attributed to being a consequence of a strongly viscoelastic beta transition near the ambient test temperature.

Most studies in which the fracture toughness of PMMA bone cement with and without added antibiotic have concluded that the antibiotic did not have any statistically significant effect on the fracture toughness.⁽¹⁾ In fact, Rinnac et al.⁽¹⁰⁹⁾ and Wright et al.⁽¹²⁴⁾ found that fracture toughness of Palacos R was increased by up to 4% by the addition of antibiotic. However, Askew et al.⁽¹²⁵⁾ found that the fracture toughness of simplex P was significantly

increased ($P < 0.05$) by the addition of Tobramycin, suggesting that antibiotics added to PMMA based cement may act as toughening agents for cement.

The process of rubber toughening involves addition of a small quantity (around 5-20%) of rubber particles (0.1-2 μm in diameter) as a disperse phase to the matrix of the polymer.⁽¹⁾ It results in a material with a superior fracture resistance, but with expected and observed reduction in the modulus and **tensile** strength of the matrix.^(126,127,128) Indeed, Villa et al.⁽¹⁰³⁾ found that the addition of elastomeric copolymer Acrylonitrile-Butadiene-Styrene (ABS) to a conventional acrylic bone cement matrix reduced significantly the **tensile** and **compressive** strengths and the **tensile** modulus, in contrast, toughened the cement. The mechanisms leading to these observed increases in fracture toughness are not yet completely understood.⁽¹⁾ Most theories are concerned with the role of the added particles in the energy absorption by the composite.^(126,127) The elastomeric particles may act as additional nucleation sites for crazes or microcracks, which extend the damage zone energy absorbing. As they can hinder the craze or microcracks propagation by acting as a barrier to its growth.⁽¹⁰³⁾

Fracture surfaces for conventional bone cement, produced by monotonic loading during fracture toughness testing were even smooth, displaying extensive evidence of PMMA bead cleavage.^(1,59,64,103) Rather, transbead fracture results in a smooth, planar fracture surface with identifiable beads outlined by matrix as depicted in Figure (II.9). Transbead fracture is associated with low energy absorption and lower fracture toughness.

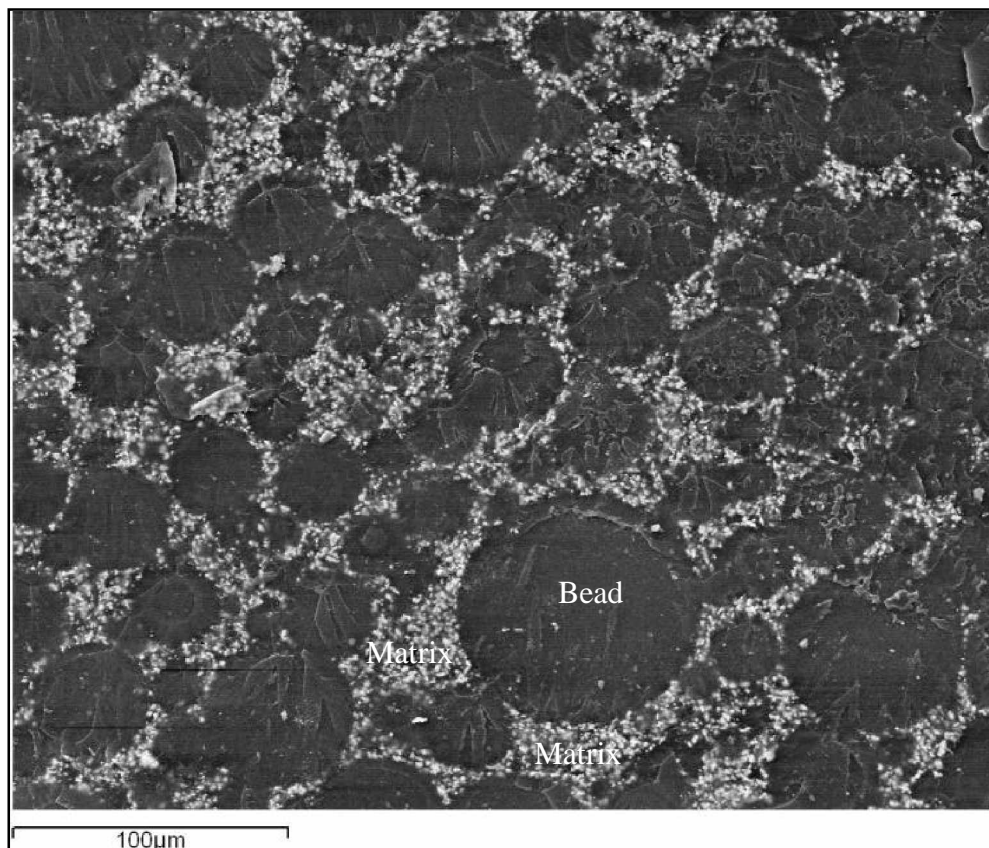


Figure II.9 Fracture surface appearance of “Simplex P” during instable crack propagation.

During toughness testing in Ringer’s solution, the crack cleaves again cleanly through the entire PMMA bead in the bone cement, leaving behind a smooth, almost flat fracture surface. When comparing the fracture surface appearance of the conventional cement in Ringer’s solution with those in air, it seems that some PMMA beads⁽⁶⁴⁾ remain uncleaved during air testing leading to relatively rough surfaces.

The fracture surface appearance of the toughened cements with ABS can be differentiated into smooth and rough regions.⁽¹⁰³⁾ In the smoothest region, the beads are not well differentiated from the matrix since the crack propagates through them. In the rough region the mechanism changes to the ductile tearing of the matrix with decohesion instead of fracture of the PMMA particles. This mechanism is more pronounced as the percent ABS increases.

II.3.2 Fatigue properties

Cyclical loads are the loads which occur during in vivo use due to the repeated actions of body weight and the muscles when subjecting to normal daily activities. Rather, the average person as cited in Ishihara's report⁽⁶²⁾ takes 1 000 000 steps in one year, and therefore in a **hip joint**, of the order of 10^6 fatigue cycles per year are applied to bone cement. Supported by microscopic studies, fatigue phenomena appear to be the cause of more frequent and dangerous mechanical failure for cement mantle itself, since it can lead to loosening and eventually malfunction of the artificial joint.^(5,38,60,62,129,130) So, it is important to understand the fatigue characteristics of bone cement. Two approaches have been used to study the fatigue properties of acrylic bone cements. The first method generally used to evaluate fatigue resistance of bone cements consists in subjecting the cement to a pre-established variable load and then evaluating the number of cycles it can resist without breaking (fatigue lifetimes). The second approach evaluates the speed of propagation of the cracks (da/dN) in the presence of defects (fatigue crack propagation), basing the evaluation on the theory of fracture mechanics.

II.3.2.1 Fatigue resistance “of bone cements”

Unfortunately, mechanical fatigue testing on bone cement is not currently regulated by any international standard and the myriad results available in literature are poorly comparable with each other.^(5,60,65,129) The difficulty in comparison arises from the differences introduced in the methods used when conducting the tests. In particular, the various shapes and sizes allotted for the experiments, the method with which the **stress** is applied, the frequency used, and finally, the various methodologies employed to analyse the trial results, make it difficult to compare the results obtained by different laboratories.^(5,60,129)

Lewis⁽¹²⁹⁾ examined critically the existed papers on the fatigue lifetimes of a large number of acrylic bone cement formulations, over the past three decades. As to that, I've taken his investigation as the main reference in the current section.

Lewis^(5,129) has identified the different types of fatigue test specimen configurations that have been used in literature. The following unnotched test specimen shapes as depicted in Figure (II.10) have been utilized: **tensile** dog bone, with a cylindrical cross-section,^(36,72,111,112,132) rectangular prismatic,^(62,133,134,135) **tensile** dog bone with a rectangular cross section,^(33,50,56,60,70,135,136) and waisted rotating beam.^(123,136) Additionally, various specimen sizes were also used, examples being: flexural test specimens with total volume V_T of 425 mm^3 ,⁽¹³⁵⁾ 2650 mm^3 ,⁽¹³⁸⁾ 4000 mm^3 ,⁽⁵⁰⁾ and 15000 mm^3 ,⁽¹³⁵⁾ and waisted specimens, with gage section volume (V_0) of 196 mm^3 ,⁽¹³²⁾ 224 mm^3 ,⁽¹³⁹⁾ and 438 mm^3 .⁽¹⁴⁰⁾ These different types of fatigue specimens may be obtained by two fabrication methods being molding into a rod or plate and then machining to final dimensions^(62,96,132) and direct molding, in a polymeric or metallic mold, without or with external pressurization, into final dimensions.^(33,55,139,140)

Various types of applied loading have been used, the test specimens were loaded in uniaxial fully reversed tension-compression,^(72,112) uniaxial zero-tension,^(70,139) uniaxial tension-tension,^(36,55,140) alternating 4-point bending,^(134,141) fully reversed bending,^(123,136,142)

3-point flexure,⁽¹⁴³⁾ sinusoidal pulsating loading,⁽¹³⁶⁾ or in a machine in which bending moments are applied by a combination of an eccentric transmission and a spring with a defined elasticity.⁽¹⁴⁴⁾

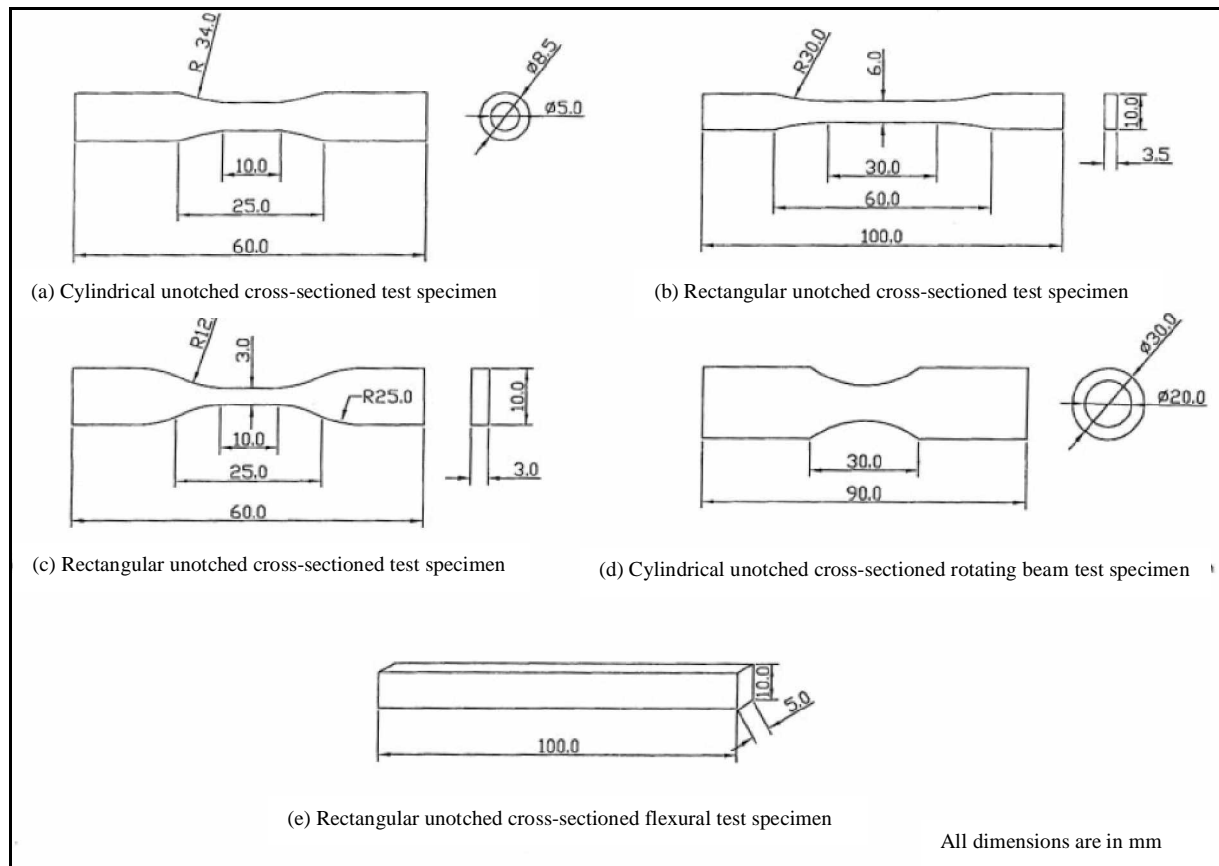


Figure II.10 Drawings of various unnotched fatigue test specimens used in literature studies.⁽¹²⁹⁾

Experiments have been run at a frequency of 1 Hz,^(37,62,137,145) 2 Hz,^(36,54,55,72,79,91,96,111,112,131,141,145) 4 Hz,⁽¹³⁴⁾ 5 Hz,^(135,136,138,145) 10 Hz,^(62,70,142,145) 20 Hz^(62,145) and 25 Hz.^(50,144)

The various methods that were used to analyse the trial results are as follows:

- Determination of the minimum, maximum, and/or mean and standard deviation of the number of **stress** cycles to failure, N_f , at a specified level of the classical applied **stress** amplitude, S ^(111,138)
- Plot the Wohler curve (applied **stress** S versus N_f or $\log N_f$)^(62,123,139,142,144)
- Estimation of the material's fatigue limit from an Olgive-type fit as the lower asymptote to the $S-N_f$ or $S-\log N_f$ results^(54,70,146) as shown in Figure (II.11). The Olgive-type equation has the form^(5,129):

$$S(N_f) = A + \frac{B - A}{\left[1 + \left(\frac{\log N_f}{C} \right)^D \right]} \quad (\text{II-5})$$

Where A, B, C, and D are material constants whose values may be obtained using nonlinear regression of the $S-N_f$ data. A is the lower asymptote to the Wohler curve (see Figure II.11)

and designated the **stress** amplitude level below which fatigue failure of the cement component will not occur for an infinite number of service load cycles.

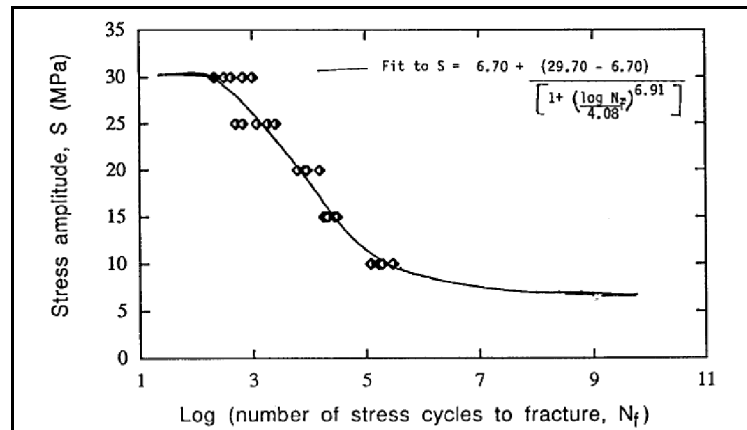


Figure II.11 Uniaxial fully reversed tension-compression fatigue test results for vacuum mixed CMW™-1 cement and their fit to the Olgive type equation.⁽⁵⁾

-Presentation of plots of probability of failure, $P(N_f)$, or survival, $\phi(N_f)[=1-P(N_f)]$ versus $\log N_f$ and, hence, determination of N_f at a specified probability level^(54,72,139,140) (see Figure II.12).

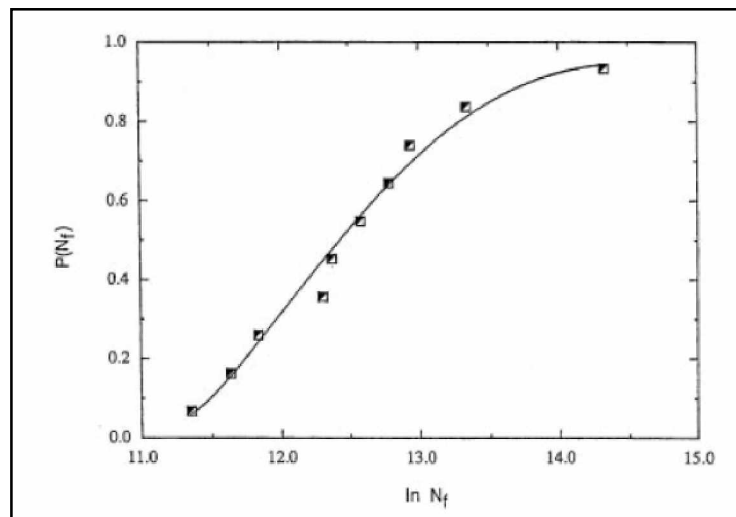


Figure II.12 Presentation of fatigue test results as a probability of failure plot.⁽¹²⁹⁾

Two different expressions have been used to estimate $P(N_f)$, these being $(M-0.3)/(G+0.4)$ ^(54,72,132,139,146) and $M/(G+1.0)$,⁽¹⁴⁷⁾ where M is the rank of the N_f result when the set of N_f results are placed in ascending order of magnitude, and G is the total number of specimens tested

-derivation of $S-N_f$, $P(N_f)-N_f$, and $P(N_f)-S-N_f$ relationships⁽⁷⁰⁾

-fit of the N_f results to the two-parameter Weibull relation using the method of least squares to obtain estimates of the Weibull characteristic fatigue life, N_a , Weibull slope, b and Weibull mean.^(139,141,142,146) The linearized form of the 2-parameter Weibull equation is

$$\ln \ln \left[\frac{1}{1 - p(N_f)} \right] = -b \ln N_a + b \ln N_f \quad (\text{II-6})$$

-fit of the N_f results to the linearized transformation of the three parameter Weibull equation, (see Figure II.13 a and b), which is

$$\ln \ln \left[\frac{1}{1 - P(N_f)} \right] = b \ln(N_f - N_0) - b \ln(N_a - N_0) \quad (\text{II-7})$$

Where N_0 is the minimum or guaranteed fatigue life, N_a is the Weibull characteristic fatigue life, and b is the Weibull slope.

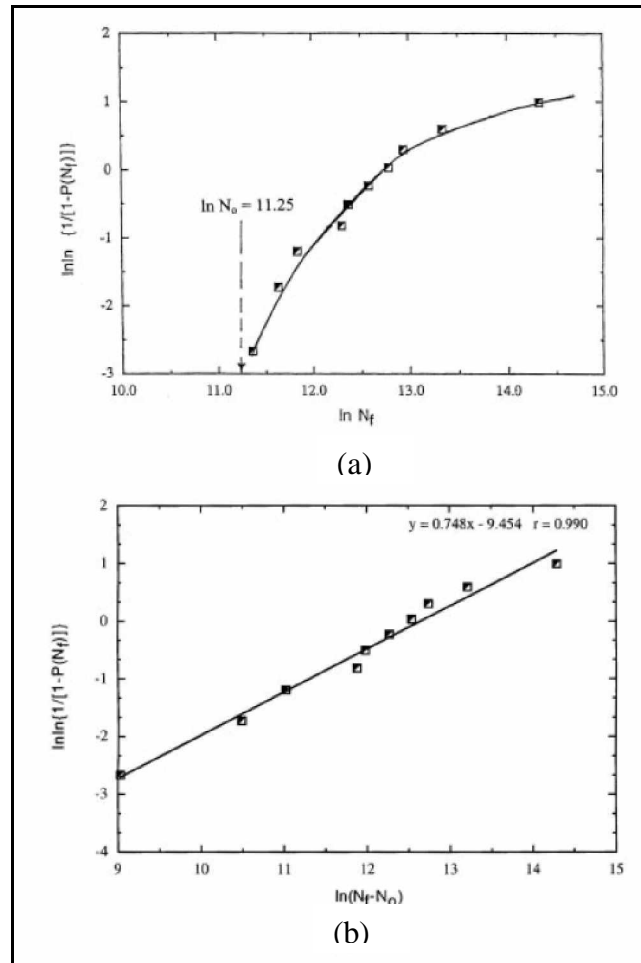


Figure II.13 Presentation of fatigue test results, with the use of the linearized form of the Weibull three-parameter equation. (a) Plot for estimation of the minimum fatigue life, N_0 . (b) Plot of $\ln \ln \{1/(1-P(N_f))\}$ versus $\ln(N_f - N_0)$.

A suitable fit to the S- N_f results and the Weibull treatment of N_f results provide more information about a cement's fatigue performance. The 3-parameter Weibull relation would provide a more meaningful fit to the S- N_f results. The combination of N_a and b factors is expressed as the fatigue performance index I ,

$$I = N_a \sqrt{b} \quad (\text{II-8})$$

Large numbers of specimens should be used in tests aimed at obtaining an estimate of an index of the cement's fatigue performance. The number of specimens used in literature, has

been 3⁽¹³²⁾, 4^(54,79), 5^(54,132,137,142), 6^(134,137,142,146), 7⁽¹³⁹⁾, 8^(96,139,147), 9⁽¹⁴⁷⁾, 10^(50,70,96,140,144), 11^(72,147), 12^(138,147), 13⁽¹⁴⁴⁾, 15^(72,111,112), 17⁽¹³⁸⁾, 18⁽³⁶⁾, 19⁽¹⁴⁸⁾ and 23.⁽¹³⁸⁾

Prendergast and co-workers^(139,149) and Dunne et al.⁽¹⁵⁰⁾ have proposed that all the test specimens fabricated should be tested. In contrast, Cristofolini et al.,^(151,152) Lewis and co-workers,^(54,132,147) Davies et al.⁽⁷²⁾ and Klekmap et al.⁽⁷⁹⁾ have taken a very different view; namely, that only a select subset should be tested. The methods that have been used by them for selecting the specimens to be tested from the collection of those fabricated may be classified as qualitative^(72,79) and quantitative.^(54,132,147,151,152) The qualitative rejection criterion stated that specimens with large voids were rejected without providing any information about what constituted large voids. According to Lewis,⁽¹²⁹⁾ Cristofolini et al.^(151,152) have proposed a rational quantitative criterion for selection of the subset based on the critical macropores, defined as having a diameter greater than 1 mm in the specimens.

Test environment affects cement's fatigue performance. It's better when tested in saline compared to when tested in air.^(62,123,145) Although, Ishihara et al.⁽⁶²⁾ reported little effect of the environment, i.e. air vs. Ringer's solution, on the fatigue lifetimes.

Soltész⁽¹³⁶⁾ found that fatigue life obtained under load controlled conditions was considerably lower than when the tests were conducted using displacement control. Rather, fatigue performance of bone cements is better when tested using displacement rather than load control. This behaviour is due to the viscoelastic nature of bone cement.

As reported in the existed literature reports,^(62,145,147) fatigue life increases with increase in test frequency, f , but there is disagreement as to the statistical nature of the increase. It's known that bone cements are viscoelastic materials, so that more **strain** develops at low frequency as compared to high. A higher local **strain** at the initiating pore due to a lower frequency will promote crack initiation, and hence have an adverse effect on fatigue life.⁽⁶²⁾

There is agreement that the following factors exert a strong positive effect on the fatigue life of a cement material:

- Molecular weight ;^(2,33,54,55) the higher the molecular weight of the powder or the fully cured cement (all other parameter being the same), the higher is the cement's fatigue performance
- Radiopacifiers,^(61,123,138) such as BaSO₄, ZrO₂, methacrylate-type iodide-containing copolymer (ICCP), etc
- Toughening/reinforcing agents,^(55,137,142) incorporation of a toughening/reinforcing agent into a cement increases its fatigue life markedly by increasing fatigue energy dissipation. One of these agents is incorporated in either the particulate or fibrous form into the cement powder. Examples of reinforcing agents being: PMMA particles, hydroxyapatite, Titanium, carbon, etc.

Lewis⁽¹²⁹⁾ based on previous literature studies,^(79,153,154) reported an unclear effect of the presence of an antibiotic as part of the powder constituents on a bone cement's fatigue performance.

Porosity, pore size, and pore size distribution were found to affect the crack initiation and fatigue behaviour of bone cement.^(24,33,37,62,96,139,150) Indeed, porosity reduction by centrifugation or vacuum mixing improves the fatigue life of PMMA bone cement.^(36,96,112,155)

All fatigue cracks initiated at pores which act as **stress** concentrators and propagated outward. Murakami et al.⁽¹⁵⁶⁾ proposed two expressions which can evaluate an equivalent initial maximum **stress** intensity factor $K_{I_{max}}$ for a pore.

$$K_{I_{max}} = 0,65\sigma_{max} \left\{ \pi \sqrt{area} \right\}^{1/2} \text{ (Superficial hole)} \quad \text{(II-9)}$$

$$K_{Ii\max} = 0,50\sigma_{\max} \left\{ \pi \sqrt{\text{area}} \right\}^{1/2} \text{ (Internal hole)} \quad (\text{II-10})$$

Where the area is the pore area at which fatigue cracking occurs.

The largest pores initiated more and larger fatigue cracks than smaller pores. So, fatigue cracks initiated at larger pores will propagate more rapidly and hence reduce the fatigue life as compared to those cracks initiated at smaller pores. It was found that pore distribution played a role in fatigue crack initiation. Small pores immediately adjacent to large pores caused larger **stress** concentrations than large pores alone. The net effect of the adjacent small pores is to sharpen the large pore, thus causing larger **stress** concentrations, and initiating more fatigue cracks, at the edge of the small hole than those initiated by the large hole alone (see Figure II.14).

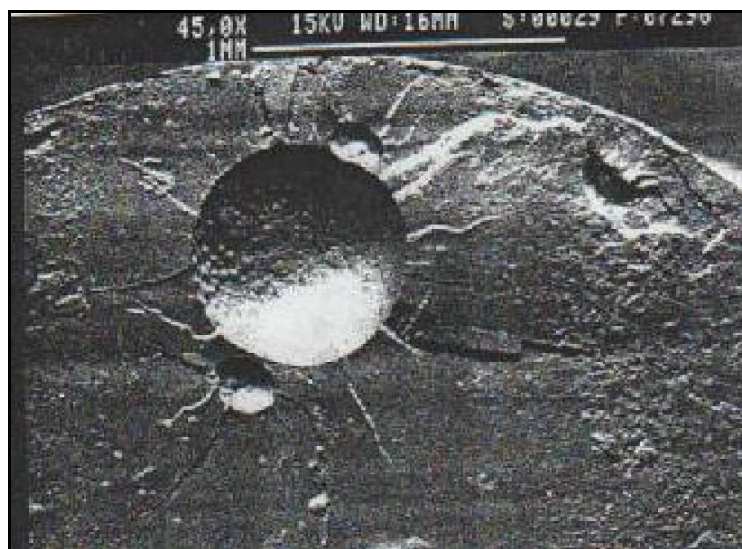


Figure II.14 SEM micrograph of fatigue fracture surface. The two small pores adjacent to the large pore caused stress concentrations which initiated several cracks.⁽⁹⁶⁾

As aforesaid, methods of cementing mixing, cementing inserting, prosthesis and bone surface properties or prosthesis temperature may affect the final pore distribution in the cement mantle: it is possible that pore formation may be favoured at the metal/cement interface, bone/cement interface, or cement interior.

II.3.2.3 Fatigue Crack Growth (FCP)

Bone cement fails through crack initiation, propagation and fracture whether at an interface or within the bulk material. These events play a key role in aseptic loosening of the cemented total joint prosthesis and, eventually its clinical life.^(5,38,157)

Acrylic cements used in **total hip replacement** contain small pockets of trapped air or monomer and exhibit regions of incomplete mixing between polymerized methyl-methacrylate (MMA) monomer and the PMMA powder. In addition to voids created by radiopacifier particles (such as BaSO₄).^(10,24,37,39) These porous regions can become highly stressed due to the **stress** concentrating effects of the voids and may act as sites for the initiation of small cracks. The formation of these microcracks may take place during the cure of the acrylic cement (by thermal stressing and residual stressing due to the shrinkage of the cement) or when the prosthesis becomes loaded in uses.⁽¹⁵⁸⁾ These flaws (micro-voids or small cracks), under in vivo loading first extend slowly by coalescence of voids and microcrack

propagation (stable crack) and then later there is fast (unstable) growth culminating in the fracture of the cement layer. According to Molino et al.,⁽¹⁵⁷⁾ some authors report that crack propagation behaviour dominates over crack initiation behaviour in vivo, and therefore the fatigue life of bone cement is controlled by propagation. Accordingly, it's important to have knowledge of the crack growth rate of the cement, which characterizes a material's resistance to fatigue crack extension under cyclic loading.

Once the crack starts to grow, the fatigue crack growth can be presented with the help of the Paris-Erdogan model,⁽¹⁵⁹⁾ which expresses the crack propagation rate $\left(\frac{da}{dN}\right)$ as a function of the **stress** intensity factor range (ΔK_I):

$$\frac{da}{dN} = A(\Delta K_I)^m \quad (\text{II-11})$$

Where A and m are constants which depend on the material and environmental conditions. When plotted in a log-log scale, as seen in Figure II.15, A represents the intercept at the $\frac{da}{dN}$ axis when $\Delta K_I=1$, and m is the slope, which is a measure of the rate of increase of the crack velocity as its increases its length. This means that for materials with a large m the crack has a greater acceleration.

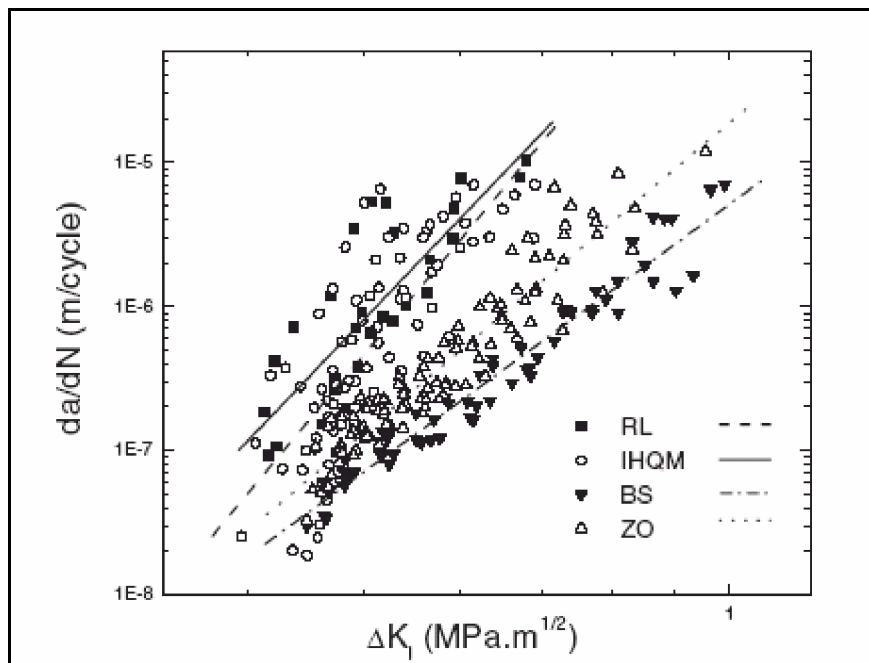


Figure II.15 Relationship between $\frac{da}{dN}$ and ΔK_I for different cements.⁽¹⁰⁾

The variation in the **stress** intensity factor ΔK_I is a function of the applied load, the specimen geometry, and the crack length.⁽¹⁰⁸⁾ Since bone cement standard fatigue crack propagation tests do not exist, many types of specimens (double torsion (DT),⁽¹⁵⁸⁾ standard compact tension (RCT),^(10,61,69,157,160,161) disc shaped tension, (DCT),^(64,109) and the single edge notched tension (SENB),⁽¹⁶²⁾ and a variety of cement mixing methods and specimen curing and aging conditions, have been used. In addition, two types of applied loading have been

used in literature. The test specimens were cyclically loaded in Zero-tension,^(61,162) and in tension-tension.^(10,69,157,160,161) Tests have been run at a frequency of 1 Hz,⁽⁶²⁾ 2 Hz,^(10,69,160,161) 4 Hz,⁽⁶¹⁾ 5 Hz,^(109,157) 16 Hz,⁽¹⁶³⁾ 20 Hz,⁽⁶²⁾ and 25 Hz.⁽⁶²⁾

Various methods were used to measure crack length extension (a special sensors, digital camera, cathetometer, etc.).

Test environment as aforementioned, influences cement's fatigue performance. Acrylic bone cement was found to be more resistant to fatigue crack propagation in an aqueous medium than in air.^(64,69,123) This is due to the fluid sorption ability of the bone cement and the plasticizing effect of the intake of water at the crack tip.⁽⁶⁹⁾ In addition, the hydrodynamic pressures induced in the fluid as it is pumped in and out of the crack act to oppose the opening or closing of the crack and therefore essentially protect the crack tip from the full applied **stress** intensity range.⁽⁶⁴⁾ Nguyen et al.⁽⁶⁴⁾ reported that the fracture surfaces produced in Ringer's solution were markedly more rougher than those produced in air environment.

There is agreement that a crack propagation resistance (slower crack propagation rate) is increased by the following factors:

- increase in the molecular weight of the cement powder and, hence, the fully cured cement;⁽⁵⁶⁾
- increase in the particle size of the PMMA beads (larger PMMA beads)⁽¹⁶¹⁾,
- incorporation of a toughening/reinforcing agent, such as carbon fiber,^(164,165) Acrylonitrile-Butadiene-Styrene (ABS);⁽⁶⁹⁾
- inclusion of inorganic radiopacifier in the cement such as BaSO₄, ZrO₂.^(10,61,157,161)

The fatigue crack in the cement containing larger PMMA beads, in the toughened cement and in the radiopaque cement seems to propagate mainly within the matrix surrounding the beads, resulting in rougher morphology of the fatigue fractured surface, and slower fatigue crack propagation.

Porosity has a controversial effect on fatigue crack propagation. It may enhance fatigue crack initiation and increase the propagation rate^(24,39,40,68,69,142,150) or conversely may absorb energy and decrease fatigue crack propagation.^(39,40,69)

Dennis et al.⁽⁴⁰⁾ elucidated by simulation "using a finite element model" the contradictory effect of pores on fatigue crack propagation. They found that the effect of a pore depended on its location with respect to the crack path. This finding was also reported by Villa et al.⁽⁶⁹⁾ When a pore was located directly on a crack path the **stress** at the tip of a crack was elevated, which accelerated the crack propagation (see Figure II.16a). When a pore was located in the neighbourhood of the crack path, the distance of the pore to the crack path determined the effect of the pore. When a pore was sufficiently close to the crack, the elevated **stress** level deviated the crack from its path (see Figure II.16b). If it was located a little further away from the crack, the pore was not able to deviate the crack, but decelerate the crack growth (see Figure II.16c). Due to the presence of the pore, the crack energy was dispersed, which in most cases caused secondary cracks to be formed at the pore. When a pore was located even further away, the effect of the pore on the crack propagation was diminished (see Figure II.16d).

In Dennis et al.⁽⁴⁰⁾ report fatigue failure process was independent of pore size (similar effect with smaller pores), whereas it was dependent of pore size in Villa et al.⁽⁶⁹⁾ investigation. Dennis et al.⁽⁴⁰⁾ reported also that the level of porosity had no effect on failure of the cement mantle. This last was, however, affected by the distribution of the pores in the region of the **stress** intensity caused by the primary crack propagating

II.3.3 Creep

Beyond fatigue phenomena, creep is the other critical aspect in the performance of bone

cement.^(5,60) It is currently not fully known what the consequence(s) of such visco-elastic behaviour are, especially in relation to the aspect loosening of the Arthroplasty.^(5,60)

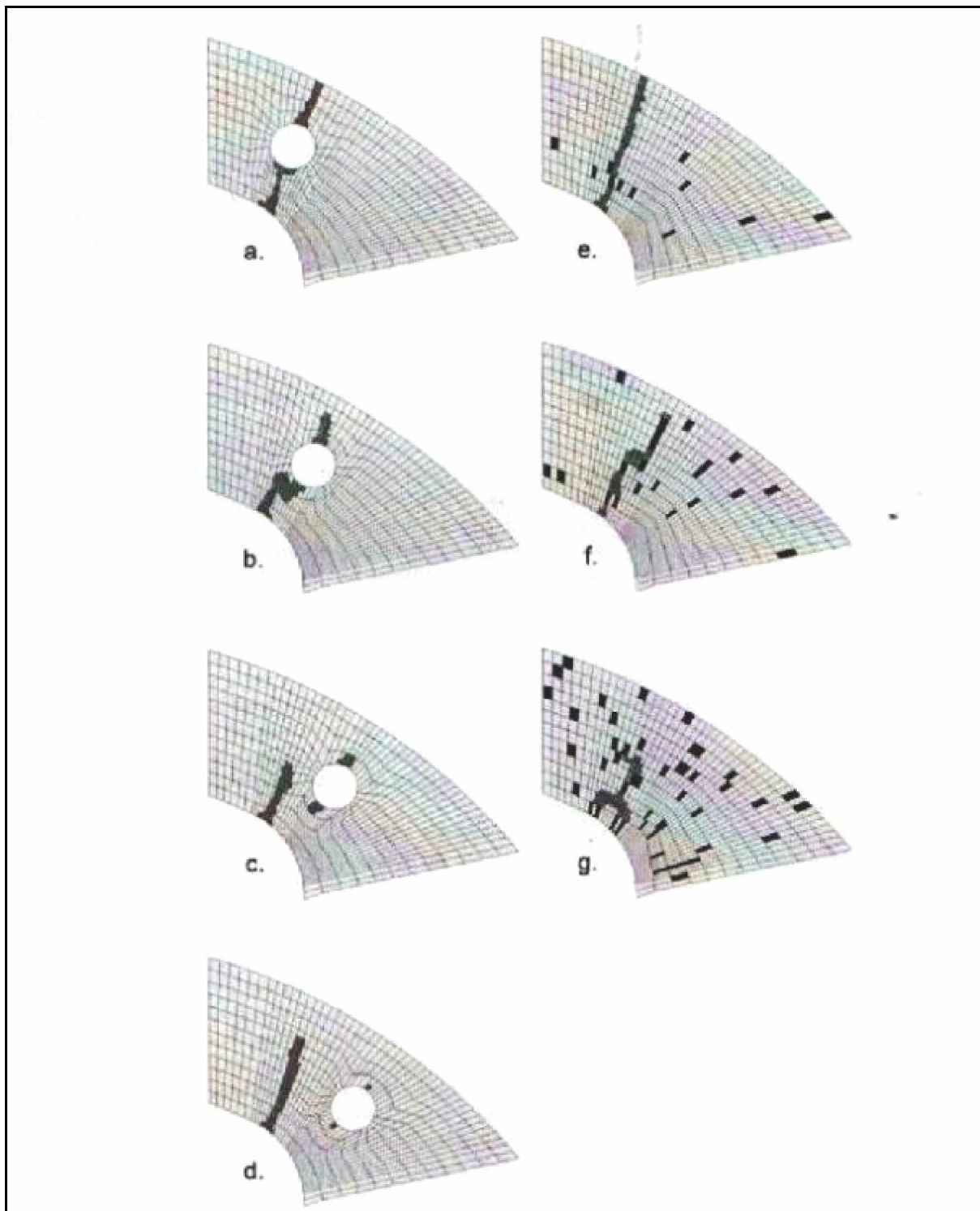


Figure II.16 Crack formation patterns in the upper right corner of the cement mantle with a single large pore (1 mm diameter) at a distance of 0.0, 0.5, 1 and 1.5 mm from the original crack.⁽⁴⁰⁾

The various clinical observations exhibit that the creep occurs in bone cement in vivo and causes, for example, the subsidence of the prosthesis in the femoral canal.^(166,167) This phenomena implies a redistribution in the **stresses** in the cement, which, depending on the case, can have beneficial^(60,168,169) or detrimental^(60,167) effects on the entire prosthetic system.

An experimental study is essential in order to evaluate the quantity of the deformations to which the in vivo cement is subjected. Various studies of the in vivo determination of the creep properties of bone cement were found in literature with both static^(168,170) and dynamic loading.^(169,171) Chwirut⁽¹⁷⁰⁾ presented the following expression to describe the dependence of creep **strain**, ϵ_c , on creep time, t , and applied static **compressive stress**, σ_{cs} , for Zimmer Regular hand mixed cement aged in saline at 37 °C:

$$\epsilon_c = 1.76 \times 10^{-9} t^{0.283} \sigma_{cs}^{1.858} \quad (\text{II-12})$$

Verdonshot and Huiskes⁽¹⁷¹⁾ presented the following expression to describe the dependence of creep **strain**, ϵ_c , on the number of loading cycles to failure N_f , and applied dynamic compression (0 to 7, 11, 15 or 20 MPa, 1 Hz) for simplex P, hand mixed cement aged in saline solution at 37°C for 3 to 6 months while immersed in saline solution at 38.5°C:

$$\epsilon_c = 1.225 \times 10^{-5} N_f^{0.314} 10^{0.033 \sigma_{cd}} \quad (\text{II-13})$$

As expected, the values of creep deformation are affected by the usual variables: cement formulation, mixing method, and curing and aging conditions.

Summary

This chapter allows us to retain the following points:

- When used in total hip Arthroplasty, PMMA fill the free space between the metallic component and the predetermined bone site.
- The main task of PMMA is to transfer complex, varying physiological loads from the prosthesis to the bone.
- In clinical service the **hip implant** is subjected to static or quasi-static **tensile, compressive, and shear** forces during daily activities.
- If the external **stress** factors are superior to the ability of the cement to transfer the force, a break will result. PMMA fragments thus formed could trigger phenomena of peri-prosthetic osteolysis and lead to the mobilisation and even failure of the prosthesis.
- It is believed that mechanical failure of the bone cement layer at any or all of the weak link zones (the implant-cement interface, the cement mantle, and the cement-bone interface) is the cause of aseptic loosening.
- Numerous studies have focused on improving the static and dynamic properties of bone cement in order to maximise its resistance to applied **stress**.
- The American Society for Testing and Materials (ASTM-F451) and the International Standards Organization (ISO 5833) have fixed minimum values for the critical properties; these standards are limited as they cover some mechanical properties in compression and bending.
- Several data on the mechanical properties of bone cements can be found in literature. However, there is no consensus on any unique value for any of the mechanical properties due to the different kind of cements and many trial techniques and conditions that have been used.
- The manner in which the cement is prepared, handled and chemically composed affects its mechanical properties. Temperature and loading rate at the time of testing, also affect the measured mechanical properties.
- PMMA bone cement fails during in vivo use at **stress** levels far below the critical values seen in their static tests. In reality, the cement mantle is subjected to cyclical loads (repeated loads) and the fatigue phenomena appear to be the cause of mechanical failure of the PMMA mantle. Failure of the cement most commonly occurs by the growth of fatigue cracks until a critical size when unstable propagation of the crack occurs and cement fractures.
- Mechanical fatigue testing can be conducted as **tensile, compressive** or bending tests. Unfortunately, mechanical fatigue testing on bone cement is not currently regulated by any international standard.
- Beyond fatigue phenomena, creep is the other critical aspect in the performance of bone cement.

MATERIALS AND METHODS

Chapter

III

This Chapter describes the experimental procedure used to obtain and analyse fatigue fractured surfaces of six commercial bone cements, carried out in Rizzoli Orthopaedic Laboratory.

III.1 Experimental Groups

Six experimental groups were investigated, which were as follows:

Experimental Group 1: Simplex P Bone cement (Shannon Industrial Estate Co. Clare, Ireland). A commercial package (see Figure III.1) of this bone cement consists of a 40 g powder component and a 20 ml liquid monomer component. The chemical compositions of these components are given in table I-1 (see Chapter I).



Figure III.1 The packaging of surgical Simplex P.⁽¹⁷¹⁾

Experimental Group 2: Cemex Rx Bone cement (Tecres SPA, Sommacampania, Verona, Italy). A commercial package (see Figure III.2) of this bone cement consists of a 40 g powder component and a 14.13 ml liquid monomer component. The chemical compositions of these components are given in table I-1 (see Chapter I).



Figure III.2 The packaging of Cemex Rx.⁽⁴⁵⁾

Experimental Group 3: Cemex Isoplastic Bone cement (Tecres SPA, Sommacampania, Verona, Italy). A commercial package (see Figure III.3) of this bone cement consists of a 40 g powder component and a 14.13 ml liquid monomer component. The chemical compositions of these components are given in table I-1 (see Chapter I).

Experimental Group 4: Cemex Genta Bone cement (Tecres SPA, Sommacampania, Verona, Italy). A commercial package (see Figure III.4) of this bone cement consists of a 40 g powder component and a 14.2 ml liquid monomer component. The polymer powder consists of 82.8%

PMMA, 3.0% BPO, 4.2% gentamicyn sulfate and 10% barium sulfate. The colorless monomer contains 98.2% MMA, 1.8% DMPT and approximately 75 ppm of hydroquinone.



Figure III.3 The packaging of Cemex Isoplastic.⁽⁴⁵⁾

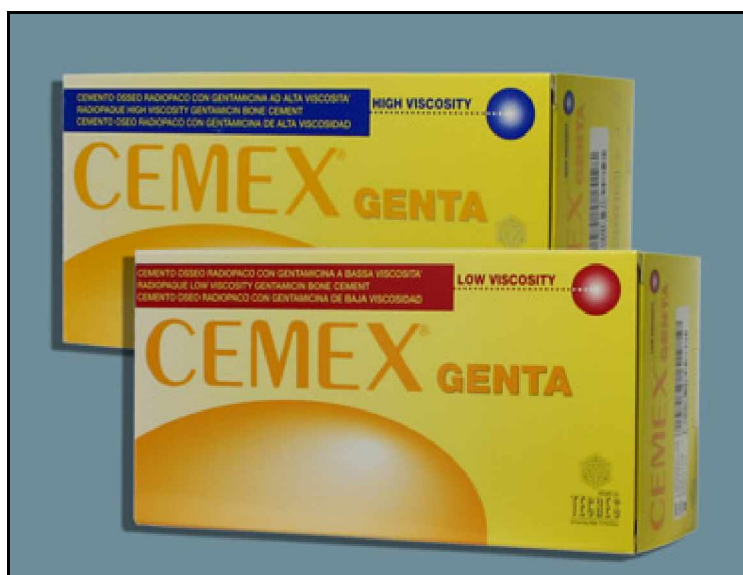


Figure III.4 The packaging of Cemex Genta.⁽¹⁷²⁾

Experimental Group 5: Cemex System Bone cement (Tecres SPA, Sommacampania, Verona, Italy).



Figure III.5 The packaging of Cemex System.⁽⁴⁵⁾

A commercial package (see Figure III.5 above) of this bone cement consists of a 40 g powder component and a 14.13 ml liquid monomer component. The chemical compositions of these components are given in table I-1 (see Chapter I).

Experimental Group 6: Cemex Fluoride Bone cement (Tecres SPA, Sommacampania, Verona, Italy). A commercial package of this bone cement consists of a 40 g powder component and a 14.13 ml liquid monomer component. The chemical compositions of these components are given in table I-1 (see Chapter I).

III.2 Preparation of the cement specimens

A hand mixing method of bone cement preparation was applied to all cements according to the manufacturer instructions at a controlled temperature of $23\pm 1^\circ\text{C}$ and at a relative humidity (R.H) ranging between 40 and 60%.^(61,94) The liquid and powder components were thoroughly mixed, so, there was no remaining dry powder visible in the mixture.

The cement mixture was then poured into two types of molds in order to prepare two different specimen geometries for mechanical testing. Fatigue crack propagation (FCP) specimens were prepared as suggested by the ASTM-E647-05 standard, while K_{IC} specimens were adapted from the ASTM-E399-05 standard. The dimensions of the FCP and K_{IC} specimens are shown in Figure III.6. All specimen geometries were seasoned in water at 37°C for at least 15 days before testing in order to simulate physiological environment.

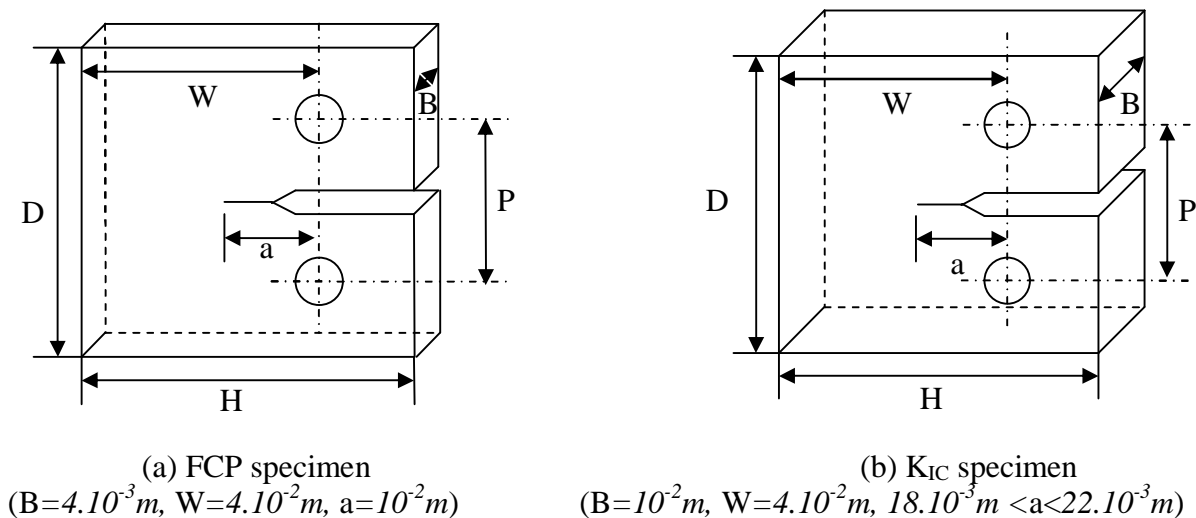


Figure III.6 Specimen tested geometries.⁽¹⁷³⁾

III.3 Fatigue crack propagation tests

Fatigue crack rates of the cements tested were performed in accordance with the ASTM E-647-05 standard. Fatigue crack propagation (FCP) specimens were mounted, by clevis pins through its 10 mm diameter loading holes, as outlined in Figure III.7, on a servo-hydraulic testing Machine (MiniBionix 858, MTS, Minneapolis, MN, USA), exhibited in Figure III.8. The same was done for K_{IC} specimens. A sinusoidal Zero-tensile load ranging up to 60 N was applied to each specimen at frequency of 4 Hz, so as to obtain failure in the range of 10^6 - 10^7 cycles. The crack growth was monitored using a crack gauge (KraK-Gage B20CE, Rumul, Neuhausen, Switzerland) placed on either side of each specimen as shown in Figure III.7. Crack-gauge signals were recorded continuously by the testing machine in order to correlate the crack length to the crack growth rate. All tests were performed in air at $23\pm 1^\circ\text{C}$.

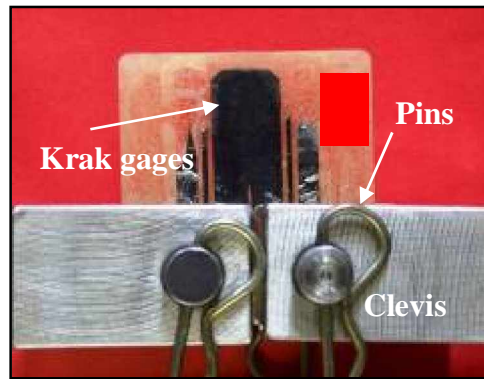


Figure III.7 Krak gages used to measure crack length.⁽¹⁷³⁾



Figure III.8 MiniBionix 858 testing machine.

The experiment using K_{IC} specimens had two phases: the pre-crack phase and the ramp load to failure phase. In fact, the specimens were cyclically pre-cracked at a frequency of 4 Hz with four decreasing load levels as prescribed by the ASTM-E399-05 standard, to maintain the crack growth rate of about 10^{-3} mm/cycle. The pre-crack length “notch” was grown to an overall length of 18-22 mm. Thus, the final value of the crack length falls into the range of 0.45-0.55 times the specimen width (criterion prescribed by the standard). The crack displacement was monitored by an Extensometer (Mod. 634.31-F24, MTS) fixed to the notch mouth. After precracking step, the crack length was highlighted by means of dye penetrants (AVIO-B spray, Rotvel, American Gas & chemical company, NJ, USA) and measured on both sides of the specimens using a profile projector (Microtecnica LTF, Helios 350V, Antegnate (BG),Italy).⁽⁹⁴⁾ The specimens that did not meet the precrack length requirements

were discarded. After that the specimens were remounted on the loading clevis and ramp loaded to failure with a preload of 100 N at a rate of 10 mm/min.

Multiple analyses were made on one half of the fractured specimens (FCP and K_{IC}) to quantify and qualify the cracked surfaces. Five specimens were used for each cement formulation. Fractured surfaces showing larger pores; i.e. greater than 1 mm were discarded from the study.^(61,94) The specimen selection was performed by means of a radiographic analysis (mammography).

III.4 Roughness measurement

In order to characterize the three different areas found in one fractured surface of each specimen tested, fractured surface roughness was measured using a Hommel profilometer (Hommel Tester-T8000, Hommelwerke, Schwenningen, Germany) with Turbo Roughness software for Windows. The measuring station is shown in Figure (III.9).



Figure III.9 Hommel profilometer.⁽¹⁷⁴⁾

The method used to determine surface roughness is based on mechanical contact between a diamond tip and the surface to be analysed (see Figure III.10).

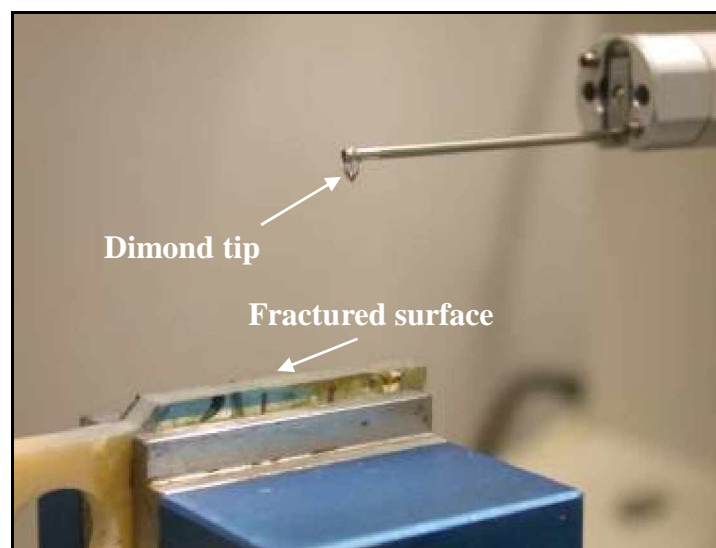


Figure 3.10 Diamond tip.

The mechanics of scanning surface is based on the principle of detection using a transducer displacement of inductive type. The tip is attached to an arm so that it can rotate vertically compared to the scanning plane. The fluctuations of voltage are evaluated from electronic contact, and converted into a proportional signal and then displayed and registered as a parameter roughness. The filter provided by the measurement system and supplied by the software package Turbo Roughness is a digital filter M1 (Gaussian filter) conforms to DIN 4777, part 1, with levels of cut-off standard and maximum adjustable wavelength.

Before start measuring, Roughness software requires entering some parameters in accordance with ISO 7206-2; their correct setting is essential in order to optimize the data acquisition roughness. The parameters to be defined are listed below:

-Length of the past (Lt): reducing the path of the diamond tip to obtain a more precise measurement;

-Feed rate (Vt): reducing the speed of diamond tip is important in order to obtain a more precise measurement;

-Cut-off (Lc) is the filter used to separate roughness and undulation. The value automatically recommended by the software is equal to one sixth of the specimen length.

In our case, the value of Lt adopted was equal to 0.48 mm, due to the limited size of the area in which the measure was performed. The values of Vt and Lc were maintained equal to 0.05 mm/s and 0.08 mm respectively.

Each specimen must be stuck on adjustable grip to secure a horizontal positioning and unique for all measurements. The contact between the diamond tip and the specimen surface was performed through an automatic command to avoid damaging of the surface to be analysed and the diamond tip.

Fifteen (15) measurements were taken by three operators; parallel to crack growth (0°), at 45° and perpendicular to crack growth (90°) for each different region of the fractured surface as shown in Figure III.11. The result of each acquisition has been put on a file with the extension ".par", creating a complete record of the tests carried out so as to make them available for subsequent statistical analysis. Areas showing micro-pores were avoided.

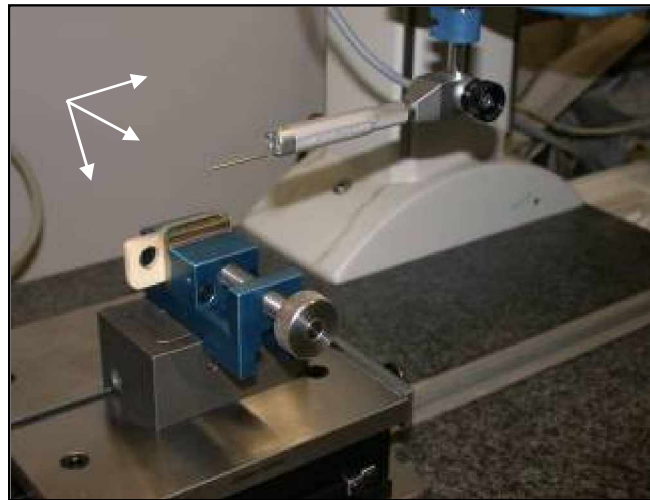


Figure III.11 Surface roughness measurement.

To assess inter-operator reproducibility, three operators were asked to perform the measurements separately at different times, thus minimising possible conditioning. To assess repeatability, each measurement was repeated 15 times, as aforementioned, for each specimen, each region, and each direction choosing different scanning spots. To assess if surface morphology is directional, roughness in three directions ($0^\circ, 45^\circ, 90^\circ$) was measured.

Different indicators were examined to establish which one was better suited for describing crack morphology: Ra, Rt, Rsm, according to the ISO 4287 standard.

III.4.1 Roughness parameters

III.4.1.1 Ra Roughness

The average roughness is the area between the roughness profile and its mean line, or the integral of the absolute value of the roughness profile height over the evaluation length (see Figure III.12):

$$R_a = \frac{1}{L} \int_0^L |r(x)| dx \quad (\text{III-1})$$

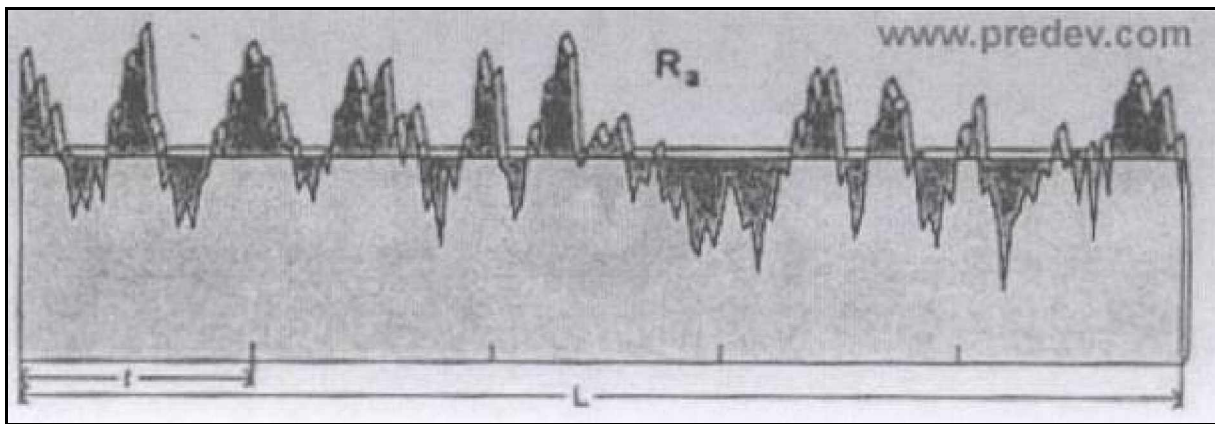


Figure III.12 The average roughness Ra.⁽¹⁷⁵⁾

III.4.1.2 Rt Roughness

The peak roughness R_p is the height of the highest peak in the roughness profile over the evaluation length see Figure III.13. Similarly, R_v is the depth of the deepest valley in the roughness profile over the evaluation length. The total roughness, R_t , is the sum of these two, or the vertical distance from the deepest valley to the highest peak.

$$R_v = |\min[r(x)]| \quad 0 < x < L \quad (\text{III-2})$$

$$R_p = |\max[r(x)]| \quad 0 < x < L \quad (\text{III-3})$$

$$R_t = R_p + R_v \quad (\text{III-4})$$

III.4.1.3 Rsm Roughness

The mean spacing R_{sm} is the mean spacing between peaks, now with a peak defined relative to the mean line. A peak must cross above the mean line and then back below it.

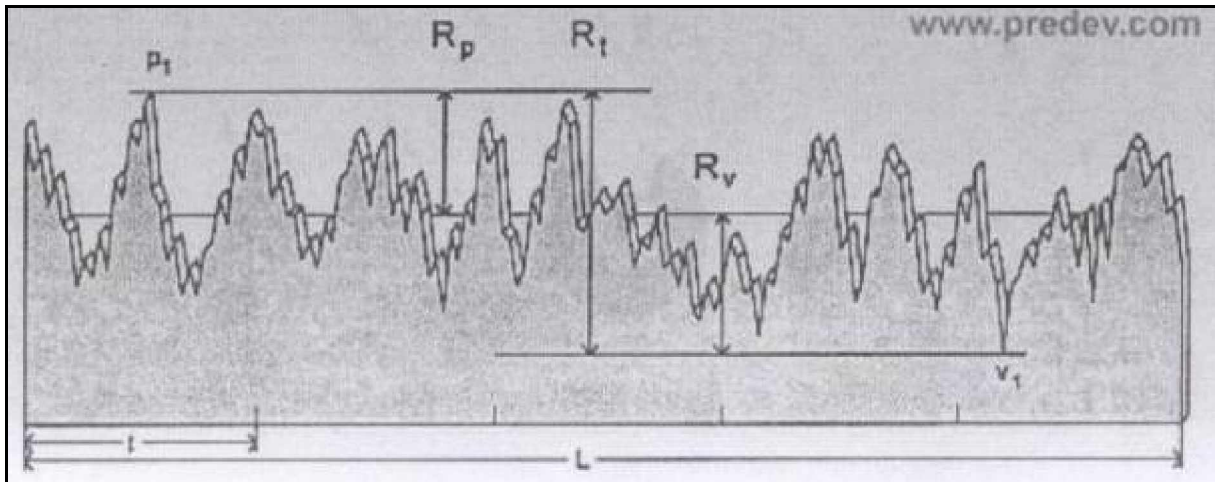


Figure III.13 Rt roughness.⁽¹⁷⁵⁾

If the width of each peak is denoted as S_i (Figure III.14), then the mean spacing is the average width of a peak over the evaluation length:

$$R_{sm} = \left(\frac{1}{N} \right) \sum_{n=1}^N S_n \quad (\text{III-5})$$

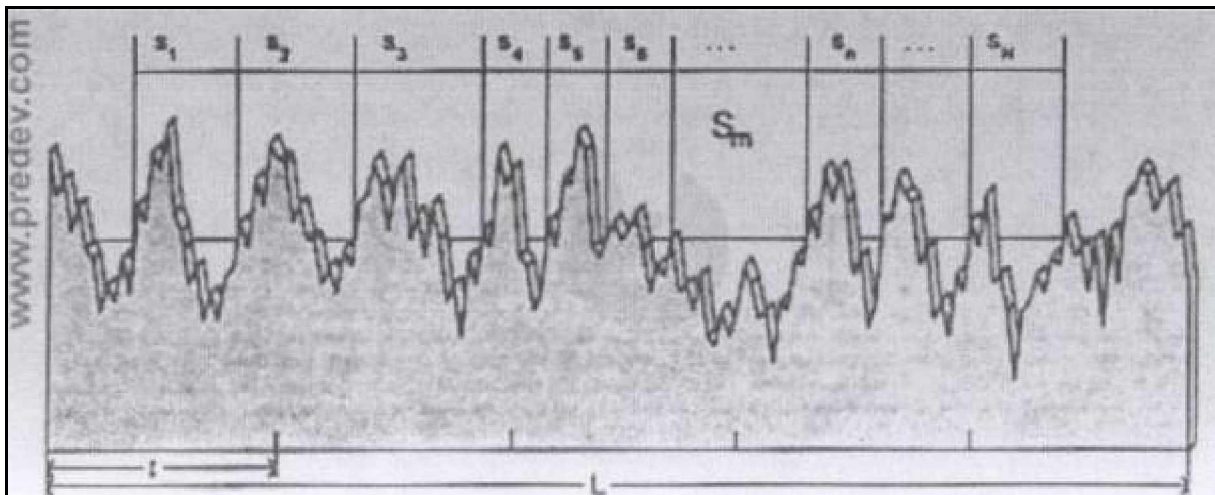


Figure III.14 Rsm roughness.⁽¹⁷⁵⁾

III.5 Treatment of fractured surfaces

To enhance contrast, all specimens were gold-sputter coated using Edwards S150B sputter coater outlined in Figure III.15. The sputter coater uses argon gas and a small electric field. The sample was placed in a small chamber which was at vacuum. Argon gas was then introduced and an electric field was used to cause an electron to be removed from the argon atoms to make the atoms ions with a positive charge. The Ar ions were then attracted to a negatively charged piece of gold foil. The Ar ions acted like sand in a sandblaster, knocking gold atoms from the surface of the foil. These gold atoms settled onto the surface of the sample, producing a gold coating.



Figure III.15 Edwards S150B Sputter Coater.⁽¹⁷⁶⁾

Specimen preparation included attaching the PMMA sample to a 25 mm aluminum stub using double sided copper adhesive tape.

The sputter time was determined using the equation given below

$$d = k \times I \times V \times T_E \quad (\text{III-6})$$

Where, d is the thickness of the coating in Angstroms (\AA), k is the proportionality constant ($k=0.07$ in air), I is the sputter current (approximately 18 mA), V is the voltage applied (approximately 1 kV) and T_E is the sputtering time in seconds(s).

III.6 Count of cleaved pre-cured beads

An optical microscope (SMZ-2T, Nikon, Tokyo, Japan) with the following characteristics:

- Maximum magnification (6.3X);
- Photographic lens (5X);
- Maximum zoom camera (3X).

was used to examine one fracture surface from each specimen (as outlined in Figure III.16). This technique allowed us to know if the crack propagated across the pre-cured beads or around them. Digital micrographs were acquired (1 pixel=0.5 μm) for each zone (avoiding micro-pores), and then treated (brightness and contrast) with Photoshop 7.0.

Pre-cured beads in the crack surface that were cleaved during crack propagation were counted (%) in 1 mm^2 using a semi-automated softwares Q Win 2001, (Leica Microsystems, Wetzlar, Germany) and Smart view. For example, a value close to 0% indicates that the crack propagated mainly through the inter grain matrix. As aforesaid, five specimens of each cement type were analysed.

To assess if the results could be changed by the operator, three persons were asked to do the entire procedure independently at different times (minimizing possible conditioning).

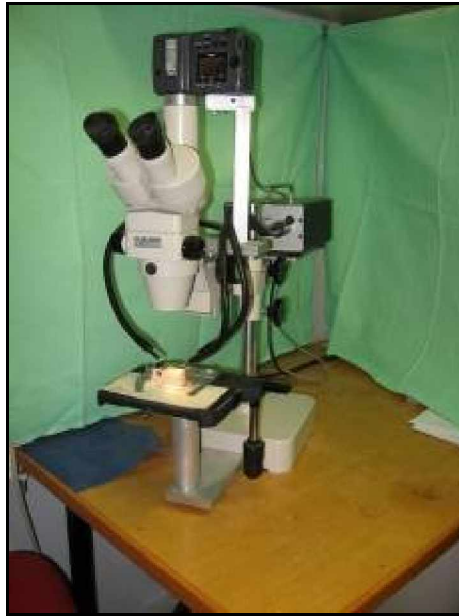


Figure III.16 Nikon Optical microscope.⁽¹⁷³⁾

III.7 Scanning Electron Microscopy

The Scanning Electron Microscope (SEM) is a microscope that uses electrons rather than light to form an image. Electrons are thermionically emitted from a tungsten cathode and are accelerated towards an anode. Tungsten is used because it has the highest melting point and lowest vapor pressure of all metals, thereby allowing it to be heated for electron. There are many advantages in using the SEM instead of a light microscope. The SEM has a large depth of field, which allows a large amount of the sample to be in focus at one time. The SEM also produces images of high resolution, which means that closely spaced features can be examined at a high magnification. Preparation of the samples is relatively easy since most SEMs only require the sample to be conductive. All specimens were gold-sputter coated using Edwards S150B sputter coater seen in the above section (III.5 Treatment of fractured surfaces). One fracture surface from each cement was examined by Scanning electron microscopy (SEM, Stereo Scan-200, Cambridge Instruments Cambridge, Uk) equipped with a tungsten filament electron source (see Figure III.17). All specimens were viewed under high vacuum, at 25 kv, perpendicularly to the facture surface.



Figure III.17 SEM, StereoScan-200, Cambridge Instruments.

The images were then scanned into electronic storage in JPEG format using a Hewlett Packard Scanjet scanner and HP Precision scan Pro3.1 scanning software. Used magnification, ranged between 15× and 3000×.

III.8 Statistical analysis

Means and standard deviations for roughness parameters and (%) number of cleaved beads were calculated.

In order to detect possible outliers, the criterion of Chauvanet⁽¹⁷⁷⁾ was applied first to the repeats under the same conditions, and then to the five specimens of each type.

Univariate Analysis of Variance for repeated measures was applied (SPSS.14.0 for Windows version 14.0.1. Chicago, Illinois) on the roughness data to assess if there was a significant variation within the 15 repeats, on each specimen, each area, each operator each direction.

Univariate Factorial ANOVA with Bonferroni post-Hoc was applied (SPSS.14.0) to assess the effect of the following factors:

- For the roughness measurements: scanning direction, operator, type of the fracture and type of the cement;

- For the account of cleaved beads: operator and type of fracture type of cement.

The statistical model had an overall significance $P < 0.0005$

Summary

The experimental procedure used to obtain and analyse fatigue fractured surfaces of six commercial bone cements, carried out in Rizzoli Orthopaedic Laboratory was as follows:

The fatigue crack growth rates of six commercial bone cements, Cement#1, Cement#2, Cement#3, Cement#4, Cement#5 and Cement#6 were determined using a test method based on ASTM-E647-05 standard. Five fatigue crack propagation (FCP) specimens of each bone were tested. Crack lengths and propagation rates were measured with Crack gages placed on either side of each specimen. Sinusoidal tensile loading (0 up to 60N) was applied to the test specimens at 4Hz. Five pre-cracked K_{IC} specimens for each cement were used following ASTM-E399-05 standard to analyze the catastrophic failure, obtained with a monotonic ramp (10 mm/min).

Optical microscope (SMZ-2T, Nikon, Tokyo, Japan) was used to examine one fracture surface from each specimen. Digital micrographs were acquired (1 pixel=0.5 μm). Pre-cured beads in the crack surface that were cleaved during crack propagation were counted (%) in 1 mm^2 using a semi-automated software. The same surfaces were analyzed by measuring their roughness Ra (15 measurements).

All specimens were gold-sputter coated and one fracture surface from each specimen was inspected using Scanning Electron Microscopy (SEM) for crack-propagation patterns.

RESULTS AND DISCUSSION

Chapter

IV

*This Chapter gives an answer to the main question:
Are Roughness measurement and count of cleaved beads quantitative analyses of the fatigue
fractured surfaces of bone cements?.*

IV.1 Crack growth rate

One approach to the study of acrylic cement fatigue is to evaluate the advancement speed of crack ($\frac{da}{dN}$) in the presence of defects; basing the evaluation on the theory of the fracture mechanics.⁽⁶⁰⁾

Once the crack initiates, the fatigue crack propagation can be presented with the help of the Paris-Erdogan model, which expresses the crack propagation rate ($\frac{da}{dN}$) as a function of the stress intensity factor range (ΔK_I):

$$\frac{da}{dN} = A(\Delta K_I)^m \quad (IV-1)$$

Where a is the crack length measured as an average of readout of the two Krak Gages, N is the corresponding number of cycles.

The mode I stress intensity factor range (ΔK_I) is calculated according to

$$\Delta K_I = \Delta P \frac{F(\alpha)}{B\sqrt{W}} \quad (IV-2)$$

Where ΔP ($P_{\max} - P_{\min}$) is the load range of the fatigue cycle, $F(\alpha)$ is a geometric factor, B is the thickness of the simple ($B = 4$ mm) and α is defined as a/W .

The geometric factor used, as calculated from the elastic theory, is

$$F(\alpha) = \frac{(2 + \alpha)}{(1 - \alpha)^{1.5}} (0.886 + 4.64\alpha - 13.32\alpha^2 + 14.72\alpha^3 - 5.6\alpha^4) \quad (IV-3)$$

As this work was a part of a big project, Baleani et al. had performed the tests related to fatigue crack growth. A typical crack growth behavior exhibited by the cement group#6 is shown in Figure IV.1.

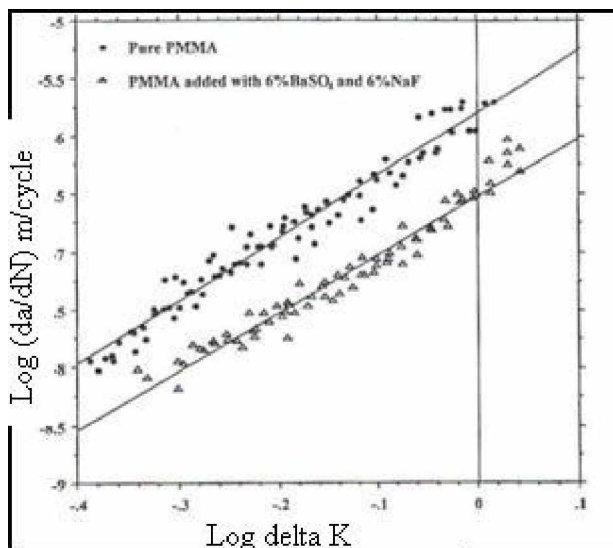


Figure IV.1 Fatigue crack propagation behavior and regression lines of Fluoride bone cement and pure PMMA.⁽⁶¹⁾

The results obtained from the $\left(\frac{da}{dN}\right)$ vs. (ΔK_I) curves showed that all the cements tested followed Paris' law.

The fractured surface appearance for the (FCP) specimens could be divided in three zones as outlined in Figure IV.2, which are consistent with crack growth rate:

The first region, *Slow cyclic propagation*, it can be found in the first part of the FCP specimens, and corresponds to crack propagation rate varying from 10^{-6} to 10^{-5} mm/cycle. This region represents the first portion of the linear crack growth region described by Paris' law. The second region is the *fast cyclic propagation* where crack growth rate varies from 10^{-4} to 10^{-3} mm/cycle. This zone corresponds to the last portion of the linear crack growth region described previously. The last one is the *catastrophic* or *sudden fracture* which occurs instantaneously. The final failure of the FCP specimens was not used as it was small (see later). This region was better seen on K_{IC} specimens (Figure IV.2), so, they were used to analyze the sudden fracture instead of the FCP specimens.

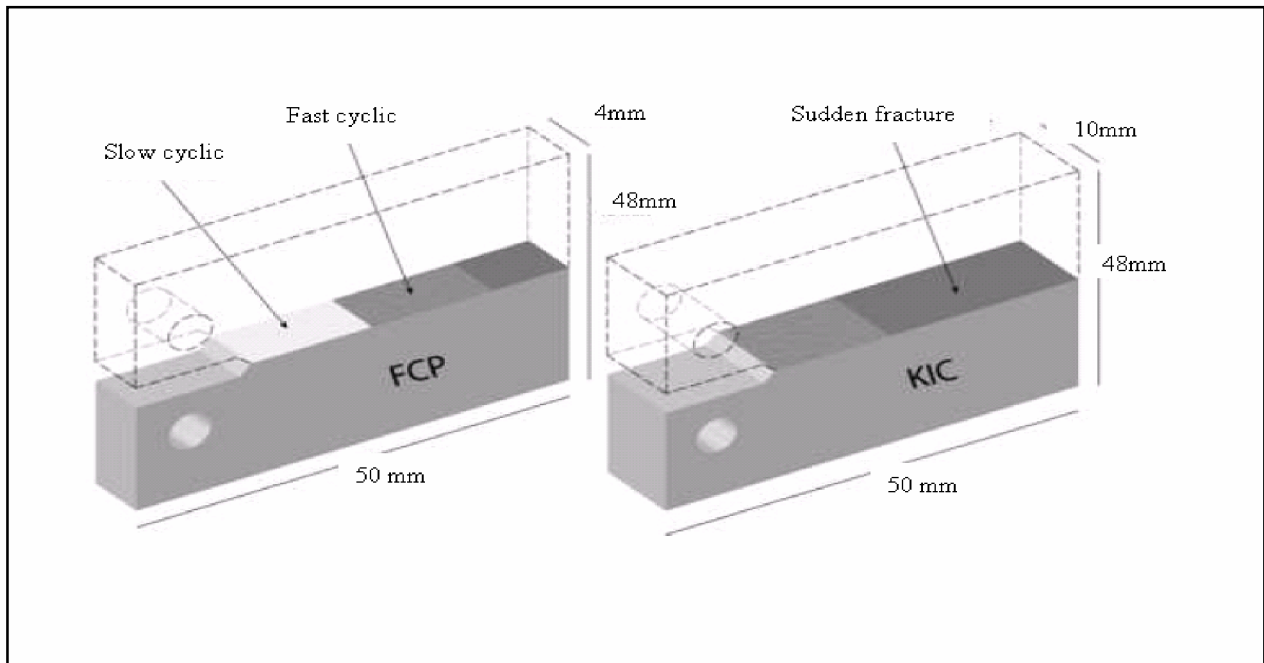


Figure IV.2 Fractured surface appearance of the specimens tested.⁽¹⁷⁸⁾

The fracture of the specimens passes through two phases:

- The first one is time dependent termed as stable crack growth or fatigue crack growth. It involves crack initiation and crack propagation.
- The second phase is time independent known as unstable crack growth or catastrophic fracture, in which, the final fracture of the specimens takes place. It is also named as rapid fracture since $\frac{da}{dN} \rightarrow \infty$.

IV.2 Roughness measurement

Taking roughness measurements is simple to do and easier to learn since roughness parameters are automatically calculated by turbo Roughness software for Windows. The roughness indicator that was most repeatable on the same specimen, reproducible between

operators and discriminated best between fracture and cement type was the average roughness (Ra). Figures IV.3-IV.5 show an example of roughness measurement indicators taken parallel to the crack growth.

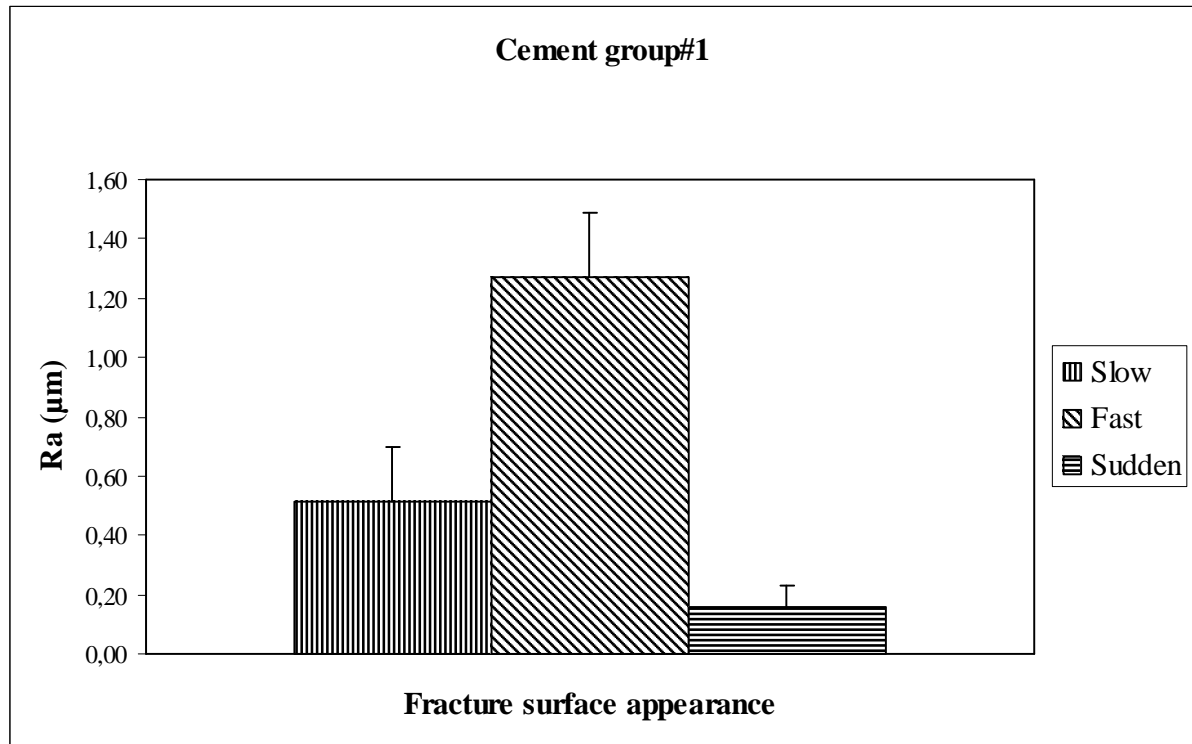


Figure IV.3 Roughness measurement using Ra indicator for cement group#1 (0°).

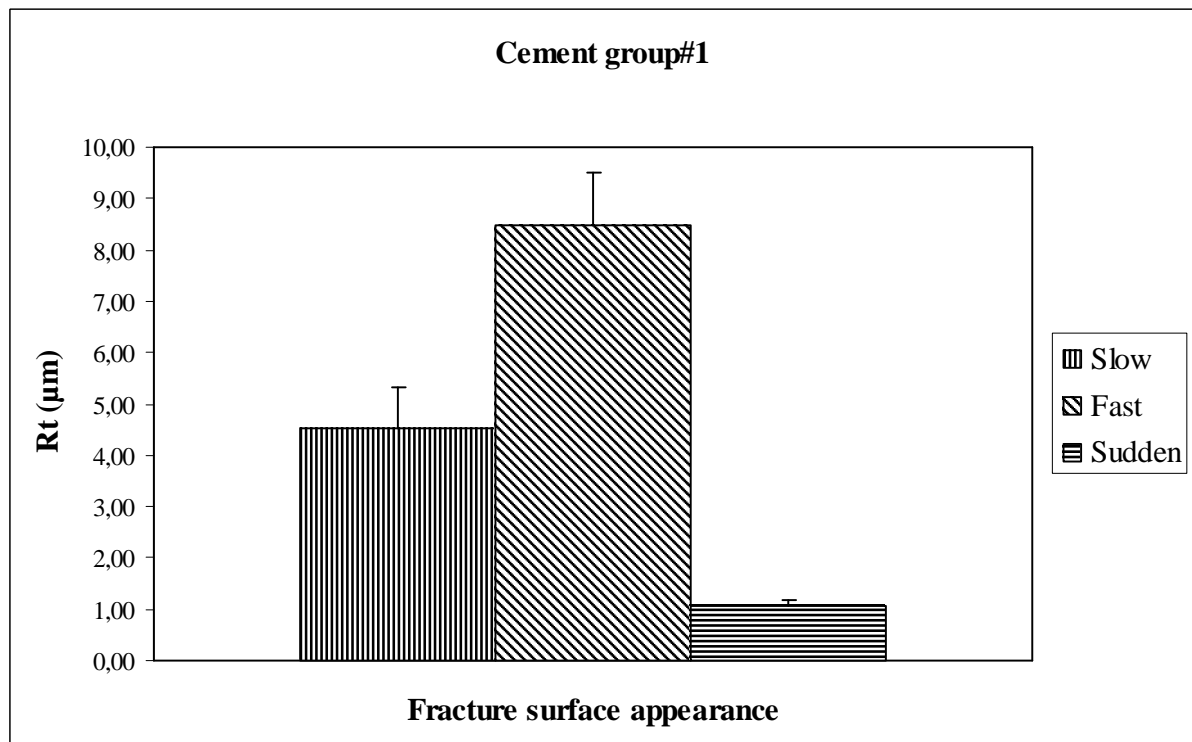


Figure IV.4 Roughness measurement using Rt indicator for cement group#1 (0°).

Ra and Rt allowed discrimination between the three zones seen on the fracture surface appearance of the specimens.

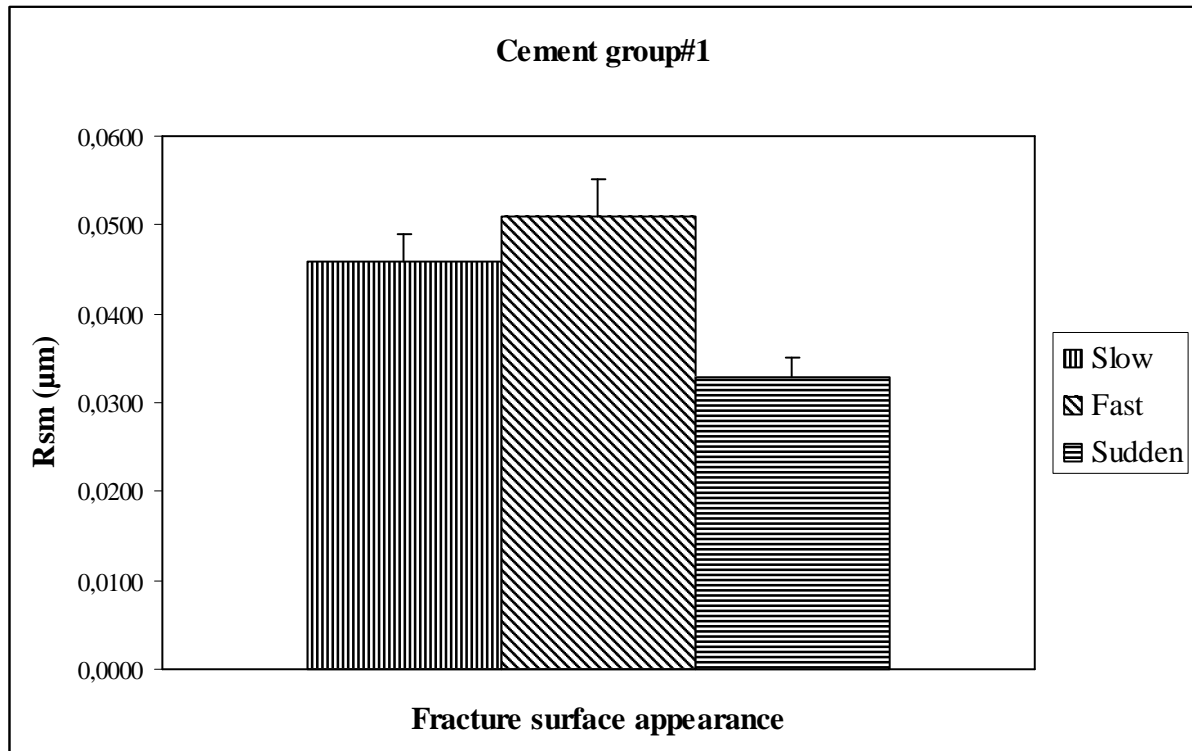


Figure IV.5 Roughness measurement using Rsm indicator for cement group#1 (0°).
(No great difference between slow and fast regions).

In fact, the statistical analysis (replication of the factorial ANOVA on all indicators) confirmed that Rt and Rsm were less powerful. Table IV-1 shows the statistical analysis between Rt and Ra indicators for all cements tested.

Table IV-1 Comparison between Ra and Rt indicators.

Ra is better powerful than Rt; Ra discriminates better between sudden and slow regions than Rt.

		Mean Difference (I-J)		Sig.	
Fracture (I)	Fracture (J)	Ra	Rt	Ra	Rt
Fast	Slow	0.6764*	3.4464*	.000	.000
	Sudden	0.8491*	3.5617*	.000	.000
Slow	Fast	-0.6764*	-3.4464*	.000	.000
	Sudden	0.1728*	0.1153	.000	1.000
Sudden	Fast	-0.8491*	-3.5617*	.000	.000
	Slow	-0.1728*	-0.1153	.000	1.000

In Table IV-2 are listed all roughness parameters Ra, Rt and Rsm for the cements tested collected by one operator parallel to the crack growth.

Therefore, *Ra* was selected for the remaining investigation as the best indicator parameter of the surface roughness.

From Figures (IV.3-IV.5) and according to Table IV-2, the following observations can be

made:

-In general, the catastrophic fracture zone appeared to be the smoothest one (i.e. lowest Ra);

-The fast cyclic propagation zone appeared to be the roughest one (i.e. highest Ra) for all cements tested.

Table IV-2 Roughness measurements taken parallel to the crack growth, for all cements tested.

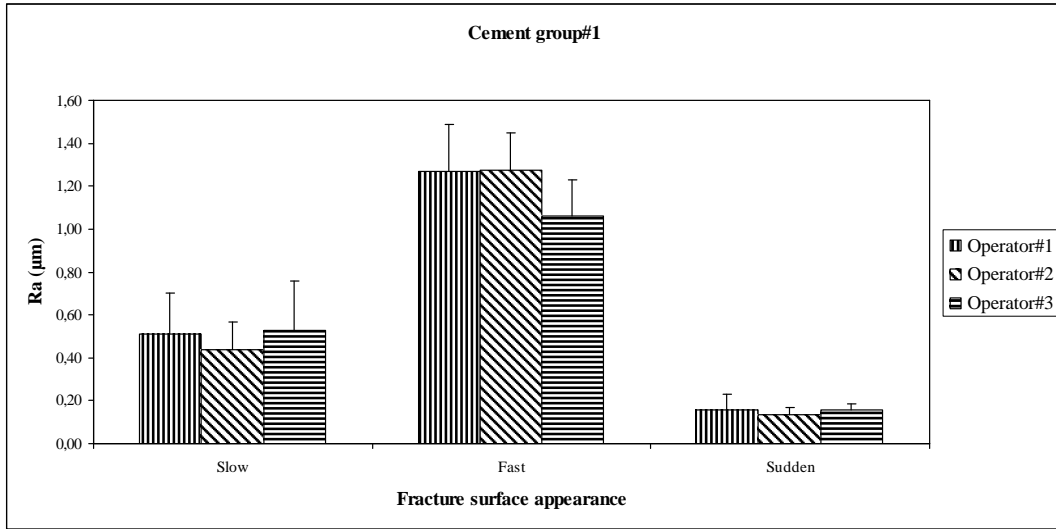
Slow cyclic propagation			
Roughness parameters	Ra (μm)	Rt (μm)	Rsm (μm)
Cement group#1	0.51 \pm 0.19	4.54 \pm 0.77	0.0459 \pm 0.0030
Cement group#2	1.16 \pm 0.10	8.04 \pm 0.62	0.0553 \pm 0.0020
Cement group#3	1.28 \pm 0.22	8.43 \pm 1.37	0.0507 \pm 0.0039
Cement group#4	1.46 \pm 0.17	9.64 \pm 0.81	0.0537 \pm 0.0005
Cement group#5	0.84 \pm 0.36	6.11 \pm 2.25	0.0499 \pm 0.0058
Cement group#6	0.83 \pm 0.09	6.02 \pm 0.50	0.0495 \pm 0.0024
Fast cyclic propagation			
Cement group#1	1.27 \pm 0.22	8.49 \pm 1.02	0.0509 \pm 0.0042
Cement group#2	1.89 \pm 0.13	12.08 \pm 1.02	0.0569 \pm 0.0023
Cement group#3	1.94 \pm 0.12	11.88 \pm 0.89	0.0552 \pm 0.0040
Cement group#4	2.09 \pm 0.05	12.51 \pm 0.18	0.0617 \pm 0.0027
Cement group#5	1.80 \pm 0.06	10.59 \pm 0.29	0.0550 \pm 0.0020
Cement group#6	1.76 \pm 0.05	11.19 \pm 1.08	0.0578 \pm 0.0028
Sudden fracture			
Cement group#1	0.17 \pm 0.03	1.46 \pm 0.59	0.0328 \pm 0.0023
Cement group#2	0.39 \pm 0.14	3.84 \pm 1.58	0.0567 \pm 0.0029
Cement group#3	1.21 \pm 0.75	8.89 \pm 3.41	0.0541 \pm 0.0036
Cement group#4	1.67 \pm 0.28	10.51 \pm 0.96	0.0600 \pm 0.0013
Cement group#5	0.75 \pm 0.26	6.08 \pm 1.35	0.0482 \pm 0.0090
Cement group#6	0.60 \pm 0.13	6.33 \pm 0.70	0.0533 \pm 0.0015

Figures (IV.6a-IV.6c) show examples of the effect of the observer on the roughness measurement parallel to the crack growth (i.e. 0°). It seems that roughness measurement is operator independent. In fact, the observer effect was not statistically significant (Factorial ANOVA, $p=0.7$ while, the statistical model had an overall significance when $p<0.0005$).

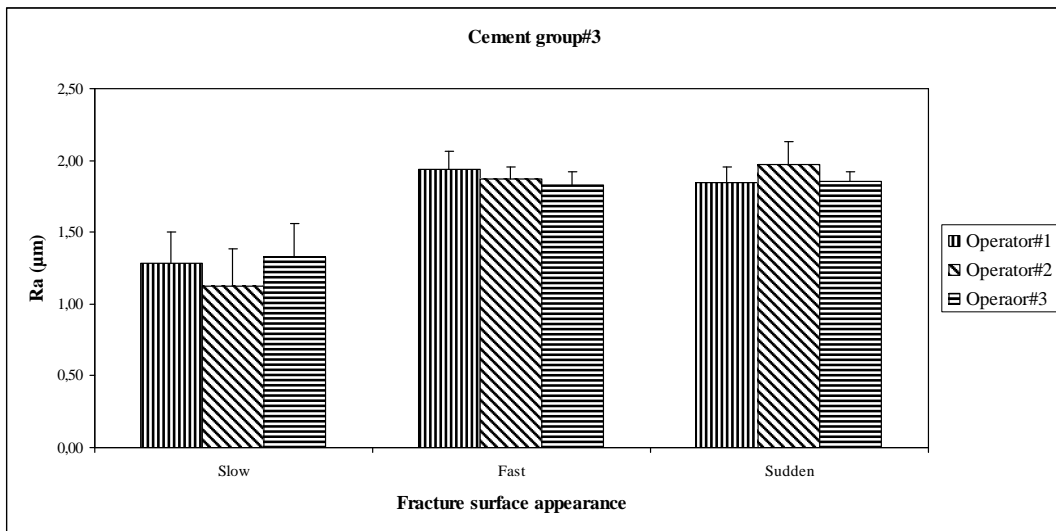
In the slow cyclic propagation zone, the Ra roughness was generally lower when measurements were taken parallel to the crack growth (0°), higher values were found at 45° (from the direction of crack growth), and even slightly at 90°. These results are depicted in Figure IV.7 for the groups tested. Conversely, the differences seen above were not pronounced in the two subsequent regions (fast and sudden) ($p>0.5$) as outlined in Figures (IV.8 & IV.9). Scanning direction effect was quite small in absolute terms (see Annex three). From these results, it appears that the slow crack propagation has a relatively smooth appearance which is in agreement with the direction roughness dependence (see later).

After collecting all measurements concerning Ra, for all cements tested Figure IV.10 will result, from which, one can say that:

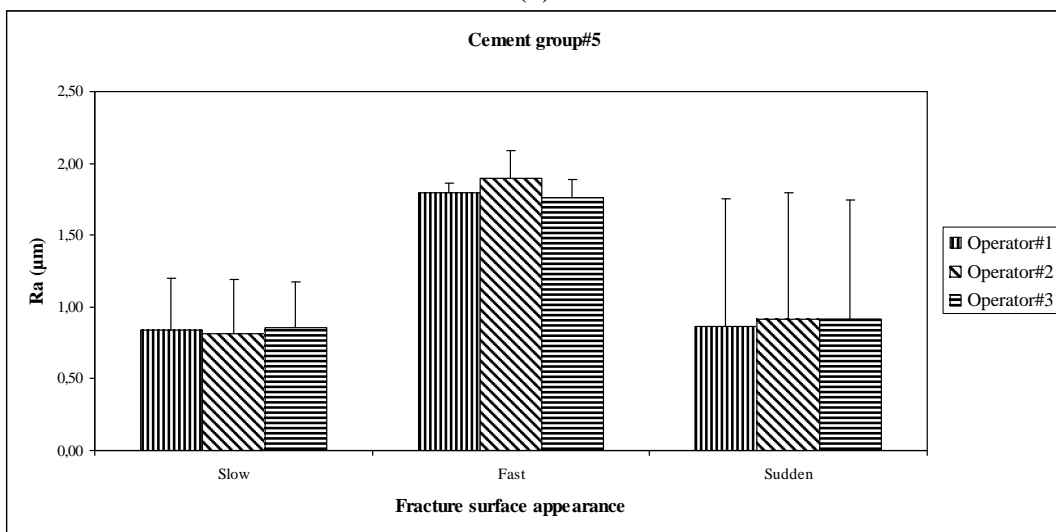
Surface roughness changed greatly in relation to the cement type and crack growth rate (slow, fast, and sudden).



(a)



(b)



(c)

Figure IV.6 Operators effect on Roughness measurement parallel to the crack growth (0°) for FCP specimens.

Therefore, roughness indicator Ra can discriminate between the crack growth zones ($p < 0.0005$) as outlined in table IV-3 and cements ($p < 0.0005$) as seen in table IV-4 (See again Annex three).

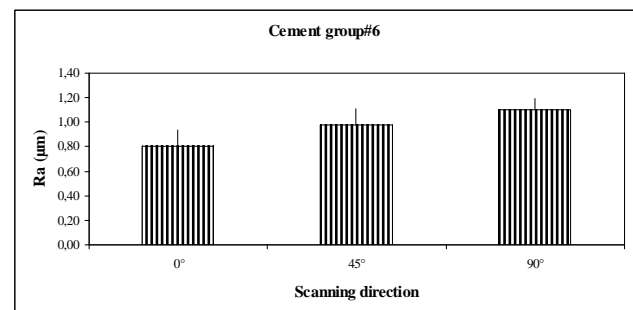
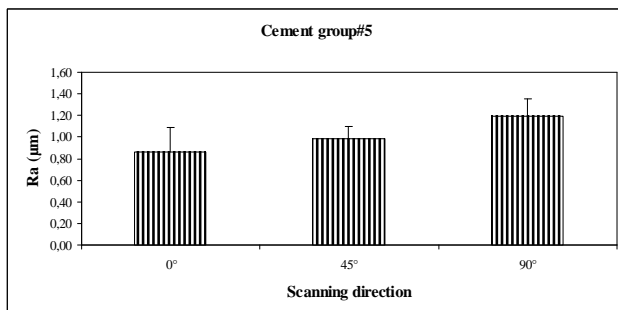
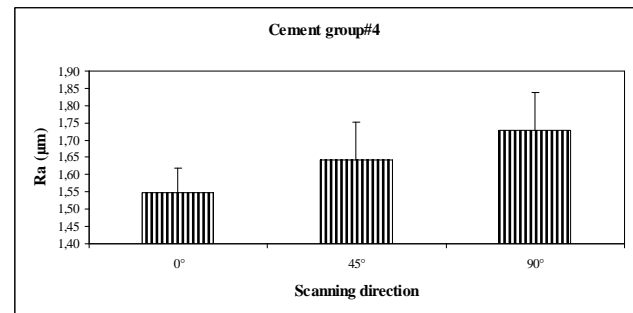
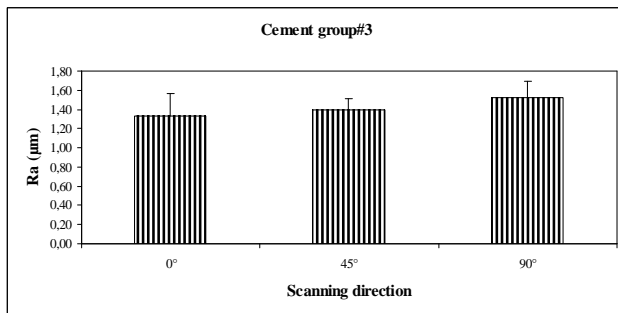
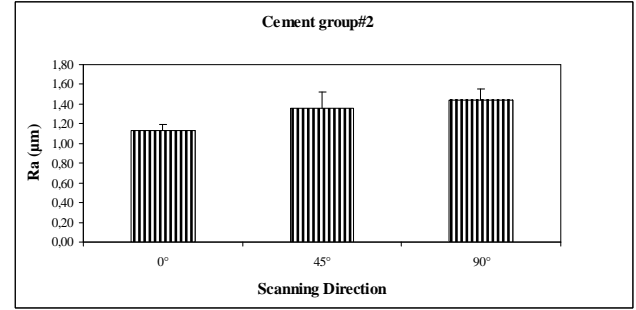
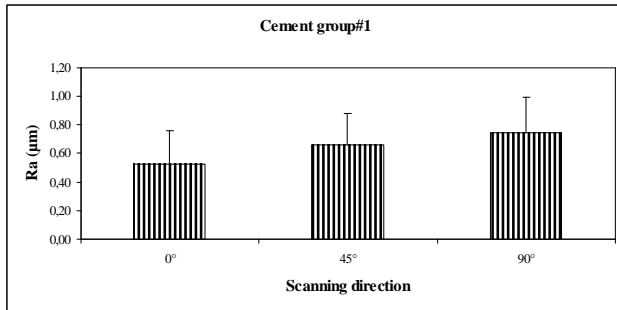


Figure IV.7 Scanning direction effect on roughness measurement for all cements tested 1-Slow region.

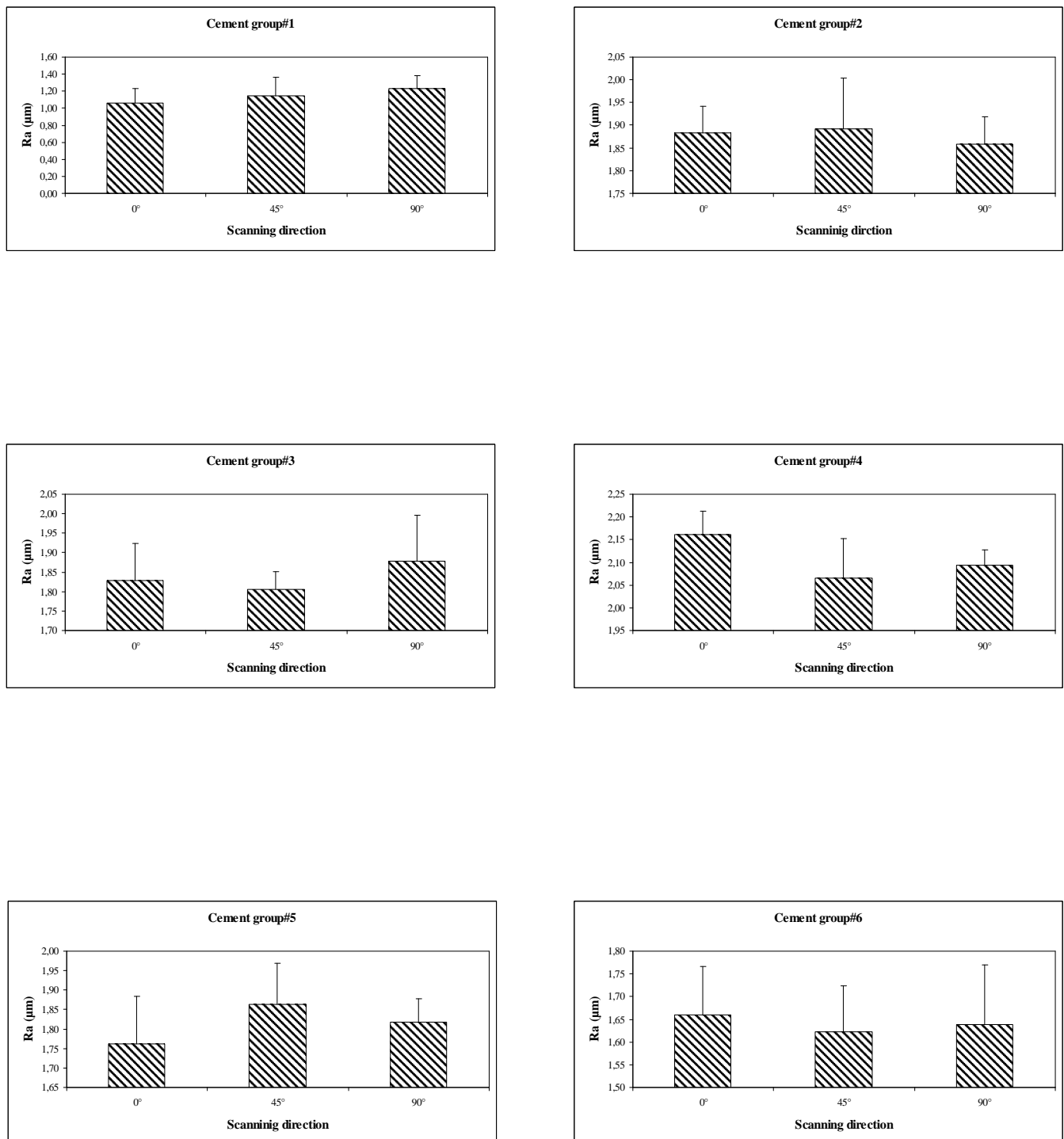


Figure IV.8 Scanning direction effect on roughness measurement for all cements tested 2-Fast region.

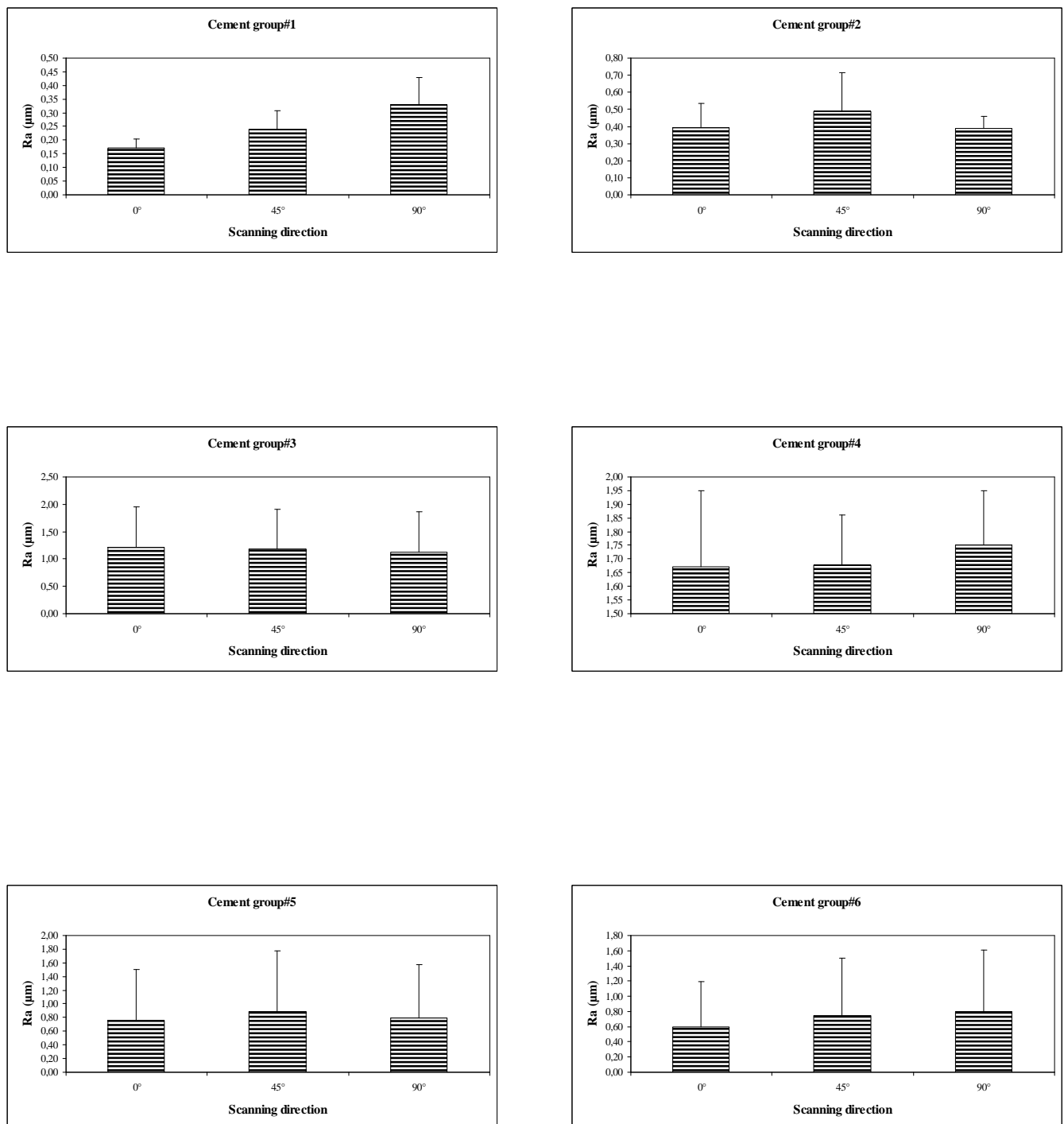


Figure IV.9 Scanning direction effect on roughness measurement for all cements tested 3-Sudden region.

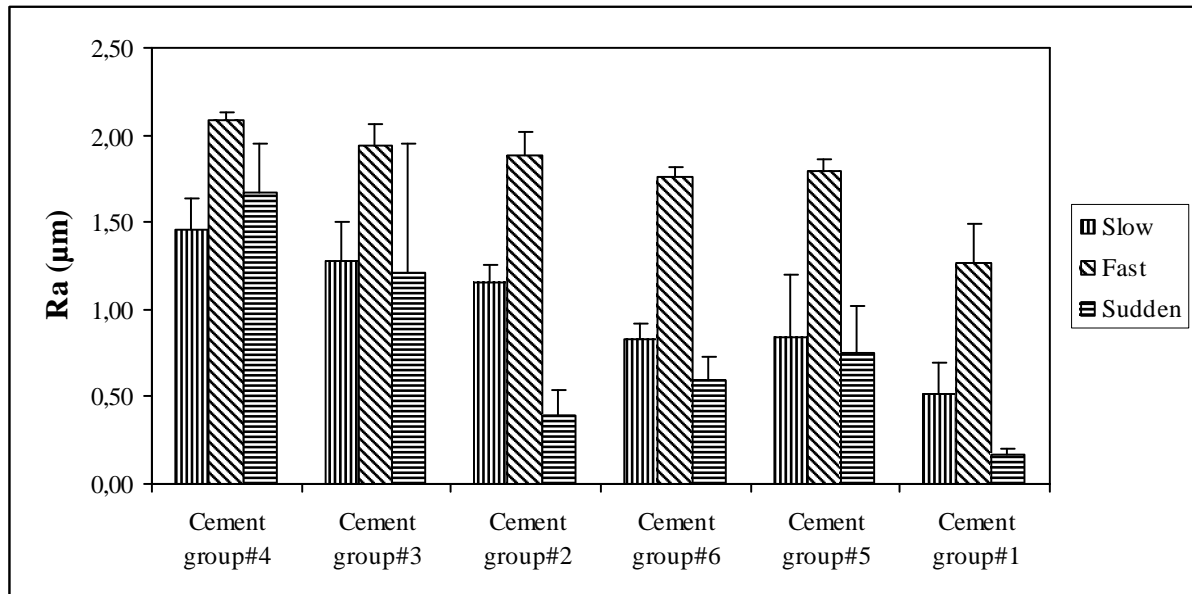


Figure IV.10 Roughness measurement (Ra) for all cements tested.⁽¹⁷⁹⁾

Table IV-3 Significance of the crack surface roughness indicator Ra.

Cement Group#1		Cement Group#2	
Crack Growth Rate	P-Value	Crack Growth Rate	P-Value
Fast, Slow	<.0001	Fast, Slow	<.0001
Fast, Sudden	<.0001	Fast, Sudden	<.0001
Slow, Sudden	<.0001	Slow, Sudden	<.0001
Cement Group#3		Cement Group#4	
Crack Growth Rate	P-Value	Crack Growth Rate	P-Value
Fast, Slow	<.0001	Fast, Slow	<.0001
Fast, Sudden	<.0001	Fast, Sudden	<.0001
Slow, Sudden	0.2306	Slow, Sudden	0.0072
Cement Group#5		Cement Group#6	
Crack Growth Rate	P-Value	Crack Growth Rate	P-Value
Fast, Slow	<.0001	Fast, Slow	<.0001
Fast, Sudden	<.0001	Fast, Sudden	<.0001
Slow, Sudden	0.5619	Slow, Sudden	0.0177

Significance level: 5%

ANOVA factorial

Table IV-4 Statistical analysis (Bonferroni tests) for Ra and cement types.

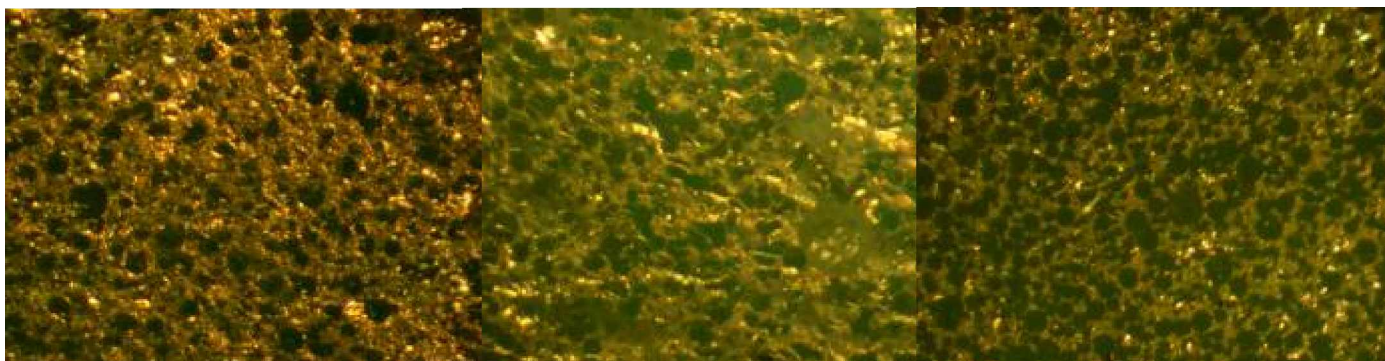
(I) Cement	(J) Cement	Mean difference (I-J)	Std. Error	Sig.
Cement group#2	Cement group#6	8.950E-02	0.042	.479
	Cement group#4	-.6002*	0.042	.000
	Cement group#3	-.2752*	0.042	.000
	Cement group#1	.4683*	0.042	.000
	Cement group#5	-2.3714E-02	0.042	1.000
Cement group#6	Cement group#2	-8.9496E-02	0.042	.479
	Cement group#4	-.6897*	0.042	.000
	Cement group#3	-.3647*	0.042	.000
	Cement group#1	.3788*	0.042	.000
	Cement group#5	-.1132	0.042	.101
Cement group#4	Cement group#2	.6002*	0.042	.000
	Cement group#6	.6897*	0.042	.000
	Cement group#3	.3250*	0.042	.000
	Cement group#1	1.0684*	0.042	.000
	Cement group#5	.5765	0.042	.000
Cement group#3	Cement group#2	.2752*	0.042	.000
	Cement group#6	.3647*	0.042	.000
	Cement group#4	-.3250*	0.042	.000
	Cement group#1	.7434*	0.042	.000
	Cement group#5	.2515*	0.042	.000
Cement group#1	Cement group#2	-.4683*	0.042	.000
	Cement group#6	-.3788*	0.042	.000
	Cement group#4	-1.0684*	0.042	.000
	Cement group#3	-.7434*	0.042	.000
	Cement group#5	-.4920*	0.042	.000
Cement group#5	Cement group#2	2.371E-02	0.042	1.000
	Cement group#6	.1132	0.042	.101
	Cement group#4	-.5765*	0.042	.000
	Cement group#3	-.2515*	0.042	.000
	Cement group#1	.4920*	0.042	.000

Based on observed means.

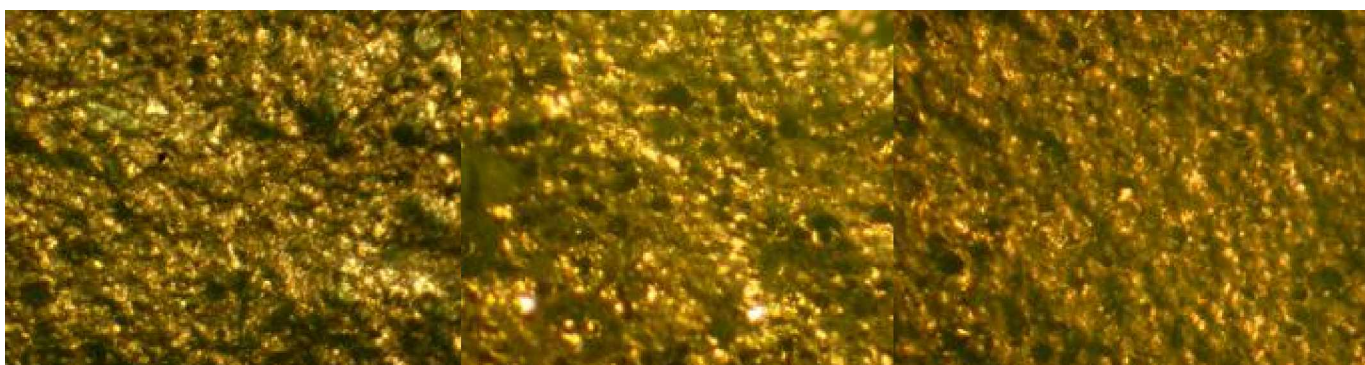
*The mean difference is significant at the 0.05 level.

IV.3 Count of cleaved pre-cured beads

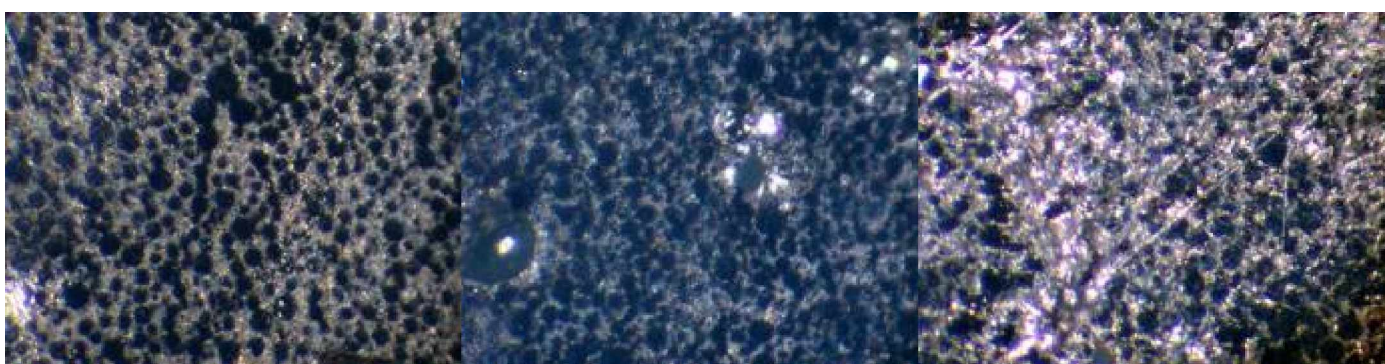
A difference in the microscopic fracture surface appearance was shown as the crack propagation progressed (see Figure IV.11). In general, more cleaved pre-cured beads were found in both the slow cyclic and catastrophic regions, a fewer in the fast cyclic region. The difference in microscopic appearance varied from one cement type to another (see again Figure IV.11).



(a) Slow



(b) Fast



(c) Sudden

Cement group#1

Cement group#2

Cement group#5

Figure IV.11 Microscopic fracture surfaces of cement group#1, cement group#2 and cement group#5; more cleaved pre-cured beads were found in the catastrophic fracture, fewer in the fast cyclic propagation region, intermediate in the slow cyclic propagation zone.

Taking good images “in focus” was not so easy to do. It was time consuming, especially, for the fast regions which were irregular and not flat. In reality we (I and my colleagues) have found a lot of difficulties in taking images of these zones because of the irregularities shown by these surfaces. This observation was consistent with Ra measurements (roughest regions).

To quantify the amount of pre-cured beads that were cleaved, the ratio between the fracture area and the area covered by cleaved beads was computed (using semi automated softwares) over the sample region of 1 mm², for each cement type and each region (see Table IV-5).

Table IV-5 Percentage of cleaved beads in the fractured surface regions carried out by one operator.

Slow cyclic propagation region	
Cement types	Percentage of cleaved beads (%)
Cement group#1	30 ± 4.7
Cement group#2	34 ± 4.1
Cement group#3	32 ± 13.2
Cement group#4	28.6 ± 3.2
Cement group#5	28 ± 11.9
Cement group#6	27.8 ± 10.5
Fast cyclic propagation region	
Cement group#1	3 ± 0.9
Cement group#2	3 ± 0.7
Cement group#3	2 ± 0.9
Cement group#4	2.8 ± 0.8
Cement group#5	2 ± 0.8
Cement group#6	3.4 ± 0.9
Sudden fracture	
Cement group#1	28 ± 5.4
Cement group#2	31 ± 8.6
Cement group#3	20 ± 19.1
Cement group#4	4 ± 1.6
Cement group#5	25 ± 15.0
Cement group#6	38 ± 5.1

Inter-observer reproducibility was excellent; variability between the three observers was on average of 3.4% of the total area.⁽¹⁷⁸⁾ Moreover, the effect of the observer was not statistically significant since p=0.9 (Factorial ANOVA). However, it was found that correct training of the observer to distinguish between cleaved-pre-cured beads and cement porosity was very demanding and extremely critical. Figure IV.12 shows one observer’s results obtained for all cements tested. In slow cyclic region the amount of cleaved beads range from 27% to 34%. In the fast it varies from 1% to 3% and in the last zone the percentage varies from 4% to 38%. The amount of cleaved pre-cured beads varied greatly in relation to the cement type and crack propagation rate. These results are given in Figure IV.13.

The interaction between cement and crack type was statistically significant (see Table IV-6) confirming that different trends along the crack path should be expected in relation to the cement type.⁽¹⁷⁸⁾ *In the first and last regions the crack propagates through the beads and inter-bead matrix without preference while it tends to propagate through the inter-bead matrix in the fast cyclic propagation.*

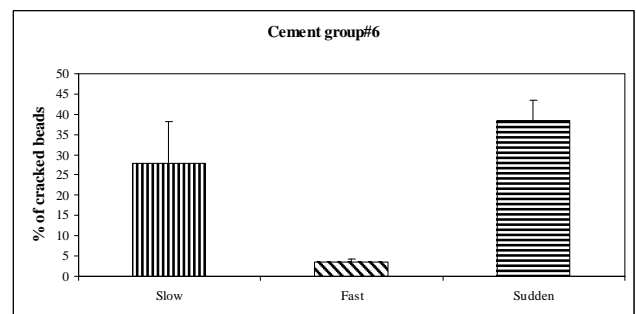
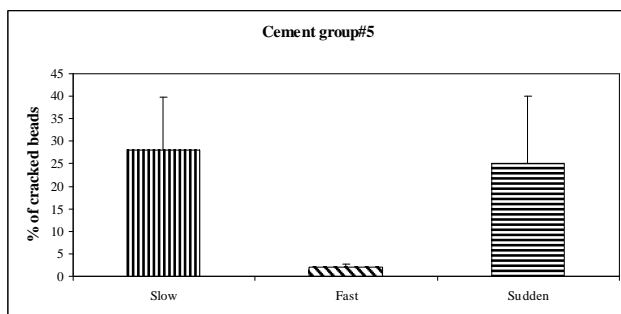
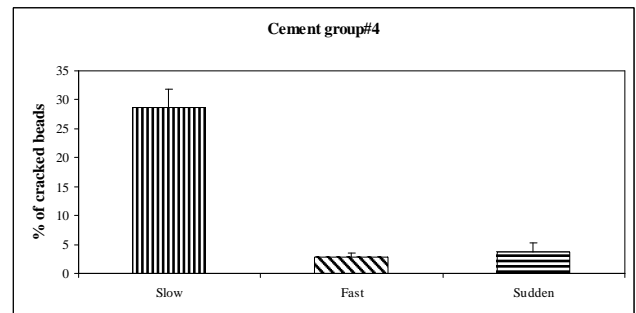
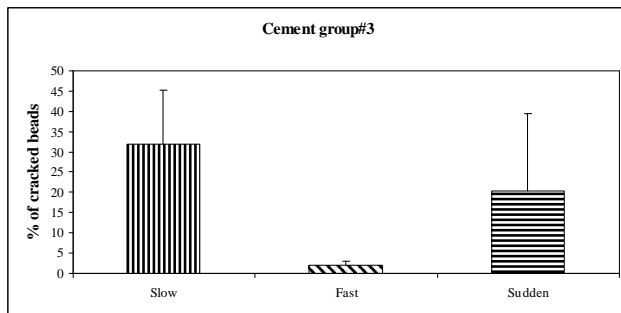
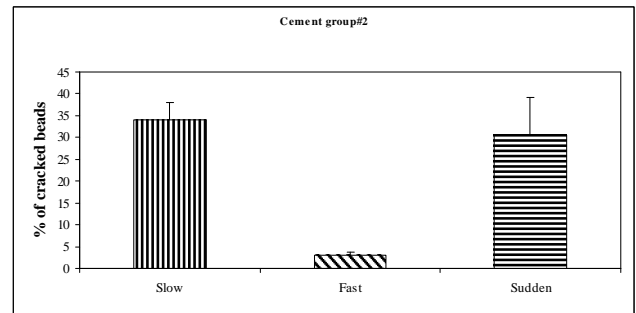
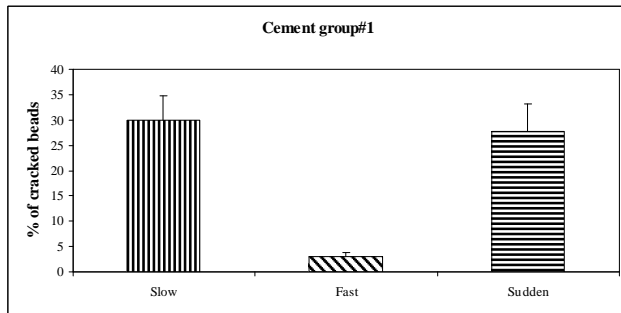


Figure IV.12 Percentage (%) of cracked beads per cement type.

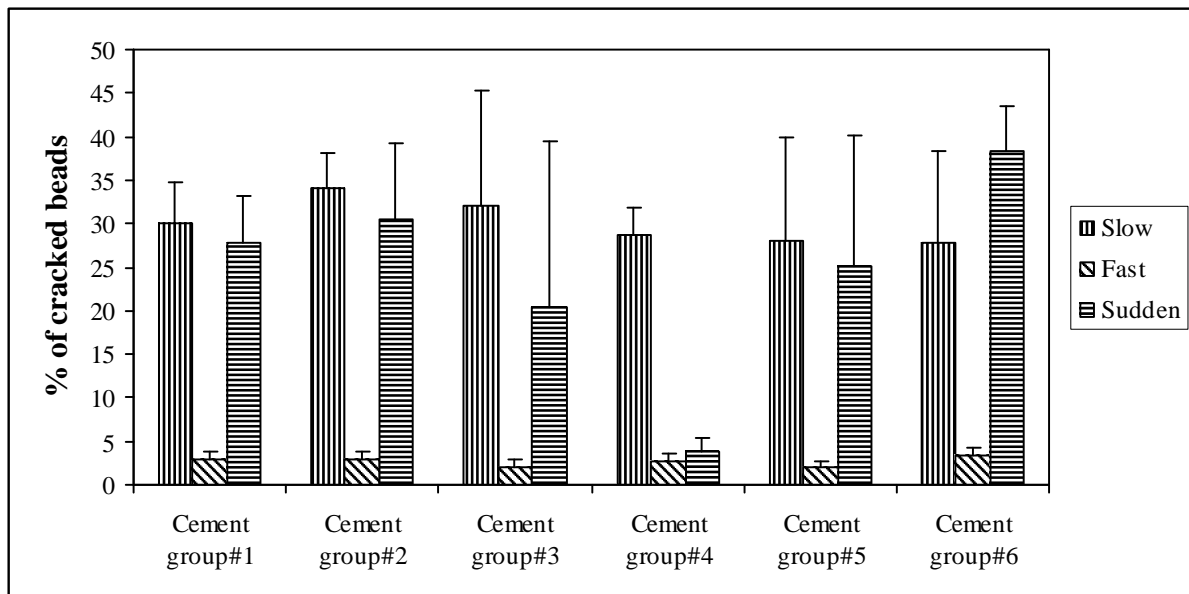


Figure IV.13 Percentage (%) of cracked beads per regions for all cemented tested.⁽¹⁷⁹⁾

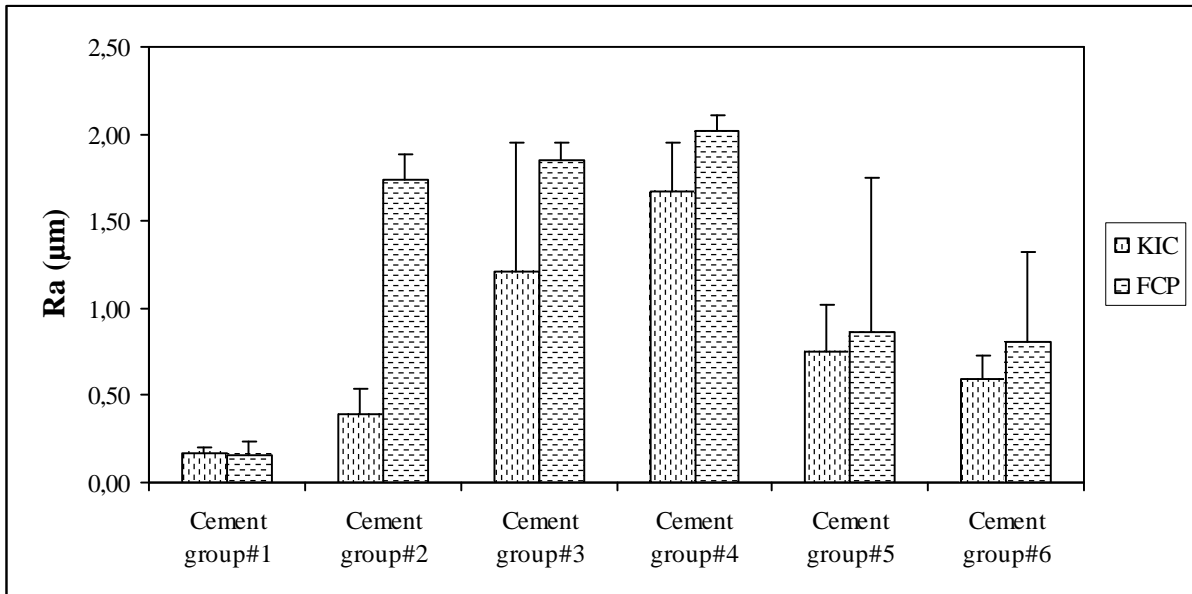
Table IV-6 Significance of the crack surface cleaved beads indicator.

Cement Group#1		Cement Group#2	
Crack Growth Rate	P-Value	Crack Growth Rate	P-Value
Fast, Slow	<0.0005**	Fast, Slow	<0.0005**
Fast, Sudden	<0.0005**	Fast, Sudden	<0.0005**
Slow, Sudden	>0.999	Slow, Sudden	>0.999
Cement Group#3		Cement Group#4	
Crack Growth Rate	P-Value	Crack Growth Rate	P-Value
Fast, Slow	<0.0005**	Fast, Slow	<0.0005**
Fast, Sudden	<0.0005**	Fast, Sudden	<0.0005**
Slow, Sudden	=0.39	Slow, Sudden	=0.86
Cement Group#5		Cement Group#6	
Crack Growth Rate	P-Value	Crack Growth Rate	P-Value
Fast, Slow	<0.0005**	Fast, Slow	<0.0005**
Fast, Sudden	<0.0005**	Fast, Sudden	<0.0005**
Slow, Sudden	=0.10	Slow, Sudden	=0.20

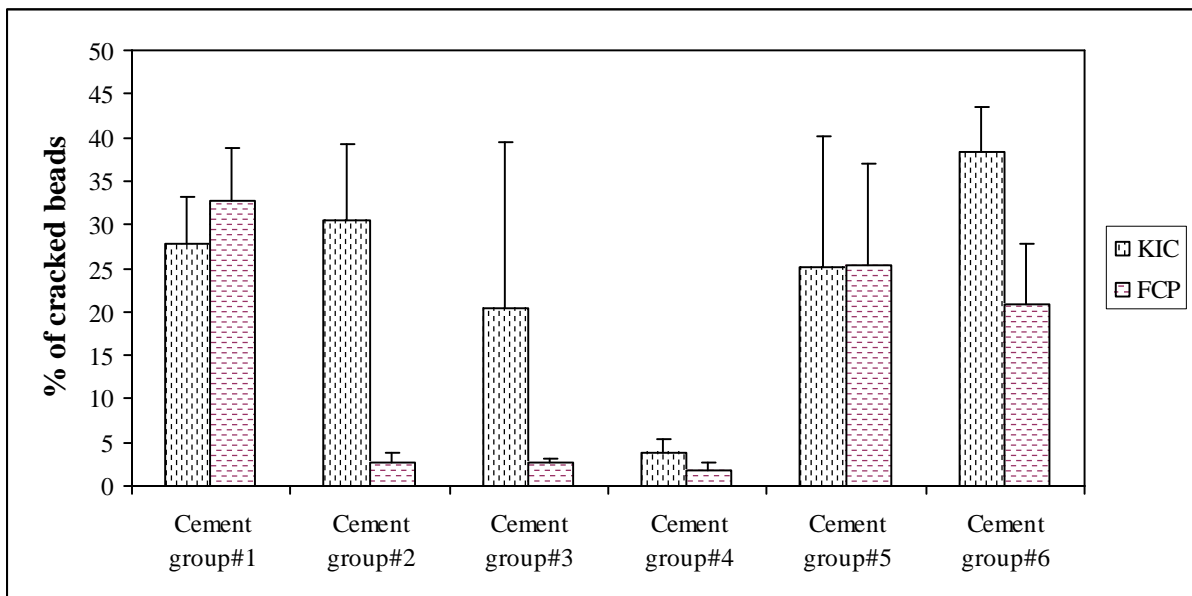
** indicates highly significant difference ($p < 0.01$).

When comparing Table IV-3 to Table IV-6, it seems that roughness indicator (automated calculation) is more accuracy than cleaved beads indicator (semi automated calculation) that includes operator calculation of the fractured beads.

During fatigue loading tests (performed on FCP specimens) micro-cracks were developed in the fast region of all (FCP) specimens tested giving the roughest appearance to the fractured surfaces corresponding to this zone (resulting from coalescence of the microcracks). These microcracks seemed to extend to the smaller third zone which appeared to be rougher in certain specimens as outlined in Figures (IV. 14a & IV.14b). For this reason K_{IC} specimens were used to analyze the unstable fractured zone. Additionally, the catastrophic fracture in the FCP specimens was smaller than that of the K_{IC} specimens (see Figure IV.2 above).



(a) Roughness indicator

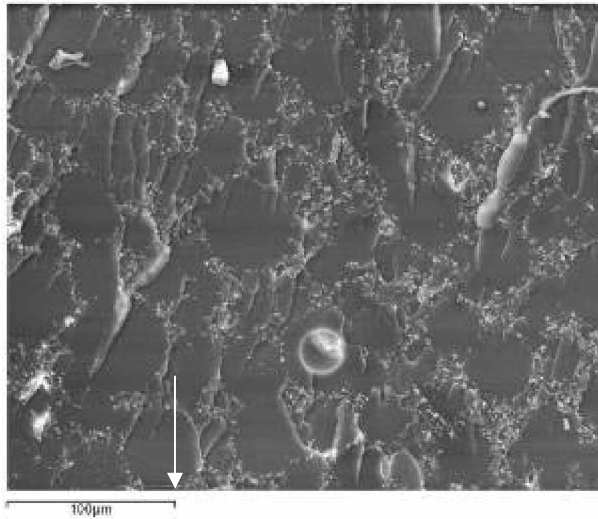


(b) Cleaved beads indicator

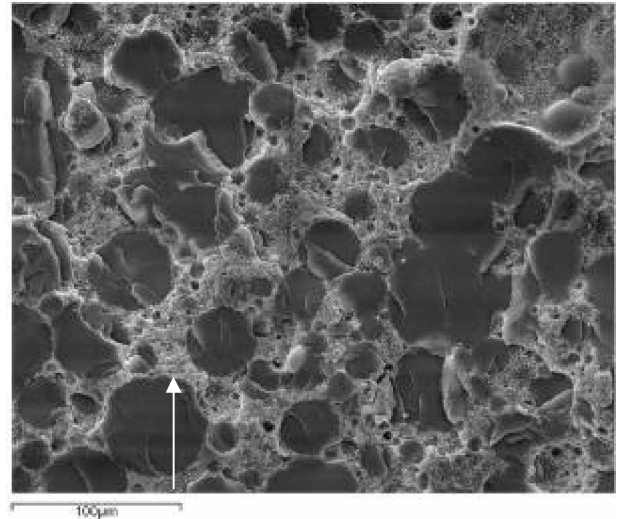
Figure IV.14 Reasons of choose of K_{Ic} specimens rather than FCP specimens.

IV.4 Fractography

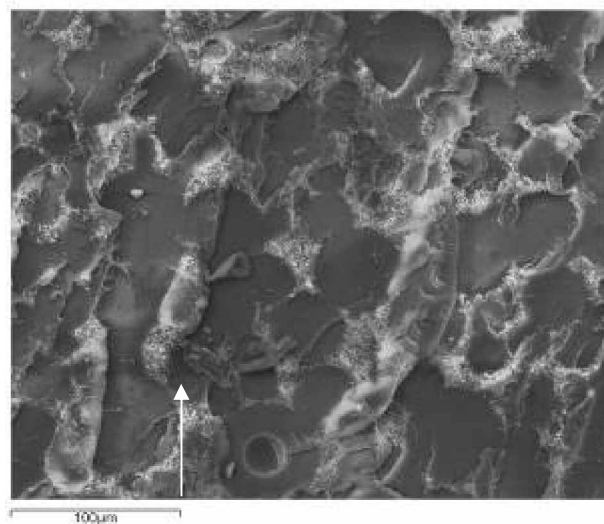
Representative specimens for the SEM analysis were chosen randomly. Three different morphologies of the fractured surface in relation with the crack propagation rate were shown by SEM for all cements tested. This qualitative inspection was found to be consistent with the above quantitative analyses (roughness measurement, amount of cleaved beads through the fractured surface). The slow cyclic propagation surface of bone cements tested was relatively smooth. Examples of the slow cyclic propagation surfaces examined under the SEM are illustrated in Figure IV.15.



(a) Cement group#1



(b) Cement group#4



(c) Cement group#2

Figure IV.15 Slow cyclic propagation morphology of three bone cements tested in air at 37°C.

(a) Cement group#1, (b) Cement group#4, and (c) Cement group #2.

Cement group#1 shows the smoothest surface.

The tailed arrow indicates the direction of crack propagation.

These pictures reveal that surgical PMMA are biphasic materials. Indeed, acrylic bone cement is a composite of spherical particles; PMMA beads (dark regions in the micrographs) embedded in a matrix of polymerized methylmethacrylate monomer. The bead cross sections were outlined by the lighter, BaSO₄, containing matrix.

These micrographs show a mixed mode of failure in the slow region with areas of transgranular (cleaved PMMA beads) and intergranular (crack propagation through the matrix) failure.

The beads were fractured in a mixed brittle and ductile mode (tensile tearing) as outlined in Figure IV.16. This fracture morphology was seen by Bhambri et al.⁽³⁷⁾ Moreover, the microcracks emanating from BaSO₄ particles may either result in a completely fracture of the bead (brittle mode) or in beads where a ligament remains unbroken which tears off under the applied load.

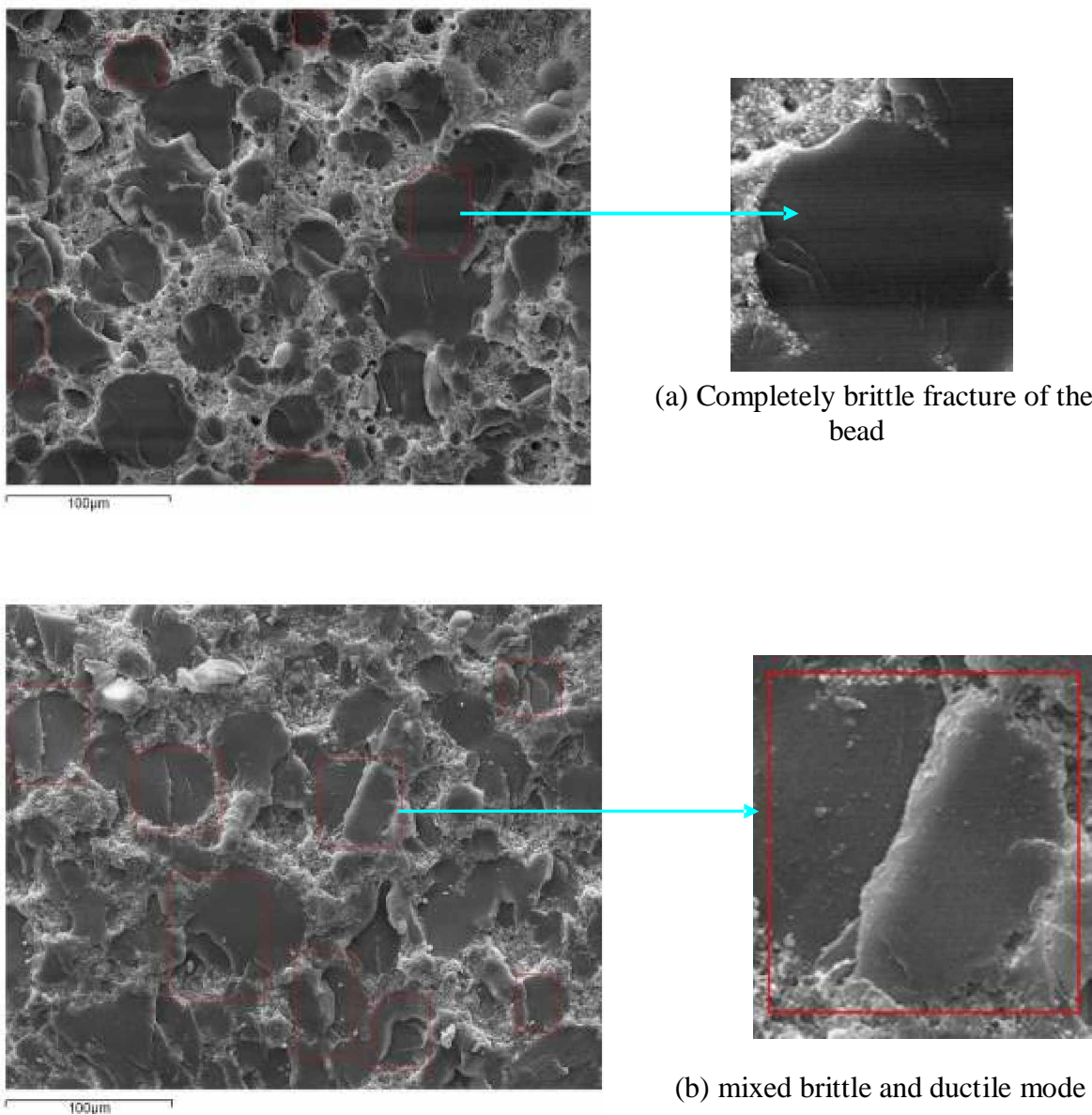
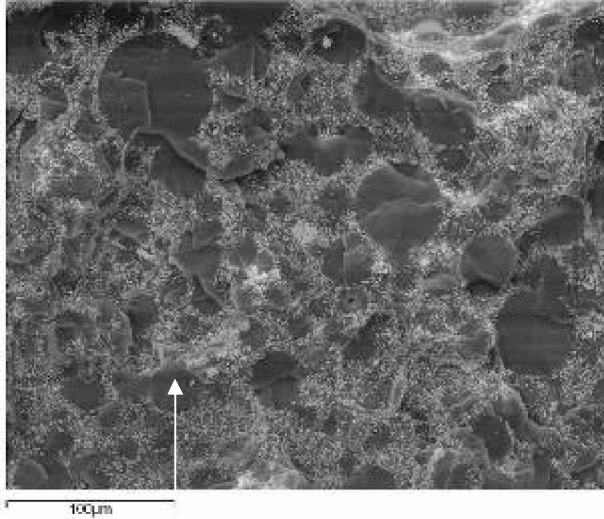


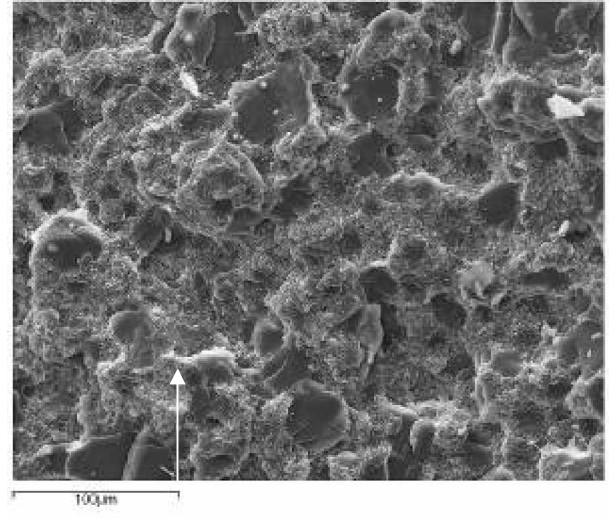
Figure IV.16 Fracture morphology of PMMA beads observed during slow cyclic propagation.

The stress intensities produced in acrylic cements tested under fatigue were apparently sufficient to propagate through the polymer beads in the slow propagation zone giving a relatively smooth appearance to this region. These important stress intensities may be attributed to the size of the pre-cracked notch 'a'.

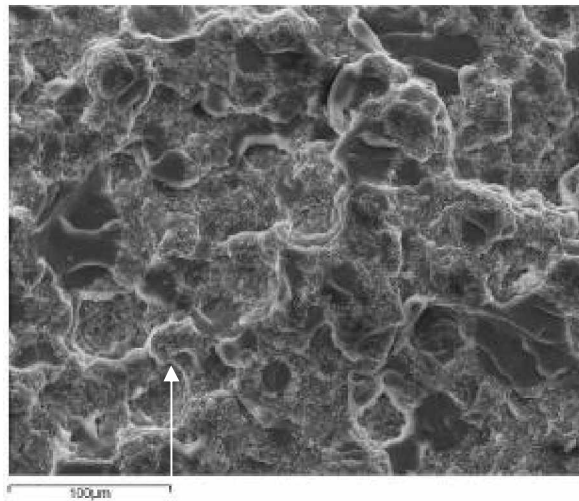
The fast fatigue crack morphology of the cements tested was rougher. Examples can be seen in Figure IV.17.



(a) Cement group#2



(b) Cement group#3



(c) Cement group#5

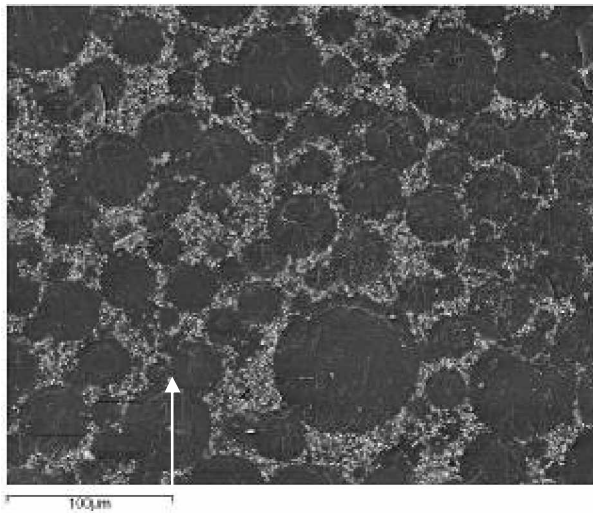
Figure IV.17 Fast cyclic propagation morphology of three bone cements tested in air at 37°C. (a) Cement group#2, (b) Cement group#3, and (c) Cement group #5.

The tailed arrow indicates the direction of crack propagation.

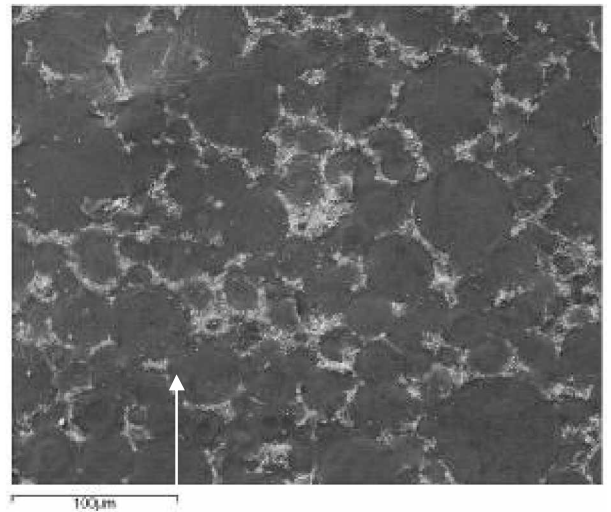
Although some sectioned PMMA beads were present, the crack propagated mainly within the matrix surrounding the beads. Again, these observations were consistent with the above quantitative analyses. The moving crack followed paths of weakness between spherical PMMA beads instead of sectioning them, resulting in a multi-plane fracture regions (rougher

aspect). The interbead matrix are weakened by the existence of the following factors (as reported by Topoleski et al.⁽³⁹⁾): BaSO₄ particles, Porosity, Residual stresses due to the shrinkage of the matrix. Microcracks, giving the roughest aspect to the fast region, were developed in all directions. This appearance may explain why the roughness measurement was independent of the direction of scanning (found in section IV.2 Roughness measurement).

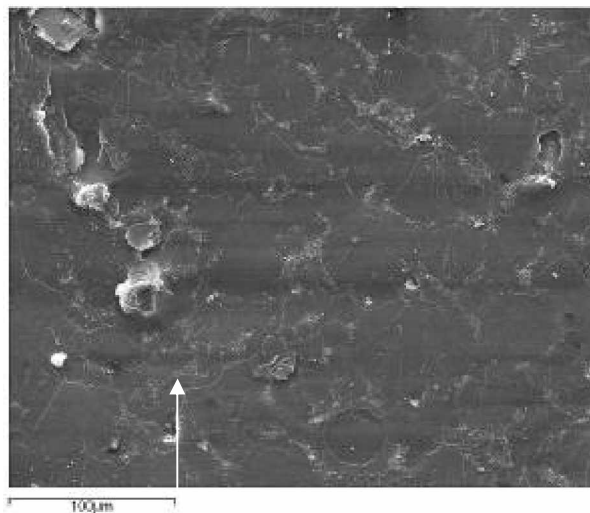
Flat surface morphology was seen in the regions of final fracture of all tested specimens except for the cement group#4. Examples of these flat surfaces were depicted in Figure IV.18. This surface inspection was in agreement with roughness measurement data (seen above). The flat surface appearance revealed that roughness was direction independent (result obtained in section IV.2 Roughness measurement).



(a) Cement group#1



(b) Cement group#3



(c) Cement group#6

Figure IV.18 Sudden fracture morphology of three bone cements tested in air at 37°C. (a) Cement group#1, (b) Cement group#3, and (c) Cement group#6. The tailed arrow indicates the direction of crack propagation.

During catastrophic fracture, where the stress intensity was greater than the critical stress intensity of the material, the unstable moving crack cut straight through the beads leaving them smooth and their surface flat. Moreover, bead crazing was observed in cement group#1, cement group#5 and cement group#6 (see Figure IV.18). This result was also reported by Topoleski et al.,⁽³⁹⁾ who attributed it to the greater polymer chain entanglement of the beads.

Figure IV.19 shows sudden fracture morphology of bone cement group#4. The crack propagated through the beads and interbead matrix without preference. The multiplane fracture of the beads gave the roughest aspect to this zone, which, explained the highest value of Ra and the lowest percentage of cleaved beads found above (last two sections).

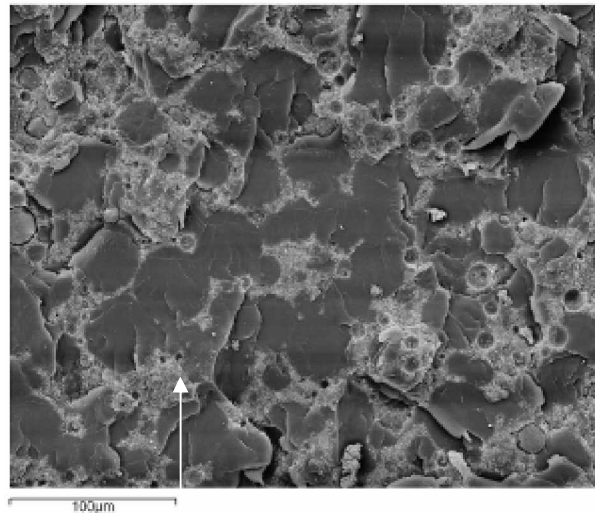


Figure IV.19 Sudden fracture morphology of Cement group#4 tested in air at 37°C. The crack propagated through the beads and interbead matrix without preference. The fractured surface is rough. The tailed arrow indicates the direction of crack propagation.

In fact, when analyzing digital micrographs (low magnification) related to this region, it was difficult to well distinguish fractured beads (see Figure IV.20).

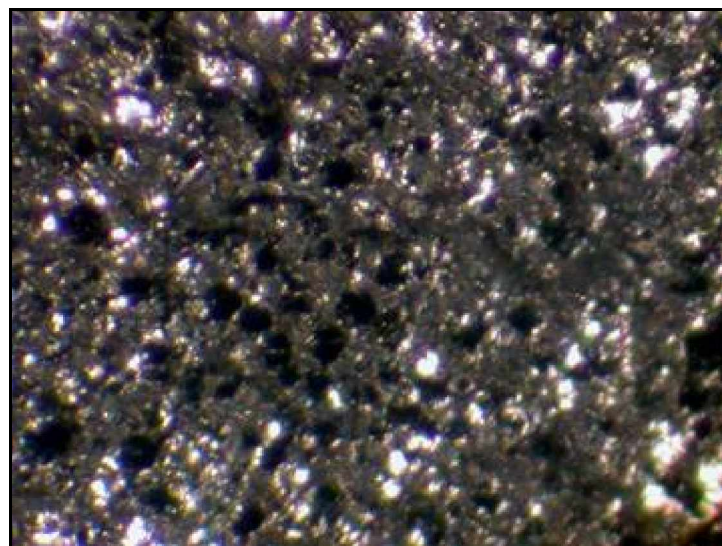


Figure IV.20 Sudden microscopic fracture surface of cement group#4.

Again, (%) of cracked beads indicator was less powerful than roughness indicator.

When analysing the cements tested porosity (see Table IV-7), it appears that cement group#4 and cement group#6 present the highest porosity.

Table IV-7 Porosity of the samples analyzed.⁽¹⁷⁵⁾

Cement types	Pore interval radius (μm)	Total porosity (%)
Cement group#1	0.0036 ÷ 26.87	7.80
Cement group#2	0.0053 ÷ 30.75	9.29
Cement group#3	0.0036 ÷ 30.75	7.26
Cement group#4	0.0036 ÷ 32.11	33.22
Cement group#5	0.0036 ÷ 29.50	7.41
Cement group#6	0.0036 ÷ 25.02	29.43

Referring to Figure IV.10, it can be said that experimental group#4 shows the roughest appearance in all three zones (slow, fast and sudden). The same cannot be said for cement group#6 despite its high porosity. Therefore, the roughest morphology of the fractured surface of the cement group#4 may be attributed to the antibiotic containing cement.

When comparing the fractured surface appearance during cyclic propagation of the five remaining cements (same components); cement group#1, 2, 3, 5 and 6, it appears that cement group#3 presents the roughest one, while, cement group#1 is the smoothest one. Moreover, in Table IV-8, for comparison, are data showing the morphological characteristics of the cements analysed. It appears that fatigue surface appearance is affected by the size of the PMMA beads. In the cement containing larger PMMA beads, the fracture surface was rougher than that containing smaller beads (see Figure IV.10).

Table IV-8 Morphological characteristics of the cements tested from Cotifava.⁽¹⁷⁵⁾

Cement types	d_{average} (μm)
Cement group#1	37
Cement group#2	48
Cement group#3	51
Cement group#4	45
Cement group#5	44
Cement group#6	45

This observation was in agreement with the results of Genebra et al.⁽¹⁶¹⁾ No relation was found between particle size and sudden fracture morphology.

In general, the effect of BaSO₄ particles on the fracture surface appearance of the cements tested was not clear in this study. An observation can be made for cement group#3 which had

the highest concentration of BaSO₄ (13%). The fractured surface of this cement was the roughest one.

Fragments of bone cement may be liberated during fast cyclic propagation (irregular surface) leading to the failure of the Arthroplasty. Furthermore, the cements debris may migrate to the surrounding tissue (biological reaction), well before bone cement fractures are radiographically distinguishable, and accelerate the failure of the Arthroplasty due to osteolysis.^(61,63) In general, no fragments were recorded during sudden fracture "flat surface".

Inspection of the fractured surface of fatigue crack propagation (FCP) and K_{IC} specimens was carried out for six different cement types, using three different methods: two quantitative analyses based on roughness measurement, and a count (%) of cleaved pre-cured beads and a qualitative analysis using Scanning Electron Microscope (SEM).

Fractured surface roughness was easily measured using a Hommel profilometer (Hommel Tester-T8000) with turbo-roughness software for windows. Roughness parameters are automatically calculated by turbo-roughness software for windows. The second quantitative analysis is a direct measurement of the percentage of crack area covered by pre-cured beads that were cleaved. This semi automated technique allows us to know if the crack propagated through the beads or around them via digital micrographs. Fractographic analysis based on SEM is the most useful method for observing failure patterns.^(24,157,158) This technique permits a qualitative inspection of the fractured surfaces (relatively smooth, rough and smooth).

The two quantitative inspections were in agreement with SEM fractographic analysis. Roughness indicator was more powerful than cleaved beads indicator. An extremely high correlation was found between the surface roughness (Ra) and the percentage of cleaved beads (Pearson correlation coefficient =0.804, P<0.0005). Ra measurements can be used to predict the amount of cleaved beads. These indicators are inversely proportional.

Fatigue fracture topographies were found to be dependent on crack growth rate and cement formulation. Moreover, for each cement type, the fractured surface appearance can be divided in three zones relative to slow, fast and sudden fractures.

The fractured surface appearance can be divided, in relation to time, into two zones: time dependent zone followed by time independent zone. The first region corresponded to fatigue crack growth named also stable crack or slow crack, the second region corresponded to sudden fracture called also rapid fracture or unstable crack. Studies found in literature^(24,64,123,157) divided the fractured surface appearance into regions rough and smooth related to fatigue and rapid fractures respectively. The results obtained in this present study appear to be consistent with those cited above when collecting the slow and fast regions. From this investigation one can say:

At every beginning an end. All processes start with a beginning change over time; slowly at first then rapidly, followed by an end.

IV.5 Limitations

The scope of this study was to assess if roughness measurement Ra, and percentage of cleaved beads were surface inspections of bone cement fractured surfaces. The present study has some limitations. First of all, only six compositions which don't cover the most common brands on the market were investigated.

The fractured surfaces were, also, inspected using Scanning Electron Microscopy (SEM). Limitations in achieving the magnifications to visualize BaSO₄, Sodium Fluoride (NaF) and antibiotic particles prevented comprehensive analysis of the fractured surfaces.

The tests were conducted in air. Tests in a fluid medium were preferable to assess the effect of physiological environment on crack path and to facilitate in vivo comparison.

CONCLUSION

1. Synopsis

The objectives of the present study were: ⁽¹⁷⁸⁾

- 1- To identify a quantitative analysis that can objectively distinguish between different zones found on bone cement fractured surfaces. This inspection measurement should provide a numerical indicator that should be repeatable (different specimens from the same cement type should provide similar results) and reproducible (different observers must draw the same conclusions).
- 2- To assess if the morphology of the crack surface (in relation to propagation rate) depends on the cement formulation.

Qualitative descriptions of microscope observation of the fracture morphology are available in the literature, but no quantitative indicators have been proposed.

This investigation was performed on six experimental groups of PMMA bone cements namely, Simplex P, Cemex Rx, Cemex Isoplastic, Cemex Genta, Fluoride bone cement and Cemex System. A hand mixing method of bone cement preparation was applied to all cements tested. Five fatigue crack propagation (FCP) specimens were prepared for each cement type according to ASTM-E647-05 standard. Sinusoidal zero-tensile load ranging up to 60 N was applied to the test specimens at 4 Hz. Five pre-cracked K_{IC} specimens following ASTM-E339-05 standard were used for each cement type (monotonic ramp) to analyse the catastrophic failure (unstable crack). Fractured specimen surfaces with pores larger than 1 mm were discarded. To enhance contrast, the fractured surfaces of all specimens tested were gold sputter coated.

Roughness measurements, as well as measuring the percentage of cleaved beads were used as means of quantifying surface morphology in relation to the type of cracking mechanism. Fractured surface roughness was measured easily using a Hommel profilometer (Hommel Tester-T8000) with turbo-roughness software for windows. Roughness parameters (Ra, Rt and Rsm) are automatically calculated by turbo-roughness software for windows. Fifteen (15) measurements were taken by three operators for each cement analysed; parallel to crack growth (0°), at 45° and perpendicular to crack growth (90°) for each different region of the fractured surface.

Pre-cured beads in the crack surface that were cleaved during crack propagation were counted (%) in 1mm^2 using a semi automated software Q Win 2001, (Leica Microsystems, Wetzlar, Germany) and Smart view. This semi automated technique allows us to know if the crack propagated through the beads or around them via digital micrographs.

The fractured surfaces were also inspected qualitatively using Scanning Electron Microscopy (SEM). This technique is the most useful method for observing failure patterns.

The main conclusions of this study were as follows:

- 1- Roughness measurement, based on Ra indicator, cleaved pre-cured beads are quantitative inspections of fractured surfaces which lead to the same result. The average roughness indicator (Ra) based on fifteen (15) measurements was repeatable on the same specimen, reproducible between operators, direction independent, and discriminate best between fracture and cement type. A direct measurement of the percentage of crack area covered by cleaved pre-cured beads was found to be repeatable on the same specimen, reproducible between operators and discriminate between fracture and cement type.
- 2- Roughness measurement takes less time and is more accuracy (automated calculation) than the account of cleaved pre-cured beads (semi automated calculation).
- 3- Fractographic analysis based on SEM pictures of the fracture surfaces revealed differences between the cements tested. The addition of antibiotic "gentamicyn" to PMMA increases crazing and micro crack formation in contrast to the addition of copolymer.
- 4- The life is time dependent, is the death time independent?

2. Future work

Future work recommendations from this study are as follows:

- 1- More PMMA bone cement kits need to be tested and compared to see if the results of this study can be generalized to all cements available on the market today.
- 2- Different varieties of powder size distributions need to be tested in order to understand their effects on the morphology of bone cements.
- 3- Determine roughness range of each cement type.
- 4- Study of relation between crack morphology and the load conditions.
- 5- Testing in fluids could be done in order to make the testing environment as close as possible to in vivo conditions.
- 6- Use of high magnifications of SEM which allows identification of the antibiotic, fluoride sodium (NaF), BaSO₄ particles on the fracture surface and highlight certain important characteristic features of the fracture surface.
- 7- Study of the existence of a relation between K_{IC} and fracture morphology.
- 8- Study of the existence of a relation between speed of crack ($\frac{da}{dN}$) and fracture morphology.

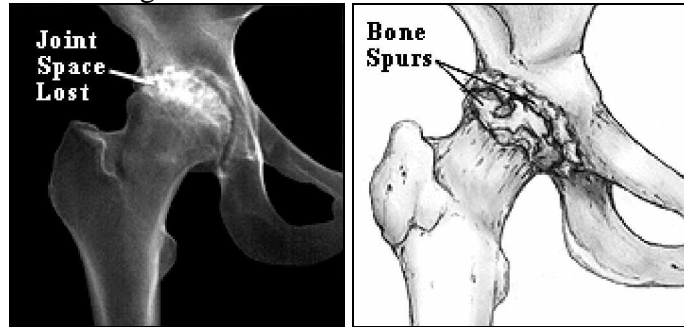
ANNEXES

1. Medical definitions

2. Mechanical and chemical definitions

3. Results”Statistical analysis”

ARTHRITIS literally means **inflammation of a joint**, but is generally used to describe any condition in which there is **damage to the cartilage**. Inflammation, if present, is in the synovium. The proportion of cartilage damage and synovial inflammation varies with the type and stage of arthritis. Usually the pain early on is due to inflammation. In the later stages, when the cartilage is worn away, most of the pain comes from the mechanical friction of raw bones rubbing on each other.



There are two broad categories of arthritis Osteoarthritis and Rheumatoid arthritis:

Osteoarthritis mainly damages the joint cartilage, but there is often some inflammation as well. It usually affects only one or two major joints (usually in the legs). **It does not affect the internal organs**. The cause of hip osteoarthritis is not known. It is thought to be simply a process of “wear and tear” in most cases. Some conditions may predispose the hip to osteoarthritis, for example, a previous fracture that involved the joint. Growth abnormalities of the hip (such as a shallow socket) may lead to premature arthritis. Some childhood hip problems later cause hip arthritis (for example, a type of childhood hip fracture known as a Slipped Epiphysis; also Legg-Perthe’s Disease). In osteoarthritis of the hip the cartilage cushion is either thinner than normal (leaving bare spots on the bone), or completely absent. Bare bone on the head of the femur grinding against the bone of the pelvic socket causes **mechanical pain**. Fragments of cartilage floating in the joint may cause **inflammation in the joint lining**, and this is a second source of pain. X-rays show the “joint space” to be narrowed and irregular in outline. There is no blood test for osteoarthritis.

Rheumatoid Arthritis (R.A.) starts in the synovium and is mainly “inflammatory”. The cause is not known. It eventually destroys the joint cartilage. Bone next to the cartilage is also damaged; it becomes very soft (frequently making the use of an uncemented implant impossible). R.A. affects **multiple joints simultaneously**. It also **affects internal organs**. Another form of hip arthritis that is mainly “inflammatory” is *Lupus*. There are other more rare forms of arthritis that are also mainly “inflammatory”. They are basically similar to R.A.. X-ray changes in R.A. are essentially similar to osteoarthritis plus a loss of bone density.

BIOCOMPATIBILITY

is related to the behavior of biomaterials in various contexts. The term may refer to specific properties of a material without specifying where or how the material is used(for example, that it elicits little or no immune response in a given organism, or is able to integrate with a particular cell type or

tissue), or to more empirical clinical success of a whole device in which the material or materials feature.

Biocompatibility is difficult to measure, it is defined in terms of success at a specific task.

BIOMATERIALS

is not a new area of science, having existed for around half a century. The study of biomaterials is called biomaterial science. It is a provocative field of science, having experienced steady and strong growth over its history, with many companies investing large amounts of money into the development of new products. Biomaterial science encompasses elements of medicine, biology, chemistry, tissue engineering and materials science.

“A biomaterial is any material, natural or man-made, that comprises whole or part of a living structure or biomedical device which performs, augments, or replaces a natural function”.

BONE RESORPTION

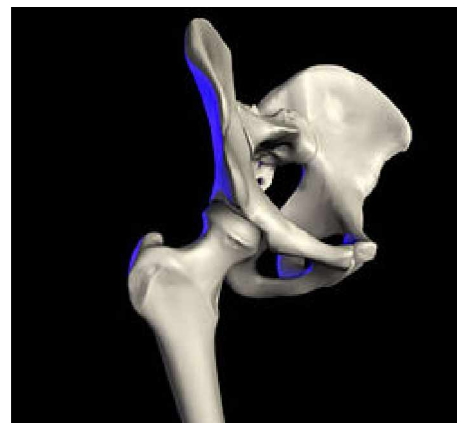
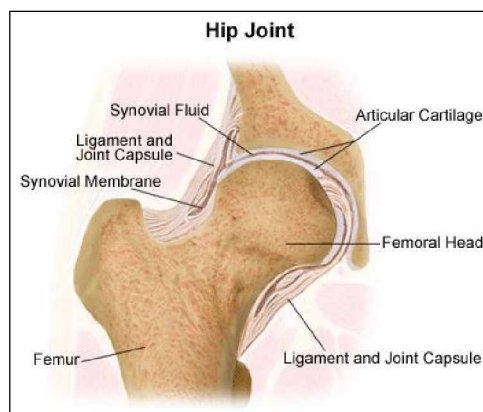
is the process by which osteoclasts break down bone^[1] and release the minerals, resulting in a transfer of calcium from bone fluid to the blood.

The osteoclasts are multi-nucleated cells that contain numerous mitochondria and lysosomes. These are the cells responsible for the resorption of bone. Attachment of the osteoclast to the osteon begins the process. The osteoclast then induces an infolding of its cell membrane and secretes collagenase and other enzymes important in the resorption process. High levels of calcium, magnesium, phosphate and products of collagen will be released into the extracellular fluid as the osteoclasts tunnel into the mineralized bone. Osteoclasts are also prominent in the tissue destruction commonly found in psoriatic arthritis and other rheumatology related disorders.

Bone resorption can also be the result of disuse and the lack of stimulus for bone maintenance. Astronauts, for instance will undergo a certain amount of bone resorption due to the lack of gravity, providing the proper stimulus for bone maintenance.

HIP

In anatomy, the **hip** (or "coxa" in medical terminology) is the bony projection of the femur which is known as the **greater trochanter**, and the overlying muscle and fat. The **hip joint**, scientifically referred to as the **acetabulofemoral joint**, is the joint between the femur and acetabulum of the pelvis and its primary function is to support the weight of the body in both static (e.g. standing) and dynamic (e.g. walking or running) postures.



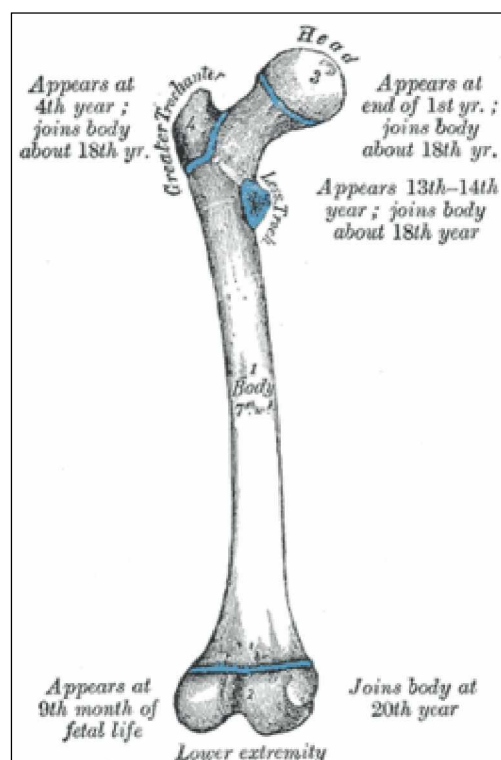
HIP REPLACEMENT

also hip **arthroplasty**, **total hip replacement**, **hip hemiarthroplasty** is a **surgical** procedure in which the **hip** joint is replaced by a prosthetic **implant** (artificial joint). The artificial hip joint has 4 parts:

- A socket that replaces your old hip socket. The socket is usually made of metal.
- The liner fits inside the socket. It is usually plastic, but some surgeons are now trying other materials, like ceramic and metal. The liner allows the hip to move smoothly.
- A metal or ceramic ball that will replace the round head (top) of your thigh bone.
- A metal stem that is attached to the shaft of the bone to add stability to the joint.

FEMUR

or **THIGH BONE**, is the most **proximal** (closest to the body) **bone** of the **leg** in **vertebrates** capable of **walking** or **jumping**, such as most land **mammals**, **birds**, many **reptiles** such as **lizards**, and **amphibians** such as **frogs**. In **humans**, the femur is the **longest** and largest bone. Along with the **temporal bone** of the **skull**, it is one of the two strongest bones in the body. The average adult human femur is 48 centimeters (19 in) in length and 2.34 cm (0.92 in) in diameter and can support up to 30 times the weight of an adult.^[3] It forms part of the **hip** (at the **acetabulum**) and part of the **knee**. There are four eminences, or protuberances, in the human femur: the **head**, the **greater trochanter**, the **lesser trochanter**, and the **lower extremity**. They appear at various times from just before birth to about age 14. Initially, they are joined to the main body of the femur with **cartilage**, which gradually becomes **ossified** until the protuberances become an integral part of the femur bone, usually in early adulthood.



From the following sites:

<http://www.thefreedictionary.com/hip>

http://www.childrenscentralcal.org/HealthE/PublishingImages/em_0244.gif

<https://catalog.ama->

[assn.org/MEDIA/ProductCatalog/m890153/%20Function%20%20Anatomy%20Ch%207.pdf](https://catalog.ama-assn.org/MEDIA/ProductCatalog/m890153/%20Function%20%20Anatomy%20Ch%207.pdf)

<http://www.hipsandknees.com/hip/hipdisease.htm>

<http://www.nlm.nih.gov/medlineplus/ency/article/002286.htm#Definition>

<http://www.nlm.nih.gov/medlineplus/ency/article/002975.htm>

Mechanical definitions

TYPES OF PURE FORCES

- Compressive:** a force that results in a decrease in length along the direction of the force.
Tensile: a force that results in an increase in length along the direction of the force.
Shear: a force that causes a sliding displacement of one side of a structure relative to another side.

STRESS is the force with which a structure resists an external load placed on it. It is the internal reaction to an externally applied load and is equal in magnitude but opposite in direction to the external load; although technically the internal force, this is difficult to measure and so the accepted way of measuring stress is to measure the external load applied to the cross sectional area; measured in force per area units such as kg/cm², MPa (MN/m²), or psi; is represented by the Greek letter, sigma.

$$\text{Stress} = \text{Force}/\text{Area}$$

Just as there are three types of pure force or load, there are three types of pure stress: compressive, tensile, and shear.

STRAIN is the change in length per unit length that a material undergoes when a force is applied to it; it is dimensionless because it has length per length units of measurement; is often expressed as a percentage; is represented by the Greek letter, epsilon.

$$\text{Strain} = \text{Change in Length}/\text{Original Length}$$

Strain can either be *elastic* or *plastic*. Elastic strain is strain that totally disappears once the external load that caused it is removed. Plastic strain is strain that permanently remains once the external load that caused it is removed.

STRESS-STRAIN DIAGRAM is a graphic way of displaying stress and strain. Traditionally, stress is plotted on the vertical axis and strain on the horizontal axis.

Many of the basic physical properties of biomaterials can be represented on a stress-strain diagram. For example:

- the straight part of the line represents the region of elastic deformation;
- the curved part of the line represents the region of elastic and plastic deformation;
- the slope of the straight part of the line represents modulus of elasticity;
- the length of the curved part of the line represents ductility;
- the area under the straight part of the line represents resilience;
- the area under the entire line represents toughness.

MODULUS OF ELASTICITY (ELASTIC MODULUS, YOUNG'S MODULUS)

is a measure of the relative stiffness or rigidity of a material. The unit values are those of force per area because

$$\text{Modulus of Elasticity} = \text{Stress}/\text{Strain}$$

A material with a steep line will have a higher modulus and be more rigid than a material with a flatter line.

ELASTIC LIMIT

is the maximum amount of stress that a structure can withstand and still return to its pre-stressed dimensions; it is, for all practical purposes, the same as the proportional limit.

YIELD POINT

is the point of first marked deviation from proportionality of stress to strain on the stress-strain diagram; it indicates that the structure is undergoing a pronounced degree of deformation with little additionally applied stress.

YIELD STRENGTH

is the amount of stress required to produce a predetermined amount of permanent strain (usually 0.1% or 0.2% which is called the percent offset). It is a useful property because it is easier to measure than the proportional limit. It is measured using the stress-strain diagram by locating the point 0.1% or 0.2% out on the strain axis and drawing a line up to the curve which is parallel to the line found in the elastic region.

ULTIMATE STRENGTH

is the maximum amount of stress that a material can withstand without undergoing fracture or rupture. It can be applied to compressive, tensile, or shear stresses.

FRACTURE STRENGTH

is the amount of stress required to produce fracture or rupture.

DUCTILITY

is the ability of a material to undergo permanent tensile deformation without fracture or rupture.

BRITTLENESS

is the material behaviour where a material undergoes fracture or rupture with little or no prior permanent deformation.

Brittle materials are sensitive to internal flaws/cracks/voids and do not respond well to tensile or bending forces because these forces tend to propagate the flaws/cracks/voids. Brittle materials do well under compressive forces, however, because they tend to close cracks.

TOUGHNESS

is the resistance of a material to fracture under sudden impact or the amount of energy absorbed by a material when it is stressed to a point just shy of its fracture point.

FRACTURE TOUGHNESS

is a measure of the resistance of a material to failure from crack propagation in tension.

Definitions taken from

http://airforcemedicine.afms.mil/idc/groups/public/documents/afms/ctb_108331.pdf.

Chemical definitions

MONOMER (from Greek mono "one" and meros "part") Is a small molecule that may become chemically bonded to other monomers to form a polymer.

From: [En.wikipedia.org/wiki/Monomer](https://en.wikipedia.org/wiki/Monomer)

POLYMER A large molecule consisting of chains or rings of linked monomer units, usually characterized by high melting and boiling points.

POLYMERIZATION

In polymer chemistry, polymerization is a process of reacting monomer molecules together in a chemical reaction to form three-dimensional networks or polymer chains. There are many forms of polymerization and different systems exist to categorize them.

From: [En.wikipedia.org/wiki/Polymerization](https://en.wikipedia.org/wiki/Polymerization)

COPOLYMER a polymer chain consisting of two or more types of monomeric units.

HOMOPOLYMER

a polymer consisting of only one type of monomeric unit.

CROSS-LINKING

are bonds that link one polymer chain to another. They can be covalent bonds or ionic bonds. From: [En.wikipedia.org/wiki/Cross-linking](https://en.wikipedia.org/wiki/Cross-linking)

PLASTICIZERS

chemical agents added to plastic compounds to improve flow and processibility and to reduce brittleness.

ANOVA Table for FBC_Ra

	DF	Sum of Squares	Mean Square	F-Value	P-Value	Lambda	Power
Tipo cricca	2	13.350	6.675	191.184	<.0001	382.369	1.000
Residual	77	2.688	.035				

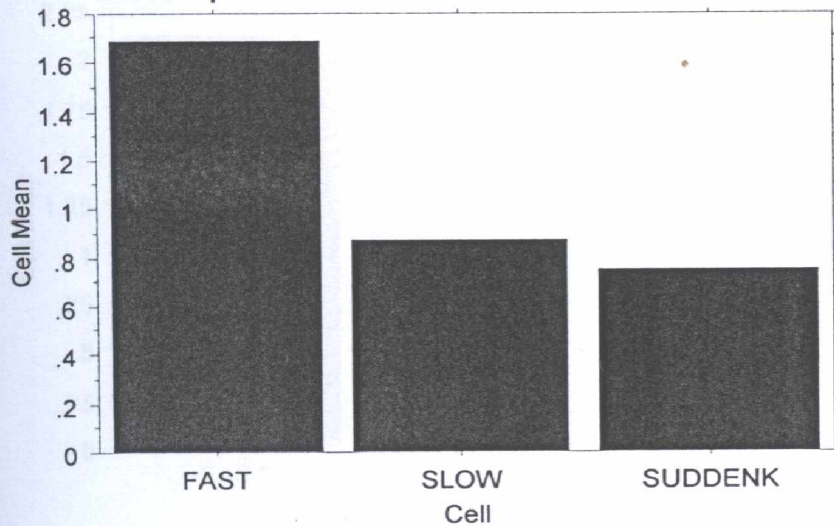
Means Table for FBC_Ra

Effect: Tipo cricca

	Count	Mean	Std. Dev.	Std. Err.
FAST	25	1.683	.104	.021
SLOW	25	.875	.185	.037
SUDDENK	30	.753	.235	.043

Interaction Bar Plot for FBC_Ra

Effect: Tipo cricca



Fisher's PLSD for FBC_Ra

Effect: Tipo cricca

Significance Level: 5 %

	Mean Diff.	Crit. Diff.	P-Value	
FAST, SLOW	.808	.105	<.0001	S
FAST, SUDDENK	.930	.101	<.0001	S
SLOW, SUDDENK	.123	.101	.0177	S

ANOVA Table for PLA_Ra

	DF	Sum of Squares	Mean Square	F-Value	P-Value	Lambda	Power
Tipo cricca	2	6.960	3.480	17.999	<.0001	35.998	1.000
Residual	77	14.887	.193				

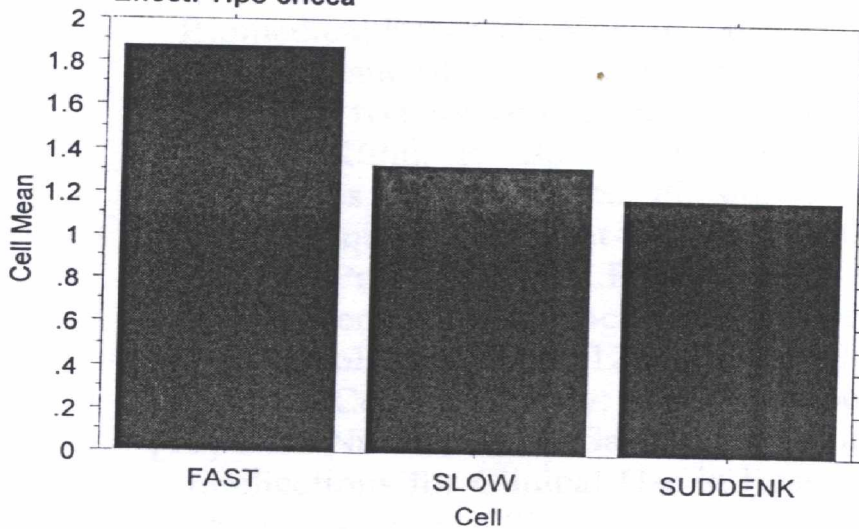
Means Table for PLA_Ra

Effect: Tipo cricca

	Count	Mean	Std. Dev.	Std. Err.
FAST	25	1.875	.101	.020
SLOW	25	1.330	.232	.046
SUDDENK	30	1.186	.679	.124

Interaction Bar Plot for PLA_Ra

Effect: Tipo cricca



Fisher's PLSD for PLA_Ra

Effect: Tipo cricca

Significance Level: 5 %

	Mean Diff.	Crit. Diff.	P-Value	
FAST, SLOW	.545	.248	<.0001	S
FAST, SUDDENK	.689	.237	<.0001	S
SLOW, SUDDENK	.144	.237	.2306	

ANOVA Table for CRX_Ra

	DF	Sum of Squares	Mean Square	F-Value	P-Value	Lambda	Power
Tipo cricca	2	25.335	12.668	526.200	<.0001	1052.400	1.000
Residual	77	1.854	.024				

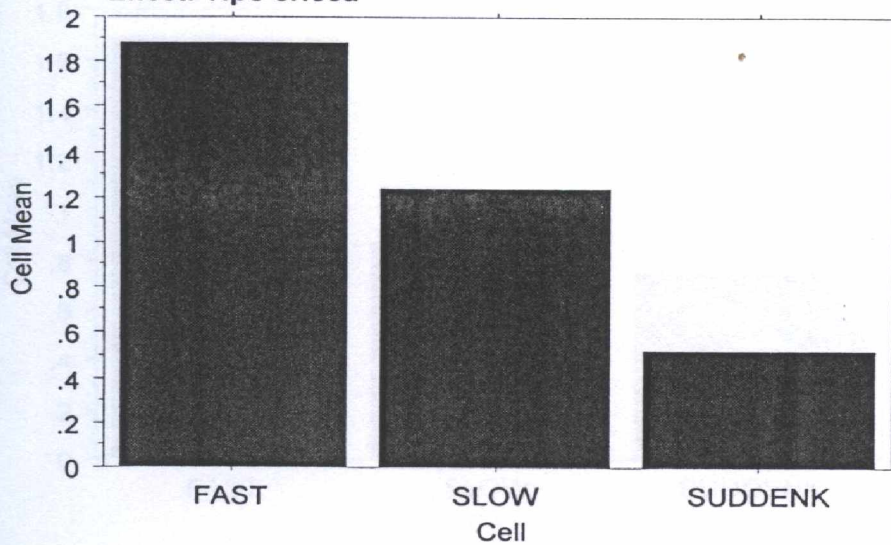
Means Table for CRX_Ra

Effect: Tipo cricca

	Count	Mean	Std. Dev.	Std. Err.
FAST	25	1.883	.112	.022
SLOW	25	1.236	.171	.034
SUDDENK	30	.524	.171	.031

Interaction Bar Plot for CRX_Ra

Effect: Tipo cricca



Fisher's PLSD for CRX_Ra

Effect: Tipo cricca

Significance Level: 5 %

	Mean Diff.	Crit. Diff.	P-Value	
FAST, SLOW	.647	.087	<.0001	S
FAST, SUDDENK	1.359	.084	<.0001	S
SLOW, SUDDENK	.712	.084	<.0001	S

ANOVA Table for SYS_Ra

	DF	Sum of Squares	Mean Square	F-Value	P-Value	Lambda	Power
Tipo cricca	2	14.376	7.188	88.847	<.0001	177.693	1.000
Residual	77	6.230	.081				

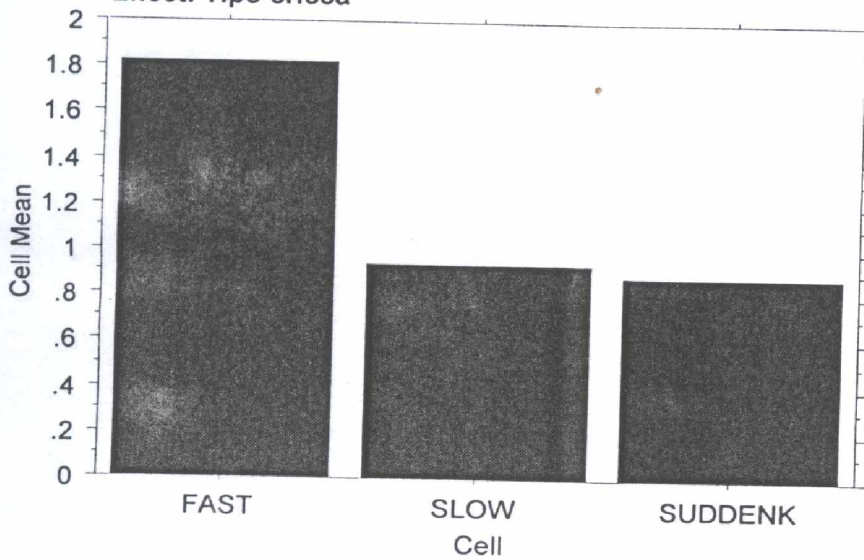
Means Table for SYS_Ra

Effect: Tipo cricca

	Count	Mean	Std. Dev.	Std. Err.
FAST	25	1.823	.108	.022
SLOW	25	.934	.356	.071
SUDDENK	30	.889	.317	.058

Interaction Bar Plot for SYS_Ra

Effect: Tipo cricca



Fisher's PLSD for SYS_Ra

Effect: Tipo cricca

Significance Level: 5 %

	Mean Diff.	Crit. Diff.	P-Value	
FAST, SLOW	.889	.160	<.0001	S
FAST, SUDDENK	.934	.153	<.0001	S
SLOW, SUDDENK	.045	.153	.5619	

ANOVA Table for GTA_Ra

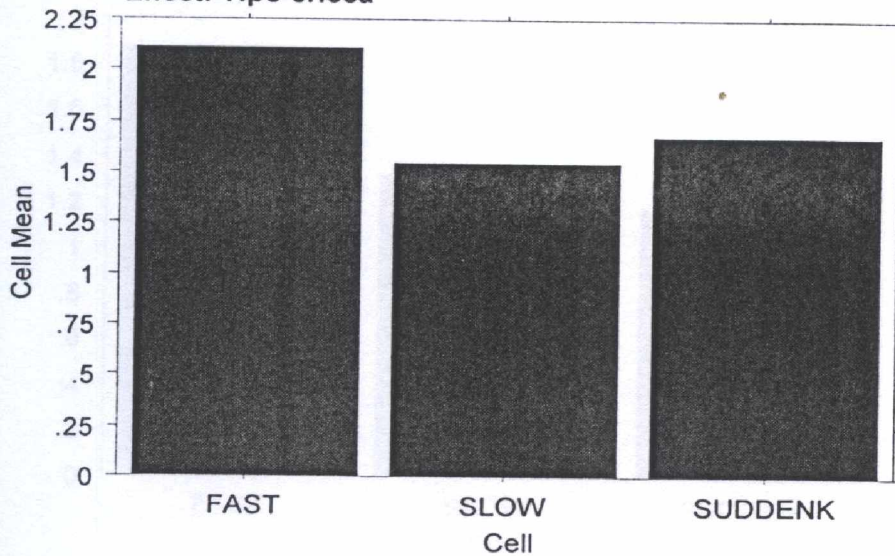
	DF	Sum of Squares	Mean Square	F-Value	P-Value	Lambda	Power
Tipo cricca	2	4.252	2.126	67.876	<.0001	135.752	1.000
Residual	77	2.412	.031				

Means Table for GTA_Ra

Effect: Tipo cricca

	Count	Mean	Std. Dev.	Std. Err.
FAST	25	2.104	.082	.016
SLOW	25	1.548	.172	.034
SUDDENK	30	1.681	.230	.042

Interaction Bar Plot for GTA_Ra
Effect: Tipo cricca



Fisher's PLSD for GTA_Ra

Effect: Tipo cricca

Significance Level: 5 %

	Mean Diff.	Crit. Diff.	P-Value	
FAST, SLOW	.555	.100	<.0001	S
FAST, SUDDENK	.423	.095	<.0001	S
SLOW, SUDDENK	-.132	.095	.0072	S

ANOVA Table for SP_Ra

	DF	Sum of Squares	Mean Square	F-Value	P-Value	Lambda	Power
Tipo cricca	2	10.016	5.008	141.583	<.0001	283.165	1.000
Residual	71	2.511	.035				

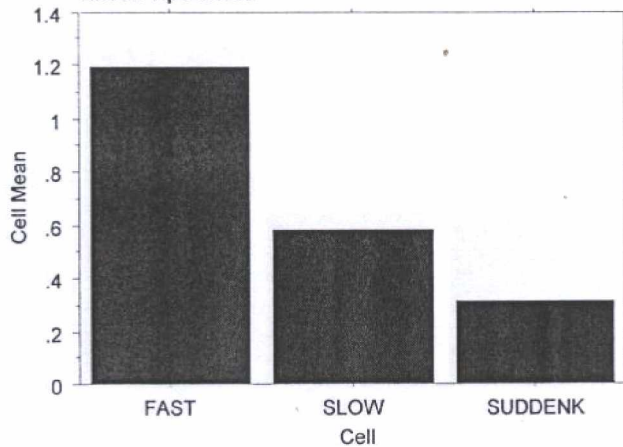
Means Table for SP_Ra

Effect: Tipo cricca

	Count	Mean	Std. Dev.	Std. Err.
FAST	25	1.196	.192	.038
SLOW	25	.581	.215	.043
SUDDENK	24	.317	.150	.031

Interaction Bar Plot for SP_Ra

Effect: Tipo cricca



Fisher's PLSD for SP_Ra

Effect: Tipo cricca

Significance Level: 5 %

	Mean Diff.	Crit. Diff.	P-Value	
FAST, SLOW	.615	.106	<.0001	S
FAST, SUDDENK	.879	.107	<.0001	S
SLOW, SUDDENK	.264	.107	<.0001	S

References

- [1] L.J. Pogula, Effect of Antibiotic Additives on The Fracture Toughness of Poly Methyl Methacrylate Bone Cement, Master Thesis of Science, August, 2005.
- [2] K.D. Kühn, Bone Cements: Up-to-Date Comparison of Physical and Chemical Properties of Commercial Materials, (Berlin, 2000).
- [3] A. Marco, S. Ajami, D. Ajami, Physicochemical, Mechanical, and Biological Properties of Bone Cements Prepared with Functionalized Methacrylates. *Journal of Biomaterials Applications*, Vol. 19, pp. 147-161, 2004.
- [4] M.C. Tanzi, The Acrylic Bone Cement: Chemistry and Chemico-Physical Properties, Bone Cement and Cemented Fixation of Implants, pp. 21-29, Zenit (Ed), (Verona, 2003).
- [5] G. Lewis, Properties of Acrylic Bone Cement: State of the Art Review. *Journal of Biomedical Research,(Appl. Biomater.)*, Vol. 38, pp. 155-182, 1997.
- [6] L.P. Tranquilli, The Biocompatibility of Bone Cements, Bone Cement and Cemented Fixation of Implants, pp. 77-82, Zenit (Ed), (Verona, 2003).
- [7] K.D. Kühn, R. Specht, Le Ciment Acrylique Osseux, Historique, Caractéristiques Chimiques et Propriétés Physiques. *Le Journal Français De l'Orthopédie, Maîtrise Orthopédique N°126*, Août-Septembre 2003.
- [8] M.J. Provenzano, K.P.J. Murphy, L.H. Rileyiii, Bone Cements: Review of Their Physiochemical and Biochemical Properties in Percutaneous Vertebroplasty. *Ajnram, J. Neurradiol.*, Vol. 25, pp. 1286-1290, 2004.
- [9] Bone Cement History: [Http://www.BoneCement.Com](http://www.BoneCement.Com), (2006).
- [10] M.P. Genebra, L. Albuixech, E. Fernández-Barragán, C. Aparicio, F. J. Gil, J. San Román, B. Vázquez, J. A. Planell, Mechanical Performance of Acrylic Bone Cements Containing Different Radiopacifying Agents. *Biomaterials*, Vol. 23, pp. 1873-1882, 2002.
- [11] The Norwegian Arthroplasty Register, Report 2005.
- [12] Istituti Ortopedici Rizzoli, Report, (Bologna), Italy, 2005.
- [13] C. Migliaresi, L. Fambri, J. Kolarik, Polymerization Kinetics, Glass Transition Temperature and Creep of Acrylic Bone Cements. *Biomaterials*, Vol. 15, pp. 875-881, 1994.
- [14] D.A. Nussbaum, P. Gailloud, K. Murphy, The Chemistry of Acrylic Bone Cements and Implications for Clinical Use in Image-Guided Therapy. *Journal Vasc. Interv. Radiol.*, Vol. 15, pp. Xxx-Xxx, 2004.
- [15] S.S. Hass, G.M. Brauer, G. Dickson, A Characterization of Poly (Methyl Methacrylate) Bone Cement. *Journal of Bone Joint Surgery*, Vol. 57-A, pp. 380-391, 1975.
- [16] A.J.C. Lee, R.S.M. Ling, J.D. Wrightson, Some Properties of Poly (Methyl Methacrylate) with Reference to its Use in Orthopedic Surgery. *Clin Orthop*, Vol. 95, pp. 281-287, 1973.

- [17] B. Pascual, B. Vázquez, M. Gurruchaga, I. Goñi, M.P. Ginebra, F.J. Gil, J.A. Planell, B. Levenfeld, J. San Román, New Aspects of the Effects of Size and Size Distribution on the Setting Parameters and Mechanical Properties of Acrylic Bone Cements. *Biomaterials*, Vol. 17, pp. 509-516, 1996.
- [18] G. Lewis, M. Carroll, Rheological Properties of Acrylic Bone Cements during Curing and the Role of the Size of the Powder Particles. *Journal of Biomedical Materials Research*, (Appl. Biomater.), Vol. 63, pp. 191-199, 2002.
- [19] R.P. Kusy, Characterization of Self-Curing Acrylic Bone Cements. *Journal of Biomedical Material Research*, Vol. 12, pp. 271-305, 1978.
- [20] F.W. Reckling, W.L. Dillon, The Bone-Cement Interface Temperature During Total Joint Replacement. *Journal of Bone Joint Surgery*, Vol. 59-A, pp. 80-82, 1977.
- [21] S. Toksvig-Larsen, H. Franzen, L. Ryd, Cement Interface Temperature in Hip Arthroplasty. *Acta Orthopædica Scandinavica*, Vol. 62, pp. 102-105, 1991.
- [22] J.B. Park, R.S. Lakes, *Biomaterials: An Introduction*, Plenum Press (2nd Ed), (New York, 1992).
- [23] J.M. Hasenwinkel, E.P. Lautenschlager, R.L. Wixson, J.L. Gilbert, A Novel High-Viscosity, Two Solution Acrylic Bone Cements: Effect of Chemical Composition on Properties. *Journal of Biomedical Materials Research*, Vol. 47, pp. 36-45, 1999.
- [24] L.D.T. Topolski, P. Ducheyne, J.M. Cuckler, A Fractographic Analysis of In Vivo Poly (Methyl Methacrylate) Bone Cement Failure Mechanisms. *Journal of Biomedical Materials Research*, Vol. 24, pp. 135-154, 1990.
- [25] S. Deb, B. Vazquez, The Effect of Cross-Linking Agents on Acrylic Bone Cements Containing Radiopacifiers. *Biomaterials*, Vol. 22, pp. 2117-2181, 2001.
- [26] R.C. Turner, P.E. Atkins, M.A. Ackley, J.B. Park, Molecular and Macroscopic Properties of PMMA Bone Cement: Free-Radical Generation and Temperature Change versus Mixing Ratio. *Journal of Biomedical Materials Research*, Vol. 15, pp. 425-432, 1981.
- [27] B. Pascual, M. Gurruchaga, M.P. Ginebra, F.J. Gil, J.A. Planell, I. Goñi, Influence of the Modification of P/L Ratio on a New Formulation of Acrylic Bone Cement. *Biomaterials*, Vol. 20, pp. 465-474, 1999.
- [28] J. Rudigier, H. Scheuermann, B. Kotterbach, G. Ritter, Restmonomerabnahme Und-Freisetzung Aus Knochenzementen. *Unfallchirurgie*, Vol. 7, pp. 132-137, 1981.
- [29] H. Wenzl, A. Garbe, H. Nowak, Experimentelle Untersuchungen Zur Pharmakokinetik Von Monomethylmethacrylat. In: Erlacher PH, Zemann L, Spitzzy K H (Hrsg), pp. 1-16, 1973.
- [30] J.B. Benjamin, G.A. Gie, A.J.C. Lee, R.S.M. Ling, R.G. Voltz, Cementing Technique and the Effects of Bleeding. *Journal of Bone Joint Surgery*, Vol. 69-B, pp. 620-624, 1987.
- [31] W.R. Krause, J. Miller, P. Ng, The Viscosity of Acrylic Bone Cement. *Journal of Biomedical Material Research*, Vol. 16, pp. 219-243, 1982.

- [32] J. S. Wang, H. Franzén, E. Jonsson, L. Lidgren, Porosity of Bone Cement Reduced by Mixing and Collecting Under Vacuum, *Acta Orthopædica Scandinavica*, Vol. 64, pp. 143-146, 1993.
- [33] J. Graham, L. Pruitt, M. Ries, N. Gundiah, Fracture and Fatigue Properties of Acrylic Bone Cement: The Effects of Mixing Method, Sterilization Treatment and Molecular Weight. *Journal of Arthroplasty*, Vol. 15(8), pp. 709-712, 2000.
- [34] E.A. Friis, L.J. Stromberg, F.W. Cooke, D.A. McQueen, Fracture Toughness of Vacuum Mixed PMMA Bone Cement. 19th Annu. Mtg. Soc. Biomater; Birmingham, Al, pp. 301, 1993.
- [35] D.W. Schreurs, P.T.J. Spierings, R. Huiskes, T.J.J.H. Sloof, Effect of Preparation Techniques on the Porosity of Acrylic Cements. *Acta Orthopædica Scandinavica*, Vol. 59, pp. 403-409, 1988.
- [36] R.L. Wixon, E.P. Lautenschlager, M.A. Novak, Vacuum Mixing of Acrylic Bone Cement. *Journal of Arthroplasty*, Vol. 2, pp. 141-149, 1987.
- [37] S.K. Bhambri, L.N. Gilbertson, Micromechanisms of Fatigue Crack Initiation and Propagation in Bone Cements. *Journal of Biomedical Materials Research*, Vol. 29, pp. 233-237, 1995.
- [38] W. Krause, R.S. Mathis, Fatigue Properties of Acrylic Bone Cements: Review of the Literature, *Journal of Biomedical Materials Research, (Appl. Biomater.)*, Vol. 22, pp. 37-53, 1988.
- [39] L.D.T. Topolski, P. Ducheyne., J.M. Cuckler, Micro Structural Pathway of Fracture in Poly (Methyl Methacrylate) Bone Cement. *Biomaterials*, Vol. 14, pp. 1165-1172, 1993.
- [40] J. Dennis, A. René, S. Jan, V. Nico, The Contradictory Effects of Pores on Fatigue Cracking of Bone Cement, *Journal of Biomedical Materials Research, (Appl. Biomater.)*, Vol. 74-B, pp. 747-753, 2005.
- [41] J.W. Wang, S.B. Goldman, H. Franzén, P. Aspenberg, L. Lidgren, Particles Accumulate Within Cement Voids. 19th Annu. Mtg. Soc. Biomater; Birmingham, Al, pp. 245, 1993.
- [42] M. Jasty, J.P. Davies, D.O. O'Connor, D.W. Burke, T.P. Harrigan, W.H. Harris, Porosity of Various Preparations of Acrylic Bone Cements, *Clinical Orthopedics Related Research*, Vol. 259, pp. 122-129, 1990.
- [43] S.C. Weker, W.L.A. Bargar, Comparison of the Mechanical Properties of Simplex, Zimmer, and Zimmer Low Viscosity Bone Cement. *Biomater. Med. Devices Artif. Org.*, Vol. 11, pp. 3-12, 1983.
- [44] C.T. Wang, R.M. Pilliar, Fracture Toughness of Acrylic Bone Cements. *Journal of Materials Science*, Vol. 24, pp. 3725-3738, 1989.
- [45] [Http://www.tecres.it](http://www.tecres.it), (2009).
- [46] L. Lidgren, H. Drar, J. Möller, Strength of Poly Methyl Methacrylate Increased by Vacuum Mixing. *Acta Orthopædica Scandinavica*, Vol. 55, pp. 536-541, 1984.
- [47] U. Linden, Mechanical Properties of Bone Cement: Importance of Mixing Technique.. *Clinical Orthopedics Related Research*, Vol. 273, pp. 274-278, 1991.
- [48] H.H. Trieu, R.D. Paxon, M.E. Carroll, J.M. Bert, A Comparative Study of Bone Cement Preparation Using a New Centrifugation

- Mixing Technique. 20th Annu. Mtg. Soc. Biomater; Boston, pp. 416, 1994.
- [49] S. Saha, A. Kumar, Improved Tensile Strength of Bone Cement by Ultra-Sonic Vibration. 5th World Biomater. Congr; Toronto, Canada, pp. 801, 1996.
- [50] E.W. Fritsch, Static and Fatigue Properties of Two New Low Viscosity PMMA Bone Cements Improved by Vacuum Mixing. *Journal of Biomedical Material Research*, Vol. 31, pp. 451-456, 1996.
- [51] M.C. Tanzi, L. Parrini, L. Quagliarella, Ageing of Cement, Bone Cement and Cemented Fixation of Implants, pp. 85-91, Zenit (Ed), (Verona, 2003).
- [52] C. Liu, S.M. Green, N.D. Watkins, A.W. McCaskie, On the Particle Size and Molecular Weight Distributions of Clinical Bone Cements. *Journal of Materials Science Letters*, Vol. 22, pp. 709-712, 2003.
- [53] A. Chapiro, *Radiation Chemistry of Polymeric Systems*, Wiley-Interscience (Ed), (New York, 1962).
- [54] G. Lewis, S. Mladi, Effect of Sterilization Method on Properties of Palacos R Acrylic Bone Cement. *Biomaterials*, Vol. 19, pp. 117-124, 1998.
- [55] E.P. Harper, M. Braden, W. Bonfield, E. Dingeldein, H. Wahlig, Influence of Sterilization upon a Range of Properties of Experimental Bone Cements. *Journal of Materials Science: Materials in Medicine*, Vol. 8, pp. 849-853, 1997.
- [56] S.L. Kim, M. Skibo, J.A. Manson, R.W. Hertzberg, Fatigue Crack Propagation in Poly (Methyl-Methacrylate): Effect of Molecular Weight and Internal Plasticization. *Polym. Eng. Sci.*, Vol. 17, pp. 194-203, 1977.
- [57] K.F Hughes, M.D Ries, L.A. Pruitt, Structural Degradation of Acrylic Bone Cements due to In Vivo and Simulated Aging, *Journal of Biomedical Material Research*, Vol. 65-A(2), pp. 126-135, 2003.
- [58] G. Lewis, Effect of Loading Rate on the Apparent Fracture Toughness of Acrylic Bone Cement. *Journal of Biomedical Material and Engineering*, Vol. 12, pp. 149-155, 2002.
- [59] C.I. Vallo, T.R. Caudrado, P.M. Frontini, Mechanical and Fracture Behaviour Evaluation of Commercial Acrylic Bone Cement. *Polymer International*, Vol. 43, pp. 260-268, 1997.
- [60] A. Gigada, M.F. Brunella, R. Chiesa, Biomedical Aspects of Bone Cement: The Effect of Dynamic Stress, Bone Cement and Cemented Fixation of Implants, pp. 41-53 Zenit (Ed), (Verona, 2003).
- [61] M. Baleani, L. Cristofolini, E. Piazza, C. Minari, A. Toni, Effect of Barium Sulphate and Sodium Fluoride on The Fatigue Behaviour of Acrylic Bone Cement, Bone Cement and Cemented Fixation of Implants, pp. 71-76, Zenit (Ed), (Verona, 2003).
- [62] S. Ishihara, A.J. Mcevely, T. Goshima, K. Kanekasu, T. Nara, On Fatigue Lifetimes and Fatigue Crack Growth Behaviour of Bone Cement. *Journal of Materials Science: Materials in Medicine*, Vol. 11, pp. 661-666, 2000.
- [63] M.D. Ries, E. Young, L. Al Marashi, P. Goldstein, A. Hetherington, T. Petrie, L. Printt, In Vivo Behavior of Acrylic

- Cement In Total Hip Arthroplasty. *Biomaterials*, Vol. 27, pp. 256-261, 2006.
- [64] N.C. Nguyen, W.J. Maloney, R.H. Dauskardt, Reliability of PMMA Bone Cement Fixation: Fatigue Crack-Growth Behaviour. *Journal of Materials Science: Materials in Medicine*, Vol. 8, pp. 473-483, 1997.
- [65] M.T. Raimondi, T. Villa, R. Pietrabissa, Mechanical Properties of Acrylic Bone Cement, Bone Cement and Cemented Fixation of Implants, pp. 31-40, Zenit (Ed), (Verona, 2003).
- [66] M. Jasty, W. J. Maloney, C. R. Bragdon, D. O. O'Connor, E. B. Zalenski, W. H. Harris, The Initiation of Failure of Bone of Cemented Femoral Components of Hip Arthroplasties. *Journal of Bone Joint Surgery*, Vol. 73-B, pp. 551-558, 1991.
- [67] M. Spector, Biomaterial Failure. *Orthop Clin NA*, Vol. 23, pp. 211-217, 1992.
- [68] B.P. Murphy, P.J. Prendergast, The Relationship Between Stress, Porosity, and Non Linear Damage Accumulation in Acrylic Bone Cement. *Journal of Biomedical Materials Research*, Vol. 59, pp. 646-654, 2001.
- [69] M.M. Vila, M.P. Ginebra, F.J. Gill, J.A. Planell, Effect of Porosity and Environment on the Mechanical Behaviour of Acrylic Bone Cement Modified with Acrylonitrile-Butadiene-Styrene Particles: Part II. Fatigue Crack Propagation. *Journal of Biomedical Materials Research (Appl. Biomater.)*, Vol. 48, pp. 128-134, 1999.
- [70] W.R. Krause, R.S. Mathis, L.W. Grimes, Fatigue Properties of Acrylic Bone Cement S-N, P-N and P-S-N Data. *Journal of Biomedical Material Research (Appl. Biomater.)*, Vol. 22-A(3), pp. 221-244, 1988.
- [71] B. Vazquez, S. Deb, W. Bonfield, Optimization of Benzoyl Peroxide Concentration in an Experimental Bone Cement Based on Poly(Methylmethacrylate). *Journal of Materials Science: Materials in Medicine*, Vol. 8, pp. 455-460, 1997.
- [72] J.P. Davies, D.O. O'Connor, J.A. Creer, W.H. Harris, Comparison of Mechanical Properties of Simplex P, Zimmer Regular and LVC Bone Cements. *Journal of Biomedical Material Research*, Vol. 21, pp. 719-730, 1987.
- [73] G. Lewis, S. Nyman, H.H. Trieu, Effect of Mixing Method on Selected Properties of Acrylic Bone Cement. *Journal of Biomedical Material Research (Appl. Biomater.)*, Vol. 38, pp. 221-228, 1997.
- [74] A.J.C. Lee, T. Duckworth, Ed, *Proceedings of the Sym. Revision Arthroplasty*, 2nd Edition London: Franklin Scientific Publications, pp. 8-13, 1983.
- [75] R.S.M. Ling, T. Duckworth, Ed, *Proceedings of Symposium on Revision Arthroplasty*, London: Franklin Scientific Publications, pp. 14, 1983.
- [76] S.M. Kurtz, M.L. Villarraga, K. Zhao, A.A. Edidin, Static and Fatigue Mechanical Behavior of Bone Cement with Elevated Barium Sulfate Content for Treatment of Vertebral Compression Fractures, *Biomaterials*, Vol. 26, pp. 3699-3712, 2005.

- [77] Súbition quirurgíco. Cemento Acrílico Para Fijaciones y Reconstrucciones Oseas, Radiopaco PROTHOPLAST SAIC Especialidades Medicinales Aprobadas por El Ministerio de Salud y Acción Social, Certificado No, 38,692.
- [78] E.P. Lautenschlager, J.J. Jacobs, G.W. Marshall, P.R.Jr. Meyer, Mechanical Properties of Bone Cements Containing Large Doses of Antibiotic Powders. *Journal of Biomedical Materials Research*, Vol. 10, pp. 929-938, 1976.
- [79] J. Klekamp, J.M. Dawson, D.W. Haas, D. Deboer, M. Christie, The Use of Vancomycin and Tobramycin in Acrylic Bone Cement. *Journal of Arthroplasty*, Vol. 14, pp. 339-346, 1999.
- [80] D.K. Kirkpatrick, L.S. Trachtenberg, P.D. Mangino, J.A. Von Fraunhofer, D. Seligson, In Vitro Characteristics of Tobramycin-PMMA Beads: Compressive Strength and Leaching. *Orthopaedics*. Vol. 8, pp. 1130-1133, 1985.
- [81] J.R. De Wyn, T.J.J.H. Sloff, F.C.M. Driessens, Characterization of Bone Cements. *Acta Orthopædica Scandinavica*. Vol. 46, pp. 38-51, 1975.
- [82] ASTM. Specification D790-95a: Standard Test Method for Flexural Properties of Unreinforced and Reinforced Plastics and Electrical Insulating Materials, 1996 Annual Book of ASTM Standards, Vol. 08.01: Plastics(I). Philadelphia, PA: American Society for Testing and Materials, pp. 155-165, 1996.
- [83] G. Lewis, S. Janna, A. Bhattaram, Influence of the Method of Blending an Antibiotic Powder with an Acrylic Bone Cement Powder on Physical, Mechanical, and Thermal Properties of Cured Cement. *Biomaterials*, Vol. 26, pp. 4317-4325, 2005.
- [84] W.L. Bargar, R.B. Martin, R. Dejesus, M.T. Madison, The Addition of Tobramycin to Contrast Bone Cement, Effect on Flexural Strength. *Journal of Arthroplasty*, Vol. 1, pp. 165-168, 1986.
- [85] M.J. Askew, M.F. Kufel, P.R. Jr. Fleissner, I.A.Jr. Gradisar, S.J. Salstrom, J.S. Tan, Effect of Vacuum Mixing on the Mechanical Properties of Antibiotic-Impregnated Polymethylmethacrylate Bone Cement. *Journal of Biomedical Material Research*, Vol. 24, pp. 573-580, 1990.
- [86] S. Saha, S. Pal, Mechanical Properties of Bone Cement: A Review. *Journal of Biomedical Material Research*, Vol. 18, pp. 435-462, 1984.
- [87] R.P. Kusy, D.T. Turner, Fractography of Poly(Methyl Methacrylates). *Journal of Biomedical Materials Research*, Vol. 9, pp. 89-98, 1975.
- [88] K.A. Mann, F.W. Werner, D.C. Ayers, Mechanical Strength of the Cement-Bone Interface is Greater in Shear than in Tension. *Journal of Biomechanics*, Vol. 32, pp. 1251-1254, 1999.
- [89] M.J. Funk, A.S. Litsky, Effect of Bone Cement Modulus on the Shear Properties of The Bone-Cement Interface. *Biomaterials*, Vol. 19(17), pp. 1561-1567, 1998.
- [90] H. Zhang, L. Brown, L. Blunt, Static Shear Strength between Polished Stem and Seven Commercial Acrylic Bone Cements.

- Journal of Materials Science: Materials in Medicine, Vol. 19(2), pp. 591-599, 2008.
- [91] T. Kindt-Larsen, D.B. Smith, J.S. Jensen, Innovations in Acrylic Bone Cement and Application Equipment. *J. App. Biomater.*, Vol. 46, pp. 75-83, 1995.
- [92] O. Kilicoglu, L.O. Koyunco, V.E. Ozden, E. Bozdog, E. Sunbuloglu, O. Yazicioglu, Effect of Antibiotic Loading on the Shear Strength at the Stem-Cement Interface (Shear Strength of Antibiotic Loaded Cement), *Int. Orthop.*, Vol. 32(4), pp. 347-341, 2008.
- [93] A. H. Wilde, A.S. Greenwald, Shear Strength of Self-Curing Acrylic Cement. *Clinical Orthopaedics Related Research*. Vol. 106, pp. 126-130, 1975.
- [94] M. Nordin, V.H. Frankel, Basic Biomechanics of the Musculoskeletal System, pp. 22-30, (2nd Ed. Philadelphia: Lea and Fibiger, 1989).
- [95] L. Guandalini, M. Baleani, M. Viceconti, A Procedure and Criterion For Bone Cement Fracture Toughness Tests, *Proc. Instn Mech. Engrs. Journal of Engineering in Medicine* Vol. 218 Part H, pp. 445-450, 2004.
- [96] S.P. James, M. Jasty, J. Davies, H. Piehler, W. H. Harris, A Fractographic Investigation of PMMA Bone Cement Focusing on the Relationship between Porosity Reduction and Increased Fatigue Life. *Journal of Biomedical Materials Research*, Vol. 26(5), pp. 651-662, 1992.
- [97] U.E. Pazzaglia. *Arch. Ortho. Traum. Surg.*, Vol. 109, pp. 83, 1990.
- [98] E.J. Cheal, M. Spector, W.C. Hayes, Role of loads and prosthesis material properties on the mechanics of the proximal femur after total hip Arthroplasty. *Journal of Orthopaedic Research*, Vol. 10, pp. 405-422, 1992.
- [99] V.M. Gharpuray, L.M. Keer, J.L. Lewis, Cracks Emanating from Circular Voids or Elastic Inclusions in PMMA near a Bone Cement Interface. *Journal Biomech. Eng.*, Vol. 112, pp. 22-28, 1990.
- [100] S.P. James, T.P. Schmalzried, P.J. Macgarry, W.H. Harris, Extensive Porosity at the Cement Femoral Prosthesis Interface; A Preliminary Study. *Journal of Biomedical Materials Research*, Vol. 27(1), pp. 71-78, 1993.
- [101] M. Jasty, E. Smith, Wear Particles of Total Joint Replacement and their Role in Periprosthetic Osteolysis. *Curr. Opin. Rheumatol.* Vol. 4(2), pp. 204-209, 1992.
- [102] J. Davies, W. Harris, Severe Weakness of Bone Cement Retrieved After In Vivo Service In Man. *Transactions of 15th Annual Meeting of The Society for Biomaterials*; Lake Buena Vista, FL, April 28-May 2, 1989.
- [103] M.M. Vila, M.P. Genebra, F.J. Gil, J.A. Planell, Effect of Porosity and Environment on the Mechanical Behaviour of Acrylic Bone Cement Modified with Acrylonitrile-Butadiene-Styrene Particles: I. Fracture Toughness. *Journal of Biomedical Materials Research, (Appl Biomater.)*, Vol. 48, pp. 121-127, 1999.

- [104] G. Lewis, S. Mladi, Correlation between Impact Strength and Fracture Toughness of PMMA Based Bone Cements. *Biomaterials*, Vol. 48, pp. 775-781, 2000.
- [105] ASTM-D5045-96: Standard Test Methods for Plane-Strain Fracture Toughness and Strain Energy Release Rate of Plastic Materials. Philadelphia: The American Society for Testing and Materials, 1999.
- [106] G.R. Irwin, *Mechanical Testing*, ASM International, Materials Park, Ohio, 1992.
- [107] M.S. Cayard, W.L. Bradley, The Effect of Various Pre-Cracking Techniques on the Fracture Toughness of Plastics, pp. 2713. In *Advances in Fracture Research*, 7th International Conference on Fracture. Pergamon Press, Oxford, 1989.
- [108] J.G. Williams, Testing Protocol. A Linear Elastic Fracture Mechanics (LEFM). Standard for Determining K_{Ic} and G_c for Plastics. EGF Newslett 8, 1988/89.
- [109] C.M. Rimnac, T.M. Wright, D.L. Gill, The Effect of Centrifugation on the Fracture Properties of Acrylic Bone Cement. *Journal of Bone Joint Surgery*, Vol. 68-A, pp. 281-288, 1986.
- [110] G. Lewis, J. Nyman, H.H. Trieu, The Apparent Fracture Toughness of Acrylic Bone Cement; Effect of three Variables. *Biomaterials*, Vol. 19, pp. 961- , 1998
- [111] J.P. Davies, W. H. Harris, Optimization and Comparison of three Vacuum Mixing Systems for Porosity Reduction of Simplex P Cement. *Clinical Orthopaedics Related Research*, Vol. 254, pp. 261-269, 1990.
- [112] D.W. Burke, E.I. Gates, W.H. Harris, Centrifugation as a Method of Improving Tensile and Fatigue Properties of Acrylic Bone Cement. *Journal of Bone Joint Surgery*, Vol. 66-A, pp. 1265-1273, 1984.
- [113] X. Lu, L.D.T. Topoleski, A Controlled-Notch Specimen to Study Fatigue Crack Initiation in Bone Cement. *Journal of Biomedical Materials Research*, Vol. 53, pp. 505-510, 2000.
- [114] L.D.T. Topoleski, P. Rutledge, X. Lu, Backscattered Electron Imaging to Enhance Microstructural Contrast in Poly(Methyl-Methacrylate) Bone Cement Fracture Analysis. *Cells and Materials*, Vol. 5, pp. 283-292, 1995.
- [115] S. Saha, In *Proceedings of the Eighth Annual Conference of IEEE/Engineering in Medicine and Biology Society*. Fort Worth, pp. 1672, November 1986, edited by G. V. Kondraske and C.J. Robinson (IEEE, New York, 1986).
- [116] G.C. Sih, A.T. Berman, Fracture Toughness Concept Applied to Methyl-Methacrylate. *Journal of Biomedical Materials Research*, Vol. 14, pp. 311-316, 1980.
- [117] M.P. Genebra, C. Aparicio, L. Albuixech, E. Fernández-Barragán, F.J. Gil, J.A. Planell, L. Morejón, B. Vázquez, J. San Román, Improvement of Mechanical Properties of Acrylic Bone Cements by Substitution of Radio-opaque Agent. *Journal of Materials Science: Materials in Medicine*, Vol. 10, pp. 733-737, 1999.

- [118] T.A. Freitag, S.L. Cannon, Fracture Characteristics of Acrylic Bone Cements: I. Fracture Toughness. *Journal of Biomedical Materials Research*, Vol. 10, pp. 805-828, 1976.
- [119] R.W. Hertzberg, Deformation and Fracture Mechanics of Engineering Materials, 2nd Ed. Wiley, (New York, 1983).
- [120] J.P. Berry, Fracture Processes in Polymeric Materials: V. Dependence of the Ultimate Properties of Polymethylmethacrylate on Molecular Weight. *J. Polym Sci*, Vol. A-2. pp.4069, 1964.
- [121] G. Lewis, Apparent Fracture Toughness of Acrylic Bone Cement: Effect of Test Specimen Configuration and Sterilization Method. *Biomaterials*, Vol. 20, pp. 69-78, 1999.
- [122] J. Shen, C.C. Chen, J. A. Sauer, Fatigue of PMMA: Effect of Molecular Weight, Water and Frequency, P.6.1. Proceedings of the international conference on polymers Plastics and Rubber; Cambridge, 1983.
- [123] T.A. Freitag, S.L. Cannon, Fracture Characteristics of Acrylic Bone Cements: II. Fatigue. *Journal of Biomedical Materials Research*, Vol. 11, pp. 609-624, 1977.
- [124] T.M. Wright, D.J. Sullivan, S.P. Arnoczky, The Effect of Antibiotic additions on the Fracture Properties of Bone Cements. *Acta Orthopædica Scandinavica*, Vol. 55, pp. 414-418, 1984.
- [125] M.J. Askew, D.A. Noe, D.A. Roush, Mechanical Property Comparisons for Bone Cement with and without Antibiotic, Proceedings of the Society for Biomaterials, Vol. 25, pp. 385, 2002.
- [126] C.B. Bucknall, Toughened Plastics. Applied Science Publishers Ltd, (London 1977).
- [127] C.K. Riew, A.J. Kinloch, Toughened Plastics II: Novel Approaches in Science and Engineering, (Washington: American Chemical Society, 1996).
- [128] R.A. Pearson, H. J. Sue, A.F. Yee, Toughening of Plastics: Advances in Modeling and Experiments. American Chemical Society (Eds), (Washington, 2000).
- [129] G. Lewis, Fatigue Testing and Performance of Acrylic Bone-Cement Materials: State-of- the Art Review. *Journal of Biomedical Materials Research (Appl. Biomater.)*, Vol. 66-B, pp. 457-486, 2003.
- [130] T.P. Culleton, P.J. Prendergast, D. Taylor, Fatigue Failure in the Cement Mantle of an artificial hip joint. *Clin. Mater.*, Vol. 12, pp. 95-102, 1993.
- [131] D.O. O'connor, D.W. Burke, J.P. Davies, W.H. Harris, S-N curve for centrifuged and uncentrifuged PMMA, Trans 31st Ann Mtg Orthop Res Soc; Las Vegas, NV, pp. 325, 1985.
- [132] G. Lewis, Relative Roles of Cement Molecular Weight and Mixing Method on the Fatigue Performance of Acrylic Bone Cement: Simplex P[®] versus Osteopal[®], *Journal of Biomedical Materials Research, (Appl. Biomater.)*, Vol. 53, pp. 119-130, 2000.
- [133] L. Lidgren, B. Bodelind, J. Moller. Bone Cement Improved by Vacuum Mixing and Chilling, *Acta Orthopædica Scandinavica*, Vol. 57, pp. 27-32, 1987.

- [134]U. Linden. Fatigue Properties of Bone Cement: Comparison of Mixing Methods. *Acta Orthopædica Scandinavica*, Vol. 60, pp. 431-433, 1989.
- [135]J.L. Gilbert, D.S. Ney, E.P. Lautenschlager, Self-Reinforced Composite Poly(Methylmethacrylate): Static and Fatigue Properties, *Biomaterials*, Vol. 16, pp. 1043-1055, 1995.
- [136]U. Soltesz, The Influence of Loading Conditions on the Life-Times in Fatigue Testing of Bone Cements. *Journal of Materials Science: Materials in Medicine*, Vol. 5 pp. 654-656, 1994.
- [137]H.Y. Kim, H. K.Yasuda, Improvement of Fatigue Properties of Poly(Methylmethacrylate) Bone Cement by means of Plasma Surface Treatment of Fillers, *Journal of Biomedical Materials Research*, Vol. 48, pp. 135-142, 1999.
- [138]H.W. Demian, A.C. Wey, S.W. Shalaby, Bone Cement with Exceptionally Uniform Dispersion of Radiopacifier. *Trans 21st Annu. Mtg. Soc. Biomater*; San Francisco, CA, pp. 368, 1995.
- [139]B.P. Murphy, P.J. Prendergast. On the Magnitude and Variability of the Fatigue Strength of Acrylic Bone Cement. *International Journal of Fatigue*, Vol. 22, pp. 855-864, 2000.
- [140]E.J. Haper, W. Bonfield, Tensile Characteristics of Ten Commercial Acrylic Bone Cements. *Journal of Biomedical Materials Research*, Vol. 53, pp. 605-616, 2000.
- [141]E.P. Lautenschlager, D.L. Menis, R.L. Wixson, E. Waida, Fatigue Crack Testing of Vacuum and Regular Mixed Simplex P. *Trans Third World Biomater. Congress (April 21-25); Kyoto, Japan*, pp. 331, 1988.
- [142]L.D.T. Topoleski, P. Ducheyne, J. M. Cuckler, The Effects of Centrifugation and Titanium Fiber Reinforcement on Fatigue Failure Mechanisms in Poly(Methylmethacrylate) Bone Cement, *Journal of Biomedical Materials Research*, Vol. 29, pp. 299-307, 1995.
- [143]J. L. Gilbert, D.S. Ney, E.P. Lautenschlager, Self-Reinforced PMMA Composites: Strength, Fatigue and Fracture Toughness Evolution, 20th Annu. Mtg. Soc. Biomater; Boston, pp. 141, 1994.
- [144]E. Fritsch, S. Rupp, N. Kaltenkirchen, Does Vacuum Mixing Improve the Properties of High-Viscosity Poly(Methyl Methacrylate) (PMMA) Bone Cement? *Arch. Orthop. Trauma. Surg.*, Vol. 115. pp. 131-135, 1996.
- [145]J.A. Johnson, J.W. Provan, J.J. Krygier, K.H. Chan, J. Miller, Fatigue of Acrylic Bone Cement: Effect of Frequency and Environment. *Journal of Biomedical Materials Research*, Vol. 23. pp. 819-831, 1989.
- [146]G. Lewis, G.E. Austin, Mechanical Properties of Vacuum Mixed Acrylic Bone Cement. *Journal of Biomedical Materials Research*, Vol. 5. pp. 307-314, 1994.
- [147]G. Lewis, S. Janna, M. Carroll. Effect of Test Frequency on the In Vitro Fatigue Life of Acrylic Bone Cement. *Biomaterials*, Vol. 24 pp. 1111-1117, 2003.
- [148]V. Paravic, P.C. Noble, J.W. Alexander, T.R. Leibs, A. Elliot, Effect of Specimen Preparation on Porosity and Fatigue Life, a Study

- of Centrifuged and Hand Mixed Cement. Trans 45th Annu. Mtg. Orthop. Res. Soc; Anaheim, CA, pp. 184, 1999.
- [149] P. J. Prendergast, B. P. Murphy, D. Taylor. Letter to the editor. Fatigue Frac. Eng. Mater. Struct., Vol. 25. pp. 315-316, 2002.
- [150] N.J. Dunne, J.F. Orr, M.T. Mushipe, R.J. Eveleigh, The Relationship between Porosity and Fatigue Characteristics of Bone Cements. Biomaterials, Vol. 24. pp. 239-245, 2003.
- [151] L. Cristofolini, C. Minari, M. Viceconti, A Methodology and Criterion for Acrylic Bone Cement Fatigue Tests. Fatigue Frac. Eng. Mater. Struct., Vol. 23. pp. 953-957, 2000.
- [152] L. Cristofolini, C. Minari, M. Viceconti, Reply to "letter to editor". Fatigue Fract. Eng. Mater. Struct., Vol. 25. pp. 317-318, 2002.
- [153] J.P. Davies, D.O. O'Connor, D.W. Burke, W.H. Harris, Influence of Antibiotic Impregnation on the Fatigue Life of Simplex P and Palocos R Acrylic Bone Cements with and without Centrifugation. Journal of Biomedical Materials Research, Vol. 23 pp. 379-397, 1989.
- [154] J.P. Davies, W.H. Harris, Effect of Hand Mixing Tobramycin on the Fatigue Strength of Simplex P. Journal of Biomedical Materials Research, Vol. 25 pp. 1409-1414, 1991.
- [155] J.P. Davies, D. O'Conner, D.W. Burke, W.H. Harris, Comparison of the Fatigue Characteristics of Centrifuged and Uncentrifuged Simplex P Bone Cement. J. Orthop. Res. Vol. 5, pp. 366-371, 1987.
- [156] Y. Murakami, S. Kodama, S. Konuma, Trans. Japan Soc. Mech. Engrs., Vol.54-A, pp. 688, 1988.
- [157] L.N. Molino, L.D.T. Topoleski, Effect of BaSO₄ on the Fatigue Crack Propagation Rate of PMMA Bone Cement. Journal of Biomedical Materials Research, Vol. 31, pp. 131-137, 1996.
- [158] P.W.R. Beaumont, R.J. Young, Slow Crack Growth in Acrylic Bone Cement. Journal of Biomedical Materials Research, Vol. 9, pp. 423-439, 1975.
- [159] L.T. Anderson, Fracture Mechanics Fundamentals and Applications. (Boston: CRC Press, 1991).
- [160] C.S.J. Van Hoog-Corstjens, L.E. Govaert, A.B. Spoelstra, S.K. Bulstra, G.M.R. Wetzels, L.H. Koole, Mechanical Behaviour of a New Acrylic Radiopaque Iodine-Containing Bone Cement, Biomaterials, Vol. 25, pp. 2657-2667, 2004.
- [161] M. P. Genebra, L. Morejon, J.A. Delgado, J.M. Manero, F.J. Gil, A. Artola, I. Goñi, M. Gurruchaga, B. Vázquez, J. San Román, J.A. Planell, Effect of Size Distribution of the PMMA Beads on the Fatigue Crack Propagation of Acrylic Bone Cements. Proceedings of the European Society for Biomaterials; London, 2001.
- [162] J. Lankford, W.J. Astleford, M.A. Asher. Microstructural Control of Fatigue Crack Growth in a Brittle, Two-Phase Polymer, J. Mater. Sci., Vol. 11, pp. 1624-1630, 1976.
- [163] Y.K. Liu, J.B. Park, G.O. Njus, D. Stienstra, Bone-Particle-Impregnated Bone Cement; an In Vitro Study. Journal of Biomedical Materials Research, Vol. 21, pp. 247-261, 1987.

- [164] T.M. Wright, R.P. Robinson, Fatigue Crack Propagation in Polymethylmethacrylate Bone Cement. *J. Mater. Sci.*, Vol. 17, pp. 2463-2468, 1982.
- [165] R.M. Pilliar, R. Blackwell, I. Macnab, H.U. Cameron, Carbon Fiber Reinforced Bone Cement in Orthopaedic Surgery. *Journal of Biomedical Materials Research*, Vol. 10, pp. 893-609, 1976.
- [166] J.L. Flower, G.A. Gie, A.J.C. Lee, R.S.M. Ling, Experience with the Exeter Total Hip Replacement since 1970. *Orthop. Clin. NA*, Vol. 19, pp. 25-37, 1984.
- [167] T.A.Gruen, G.M McNiece, H.C. Amstutz, 'Modes of Failure' of Cemented Stem-Type Femoral Components. *Clin. Orthop. Rel. Res.*, Vol. 141, pp. 17-29, 1979.
- [168] T.L. Norman, V. Kish, J.D. Blaha, T.A.Gruen, K. Hustosky, Creep Characteristics of Hand and Vacuum Mixed Acrylic Bone Cement at Elevated Stress Level, *Journal of Biomedical Materials Research*, Vol. 29, pp. 495-501, 1995.
- [169] N. Verdonschot, R. Huiskes, Creep Behavior of Hand Mixed Simplex P Bone Cement under Cyclic Tensile Loading. *J. Appl. Biomater.*, Vol. 5, pp. 235-243, 1994.
- [170] D.J. Chwirut, Long-Term Compressive Creep Deformation and Damage in Acrylic Bone Cement. *Journal of Biomedical Materials Research*, Vol. 18, pp. 25-37, 1984.
- [171] N. Verdonschot, R. Huiskes, Dynamic Creep Behavior of Acrylic Bone Cement. *Journal of Biomedical Materials Research*, Vol. 29, pp. 575-581, 1995.
- [172] <http://www.stryker.com/BoneCement/CEMEXGENTA.asp>, (2007).
- [173] <http://www.exac.com/BoneCement/CEMEXGENTA.asp>, (2007).
- [174] N. Ihaddadène, P. Erani, L. Cristofolini, M. Baleani, M. Viceconti, Fatigue Fractured Surfaces of Acrylic Bone Cements. *International Review of Mechanical Engineering (I.RE.M.E)*, Vol. 1(2), pp. 174-179, 2007.
- [175] M. Cotifava, Engineer Thesis, 2006.
- [176] <http://www.predev.com/parameters.htm>, (2006).
- [177] www.nanolab.aau.dk, (2009).
- [178] P. Erani, L. Cristofolini, M. Baleani, M.C. Bignozzi, M. Cotifava, N. Ihaddadene, F. Tomei, M. Viceconti, Quantitative Crack Surface Morphology of Bone Cement in Relation to Propagation Rate. *Fatigue Fract. Engng. Mater. Struct.*, Vol. 30, pp. 783-795, 2007.
- [179] N. Ihaddadene, P. Erani, M. Cotifava, F. Tomei, M. Baleani, M. Viceconti, S. Bouzid, L. Cristofolini, Fatigue-Fractured Surfaces of Commercial Bone Cements. *Computer Methods in Biomechanics and Biomedical Engineering*, Vol. 10 Supplement 1, pp. 157-158, 2007.

Abstract – Acrylic bone cements have been widely used in orthopaedic surgery for the fixation of artificial joints. In total hip prosthesis, the fracture of poly methyl methacrylate (PMMA), through crack initiation propagation and fracture whether at an interface or within the bulk material is of serious concern since it leads to the implant failure. In the present study, cyclic fatigue fractured surfaces of six commercial bone cements, were investigated using two methods: roughness measurement and cleaved beads indicator (percentage of cleaved pre cured beads). The same surfaces were also inspected by Scanning Electron Microscope (SEM) for crack propagation patterns. Fatigue fractured surfaces of the cement tested were obtained using a methodology based on ASTM-E647-05. All cements tested showed three different morphologies which are in relation to the crack growth rate and cement type. The two methods are able to discriminate between the three zones and thus are quantitative inspections of the fractured surfaces (factorial ANOVA, $p < 0.0005$).

Keywords: Crack propagation, Fatigue fracture, Fracture surface morphology, PMMA bone cement, roughness.

Résumé – Les ciments osseux ont été et ils sont largement utilisés en chirurgie orthopédique pour la fixation des implants articulaires. En prothèse totale de hanche, la rupture du poly méthyle méthacrylate (PMMA) se produit à travers l'initiation puis la propagation de la fissure suivie de la rupture elle-même, que ce soit à l'interface ou bien à l'intérieur du matériau. Ceci pose un grand problème puisqu'il conduit à la défaillance de l'implant. Dans la présente étude, les surfaces rompues par fatigue cyclique de six types de ciments osseux commercialement disponibles ont été analysées suivant deux méthodes : La mesure de la rugosité, Le calcul de billes de polymère (pré polymérisées) rompues (% des billes brisées). Les mêmes surfaces ont subi des inspections qualitatives grâce au Microscope électronique à balayage (SEM) afin de voir le parcours des fissures. Les surfaces rompues étudiées ont été obtenues suivant une méthodologie basée sur la norme ASTM-E647-05. Toutes les surfaces analysées montrent l'existence de trois zones de morphologie différente qui dépendent de la vitesse de propagation des fissures et du type du ciment utilisé. Ces deux méthodes sont capables de distinguer les trois zones constituant les surfaces rompues par fatigue, de ce fait, elles peuvent être considérées comme des inspections quantitatives des surfaces fracturées (facteur ANOVA, $p < 0.0005$).

Mots clés : Propagation des fissures, Fracture par fatigue, Morphologie des surfaces rompues, Ciment acrylique PMMA, Rugosité.

الموجز - يستخدم الاسمنت 'الكريليك' العظام على نطاق واسع في جراحة العظام لتثبيت المفاصل الاصطناعية. في الفخذ الاصطناعية، كسر بولي ميثيل الميثاكريليت (PMMA)، يحدث ببدء ثم انتشار التشقق مما يؤدي إلى الكسر إما في واجهة أو داخل بينية الاسمنت مما يؤدي إلى فشل عملية الزرع. في هذه الدراسة، نتطرق إلى معاينة سطوح ستة أنواع تجارية من اسمنت العظام الخاضعة لكسر التعب الدوري باستخدام طريقتين : طريقة قياس الخشونة وحساب حبات البوليمر الاصلية المكسرة (النسبة المئوية للحبات). نفس السطوح، تمت معاينتها مجهرياً باستخدام المجهر الالكتروني (SEM). تم الحصول على السطوح المعاينة باستخدام منهجية الجمعية الأمريكية لفحص المواد - 05 - E647. أظهرت الفحوصات وجود ثلاثة مناطق مختلفة تتعلق بسرعة انتشار التشقق و بنوع الاسمنت. هاتان الطريقتان قادرتان على التمييز بين المناطق الثلاثة وبالتالي تعتبر طرق معاينة كمية للسطوح الناتجة عن الكسر (العامل ANOVA: $P < 0.0005$).

الكلمات الرئيسية : انتشار التشقق ، الانكسار عن طريق التعب ، مورفولوجية السطح المتكسر ، أسمنت العظام بولي ميثيل الميثاكريليت (PMMA) ، الخشونة